Experimental Investigation on Magnetic Field Assisted PMEDM Process for Slot Cutting

A Dissertation Submitted

In Partial Fulfillment of the Requirements

For the Degree of

Master of Engineering

in

Production Engineering

By

KANIKA VERMA

(Registration No. 801282007)

to the

MECHANICAL ENGINEERING DEPARTMENT

THAPAR UNIVERSITY, PATIALA

July, 2014

CERTIFICATE

I hereby declare that the thesis entitled "**Experimental Investigation on Magnetic Field Assisted PMEDM Process for Slot Cutting**" is an authentic record of my study carried out as requirements for the award of the degree of **Master of Engineering** in **Production Engineering** at **Thapar University, Patiala** under the supervision of **Anirban Bhattacharya**, Assistant Professor, Mechanical Engineering Department, Thapar University, Patiala during July, 2013 to July, 2014. The matter embodied in this report has not been submitted in partial or full to any other university or institute for the award of any degree.

Date: 18/07/2014

KANIKA VERMA

It is certified that the above statement made by the student is correct to the best of my knowledge and belief.

ANIRBAN BHATTACHARYA
Assistant Professor
Mechanical Engineering Department
Thapar University, Patiala - 147004

Countersigned by

Dr. AJAY BATISH
Professor & Head
Mechanical Engineering Department
Thapar University, Patiala

Dr. S.K. MOHAPATRA
Dean of Academic Affairs
Thapar University, Patiala-147004

i

Dedicated to

MY DEAR PARENTS

Acknowledgement

With deep sense of gratitude I express my sincere thanks to my guide **Anirban Bhattacharya,** Assistant Professor for their valuable guidance, proper advice and constant encouragement during the my work on this seminar.

I also feel very much obliged to **Dr. Ajay Batish**, Professor and Head of mechanical Engineering Department.

I am thankful to entire faculty and staff members of Mechanical Engineering Department for their direct and indirect cooperation during my thesis work.

I am sincerely thankful to UGC sponsored projects for financial support.

I am also thankful to my friend **Sanchit Singla** for his help and cooperation.

At last but most important I am highly indebted to my dear parents for their love, support and trust.

Kanika Verma

KANIKA VERMA

iii

Abstract

In todays evovling world many new hard, difficult to machine materials are being developed. With the development of these materials the need to machine them also emerges. In order to machine theses materials many methods are being developed EDM is one of them. Electric discharge machining (EDM) is one of the maximum commonly used nontraditional processes for making accurate intricate shapes on hard materials like die steels and is most preferred process to be followed for die and mold making. Besides machining, EDM when used with powder suspension and with certain combination of electrode materials has also been helpful in developing properties like increasing surface roughness and hardness.

Experiment plan has been designed using Taguchi technique to study the effect of different parameters and their levels by conducting least number of experiments. Based on this L18 orthogonal array is been used.

As the most popularly used materials in die and mold casting industries are the die steels hence for this work AISI H11, H13 and D3 die steels are used as the workpiece materials for slot cutting. Effort has been made to find out the optimum machining conditions by varying process parameters like current, powder to be suspended in dielectric, its concentration, tool material and pulse-on duration at three levels with and without using external magnetic field. The results are analyzed using analysis of variance (ANOVA) both analytically and graphically. Significant factors affecting the output parameters have been found using F-test and percentage contribution. From the experimental investigation copper tool followed by C18000 tool has been found to give the best MRR results and high tool wear, whereas tungsten tool has been found to give the least MRR accompanied by least tool wear. The dimensional accuracy of the tools in terms of corner wear, side wear and overcut has also been studied.

Keywords : EDM, Taguchi, ANOVA, MRR.

Contents

List of Figures

List of Tables

Acronyms

ANOVA	Analysis of Variance
MRR	Material Removal Rate
TWR	Tool Wear Rate
SR	Surface Roughness
MH	Micro Hardness
EDM	Electric Discharge Machining
PMEDM	Powder mixed EDM
OA	Orthogonal Array
DOF	Degree of freedom
SEM	Scanning Electron Microscope
XRD	X-Ray Diffraction

Chapter 1

Introduction

1.1 Introduction to Non-traditional Machining Processes

In conventional machining material is removed from the workpiece with the help of a tool made up of material; harder than the workpiece material. As there are contact forces within the workpiece and the tool, a plastic deformation is produced in the workpiece material.

Non traditional machining (NTM) Processes on the other hand are characterised as follows:

- Material may be removed by forming chips or even no chips may be formed. For example in AJM (Abrasive jet machining), material is removed in the form of small pieces called chips and in case of ECM material is removed by the chemical reaction.
- In NTM, there may or may not be a tool. For example in laser jet machining, machining is done by using a laser beam but in ECM there is a need of physical tool.

1.2 Need of Non-traditional Processes

As a result of modern inventions in the field of tools and cutting methodologies many traditional macining methods like turning had transformed into a less costly, efficient manufacturing processes for manufacturing of delicate, intricate parts having complex geometry in the field of aerospace, automobile industry. For example recently milling was used to the machine aluminum alloys for manufacturing of complex parts used in the aerospace industry. In the past ten years, with the improvement of cutting tools , high-speed milling has been employed for tool steels (usually hardness >30 HRC) for making moulds and dies used in the production of a large range of automotive and electronic components.

In order tomaintain place in the market , manufacturers have to increase the quality of their products and minimize costs while meeting requirement of their customers. Major benefits of high-speed machining recognized are as: high MRR, reduced manufacturing time , less amplitud of cutting forces. However, difficulties related to the use of high-speed machining fluctuate subjected on the work piece material and required geometry. The common limitations of highspeed machining are : increased tool wear, the requirement of special cutting tools with innovative spindles and numerical controllers, fixturing, balancing

the tool holder and at last but the very importantly the need for advanced cutting tools [http://www.iste.co.uk].

1.3 Electric Discharge Machining

The invention of EDM was done in 1770 by Joseph Priestly who discovered the erosive effect of electrical arcs. It was discovered that erosion was caused by discontinuous arc discharges occurring in air among the tool electrode and work piece connected to a DC power source. It was found that these procedures were not very accurate due to high temperature of the machining area and was defined as 'arc machining' rather than 'spark machining.'

Revolutionary work on electrical discharge machining was carried out in 1940s. The damaging effect of an electrical discharge was modified to get organized process for machining materials. The RC relaxation circuit was presented around in 1950s, which was first to provide reliable regulator of pulse times with a servo system to controlthe effective gap required for sparking. In the1950s the relaxation circuit circuit was extensively used in improving the EDM technology.

It was in the 1980s when CNC control was invented a incredible development in EDM was done. Due to continuous evolution in the EDM modernized machines are relaible and stablized ones.. Any material whoch is electrically conductive can be machined with an electrically conductive tool.[Abu Zeid, 1997].

1.3.1 Working Principle of EDM

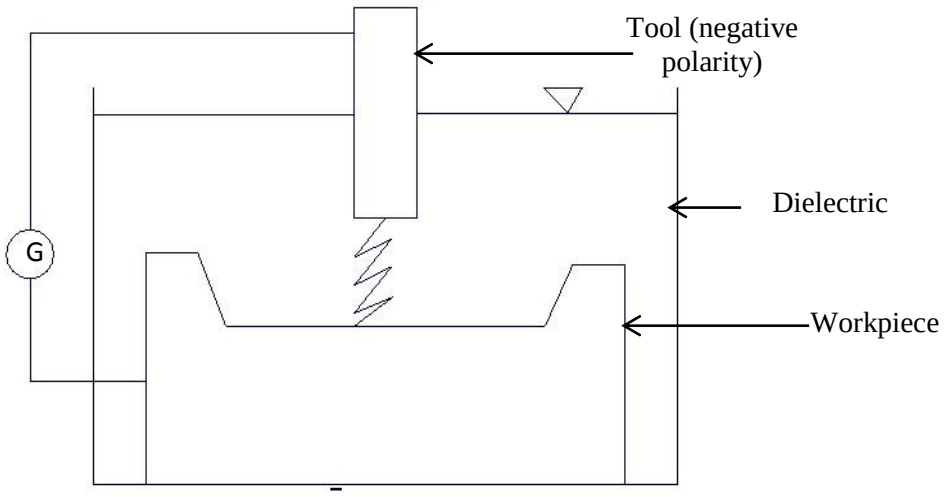

Figure1.1: Schematic representation of EDM

In EDM (as shown in Fig. 1.1) both the tool and thw workpiece material are to be conductors of electricity and have to be dipped in the dielctric medium normally kerosene is used. An effective gap also called sparking gap is sustained between the tool and the workpiece. The electric field established depends on the intensity of the potential difference. Mostly tool is made cathode and workpiece is the anode. Due to established electric field free electrons experience electrostatic forces. Depending on the work function of the tool and the workpiece material the electrons are emitted from the one having lower work function. Normally the electrons are made to be emmitted from the tool, such emission is called cold emmission. These 'cold emitted' electrons are then augmented towards workpiece through the insulating dielectric. As these electrons are emmitted they are accelerated towards the workpiece and collisons are made. These collsions result in ionisation of the molecules of the dieletric which would result in emmsion of more electrons.

This is a recurring process and as a result the number of electrons and ions in the dielectric medium will increase. Due to high number of electrons it is called as plasma channel and such a channel is having very less resistivity. Suddenly there will be a flow of large elctrons from tool to the workpiece, this type of motion is called avalanche motion. It can be seen in the form of a spark. Such movement of electrons and ions can be visually seen as a spark. Thus the electrical energy is transformed into thermal energy of the spark.

These electrons having high speed then invade on the job and ions invade on the tool. This kinetic energy of the fast moving electrons as well as ions on bearing with the surface of the job and tool respectivelyis converted into heat energy. Such heat makes the workpiece temperature rise upto 10,000 °C.

Such a high temperature leads to melting and vaporistaion of materials and hence the material is removed. This molten metal is removed with the help of dielectric.

When the voltage supplied is withdrawn there is no plasma channel and this leads to the generation of pressure waves which removes the molten material forming a crater in the area where spark has occured.

Thus summarizing the EDM process, the material is removed in EDM by spark erosion process.

Generally the workpiece is made anode and the tool is the cathode. The electrons are made to strike the workpiece leading to crater formation and a high temperature is obtained thus removing the material..

1.3.2 Parameters Affecting Performance of EDM

- **Discharge Voltage**

Discharge voltage in EDM depends on the effective gap between the tool and the workpiece. [Ghosh and Mallick]. Before the flow of current starts an open circuit voltage is supplied and it rises till an ionization path is created through the dielectric medium. As soon as the current flows the voltage descends and gets steadied when a working gap is established. It is found that with the increase in voltage MRR, tool wear rate (TWR) and surface roughness as the electric field strength increased. [Fuller, 1996].

- **Peak Current**

It is most important machining parameter. This is the amount of power used in discharge machining, measured in units of amperage. Maximum amount of amperage is controlled by the surface area of the cut. Higher amperage is used in roughing operations and in cavities or details with large surface areas. Machined cavity is a replica of tool electrode and excessive wear will affect the accuracy of machining.

- **Pulse Duration and Pulse Interval**

EDM cycle consists of an on time and off time. All the machining is done in on time, hence it is critical to know it. On and off time are calculated by the duration of the pulses. MRR is directly dependent on the quantity of energy supplied during the pulse-on time. [Singh et al., 2005]. The time during which machining is done is called pulse duration and the interval between two continuous on-time is called pulse interval. MRR increases upto a certain value for the particular combination of workpiece and tool but after that it begins to decrease.

- **Pulse Waveform**

Different types of generators are used to generate different types of waves. The shape of the pulse is usually rectangular but presently other waveforms are also being generated. Most widely used waveform is trapezoidal which is generated with the help of relaxation generator. (Fig. 1.2).

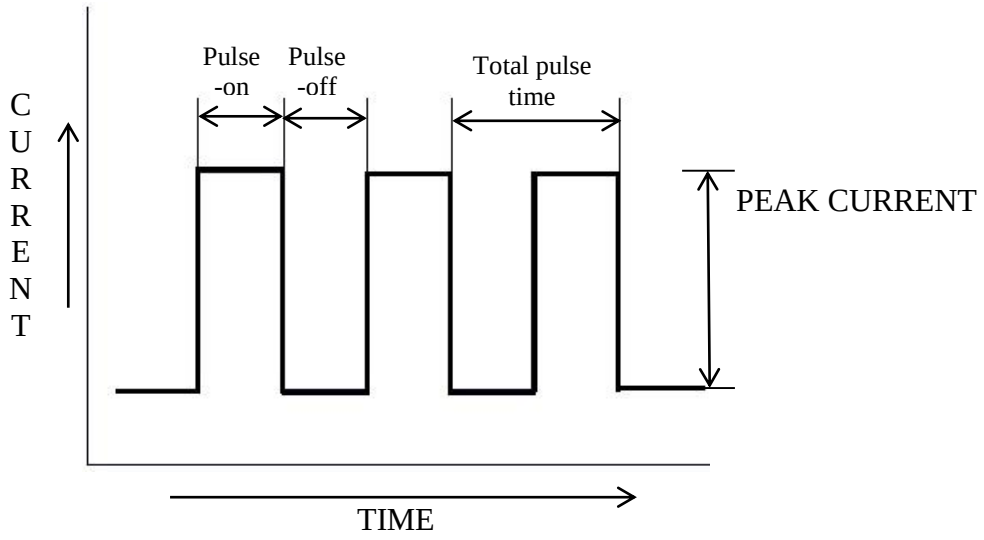

Figure 1.2: Pulse waveform of controlled pulse generator

- **Polarity**

The direction of the current is governed by the type of polarity used i.e straight or reverse polarity. In positive tool is cathode and workpiece is the anode. Today reverse polarity is being used for avoiding the occurring of arcing [Ho and Newman, 2003].

- **Electrode Gap**

To control the working gap to a set value a servo mechanism is used. Larger gap means longer ignition times and higher gap voltage. Feed control should be such that it maintains constant working gap. Its value varies between 0.005 to 0.05 mm.

- **Electrode Material**

The material of the electrode should be wear resistant one. Thus the necessary requirements of electrode materials are:

• The electrical conductivity of the material should be high.

• It should have high thermal conductivity.

• It should possess high melting point to avoid melting of material during machining.

• It should be easy to manufacture.

• It should not be expensive rather it should be easily available and should have low cost.

The followings materials possess above qualities and are mostly used

• Graphite

• Electrolytic oxygen free copper
• Tellurium copper – 99% Cu + 0.5% tellurium
• Brass

- **Dielectric**

Dielectric should possess some required properties which are

- It should have good dielectric strength and should be able to recover easily.
- It should also have required flushing properties and should provide good quenching.
- Mostly used dielectric fluids are kerosene and distilled water.

- **Pulse-on Time**

This is time period during which machining is performed. Increasing pulse-on time increases the machining. Larger the pulse on times means larger is the recast layer and more are the heat affected zones.

- **Pulse-off Time**

It is the time interval between two pulse-n durations, during this interval reionization of dielectric takes place. Increasing the pulse-off duration increases the machining time. It controls steadiness of the process.

1.4 Powder Mixed EDM

PMEDM is also known as 'Additive EDM' it was developed in the course of late seventies for attaining mirror like finish. In powder mixed EDM powder having good electrical conductivity is mixed in the dielectric of EDM, which reduces the insulating strength of dielectric also spark gap rises spark gap making the process more stable and enhancing the surface finish [Kansal et al., 2006].

1.4.1 Technology used in Powder Mixed EDM

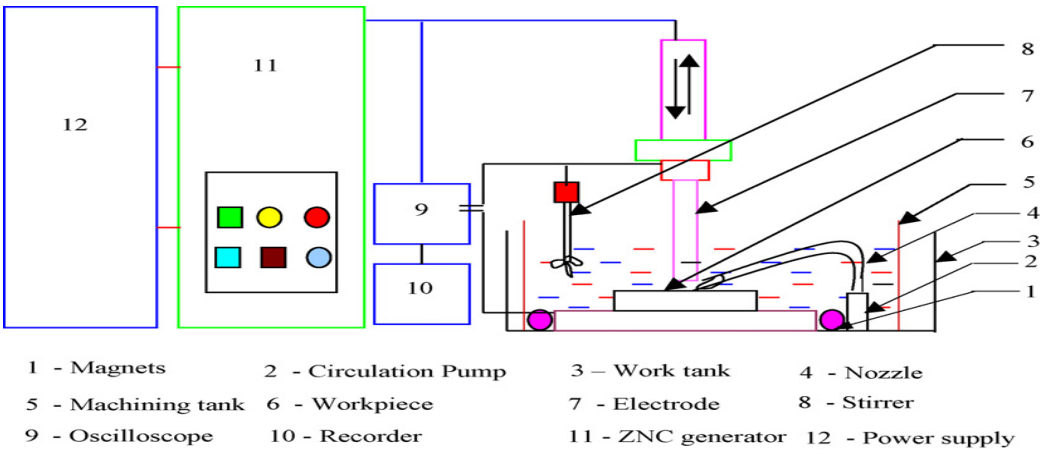

Figure 1.3: Schematic of PMEDM experimental setup [Kansal et al., 2006]

The experimental set up (as shown in Fig. 1.3) consists of transparent container in which machining is performed called machining tank. Fixture assembly is used to hold the work piece. Dielectric (kerosene oil) fluid is filled in machining tank. A stirrer system is used to avoid particle setting. Small dielectric circulation pump is used. Pump is used for circulating the powder with stirrer attached to it both are retained in the tank in which machining is performed. External magnetic field is used for separation of debris for which two bar magnets are placed on the workpiece.

Different conductive powders like aluminum, chromium, graphite, silicon, copper or silicon carbide, tungsten, tellurium can be mixed in the dielectric.

The machining gap is filled with powder particles. When voltage was applied an electric field was created. The powder particles get charged and act as conductors behaving in zigzag manner.

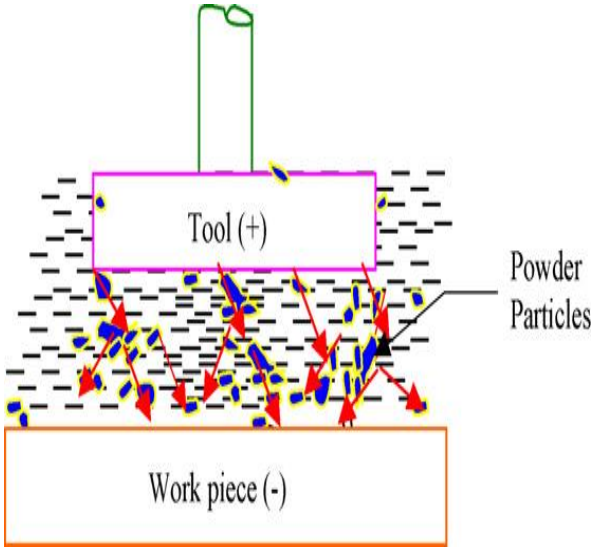

Figure1.4: Principle of PMEDM [Kansal et.al, 2006]

Under sparking area (as shown in Fig. 1.4) particles arranged themselves in chain like structures bridging the discharge gap between tool and the work piece. As a result of this bridging effect insulating strength of dielectric fluid decreases causing easy short circuit to take place thus causing faster sparking leading to faster erosion. At the same time plasma channel is enlarged and widened. [Zhao et al., 2002]

CHAPTER 2

Literature Review

2.1 Introduction

EDM was invented in 1770 by Joseph an English scientist. The different scientists carried out the following work. Literature review in section 2.1 is on powder mixed EDM and in section 2.2 is based on magnetic assisted EDM/PMEDM. Section 2.3 discusses research done on tool wear in which parameters affecting tool wear and geometrical tool wear characteristics are discussed. Based on the research papers studied and conclusion drawn the scopes and objectives are listed in section 2.4

2.2 Powder Mixed EDM

Erden and Bilgin [1980] reported experimental effects of impurities in dielectric fluid. On mixing copper, aluminum, carbon and iron as artificial impurities in kerosene machining of brass steel and copper steel pairs were performed. It was observed that reionization properties of dielectric fluid improved, machining rate was increased when the concentration of the added powder was increased, but machining becomes unstable at excessive powder concentrations due to short circuits. Surface finish and gap size also enhanced on addition of impurities.

Uno and Okada [2000] studied effect of silicon powder mixing and found that glossier surfaces were produced compared to conservative EDM with kerosene fluid. Stability of machining was increased as there was no short circuit between the tool and the workpiece. Okada et al., also found that using carbon powder with titanium carbide a hard layer of titanium carbide is formed on the surface.

Wong et al. [1998] observed “near mirror finish” occurrence in EDM on the use of silicon, graphite, molybdenum, aluminum and silicon carbide. Aluminum powder was reported to give mirror finish on SKH-51 workpiece but was unsuccessful to give same results on SKH-54. Partially conductive powders such as silicon and carbide powders gave very sufficient finish. It was also observed that parameters such as polarity, pulse parameters and powder characteristics have significant influence on mirror finish condition. Negative tool polarity was found to be necessary for mirror finish conditions. Wong et al. also studied

result of aluminum and chromium powder mixture in kerosene and initiate that their presence increased the gap distance between electrode and workpiece. The process gets steadied and improved MRR. Minor particle had advanced suspension affect in dielectric due to higher concentration as a result the likelihood of bridging the gap was higher giving good surface finish.

Furutani et al. [2001] used titanium powder of size <36 μm at concentration of 50 g/l into Mitsubishi oil and a voltage of 320 V with negative polarity and found that TiC layer was deposited to a breadth of 150 μm having hardness of 1600 Hv on surface of carbon steel. Furutani et al. also planned a seating method of lubricant layer during concluding EDM process to yield parts for ultra-high vacuum environment a solid lubricant. In order to molybdenum disulphide powder was mixed into the dielectric fluid to apply lubricant layer on carbon steel and stainless steel using high voltage, small discharge current, a short pulse duration and medium pulse interval.

Chow et al. [2000] studied machining of titanium alloy workpiece by adding SiC and aluminum powders and using kerosene as dielectric fluid, gap distance was enhanced resulting in higher debris removal as it facilitated the scattering of discharge into several boosts. However addition of powder disturbed carbon nuclei attached to the exterior of tool and increased TWR. SiC was found to give better material removal depth than aluminum powder and increased gap distance. Optimal concentration which gave highest removal depths were Al (5 g/l) and SiC (25 g/l).

Tzeng et al. [2001] studied the effect of various additives like Al, Cr, Cu and SiC and found that found that the effect of concentration, size, density, electrical resistivity and thermal conductivity of powders was noteworthy on machining performance. Adding of suitable quantity of powders to the dielectric fluid enhanced MRR and reduced TWR. For a stable concentration, the smallest size of the particle led to highest MRR and lowest TWR. Tzeng et al. also proposed approach for strong design of high speed EDM for process optimization using Taguchi method . A linear relationship was found between input value and the output value. Various input parameters that were found to affect performance powder concentration, pulse on time, duty cycle, peak current, etc.) were optimized.

Simao et al. [2006] helped in modifying the surface properties, they used Taguchi method to recognize the effect of main operating factors (open circuit voltage, peak current, pulse on time, electrode polarity and capacitance) on yield measures (electrode wear, workpiece surface hardness, etc.). It was reported that with the use of moderately sintered electrodes made from WC/Co, a uniform alloyed/altered surface layer with comparatively

few micro-cracks and an average thickness of up to 30μm was formed. Control factors such as powder concentration, pulse on time, duty cycle, peak current were optimized . Experimental results showed that most important factors that affected the EDM process are pulse on time, duty cycle and peak current.

Kunieda and Yanatori [1997] studied association of the debris in the discharge gap of EDM. It was observed that remains units move towards one electrode and return to the other frequently. Many chain particles link the gap in a very short time period. During discharge duration the area of the discharge spot, chains are cracked due to the volatile growth of a bubble of vapor from the dielectric liquid and its disconnected gases

Zhao et al. [2002] reported that principle involved in PMEDM was different from that of simple EDM. Experimental research was performed on machining efficiency and SR of PMEDM in rough machining phase. Zhao et al. also observed that the existence of conducting micro powders in the machining gap causes electric field irregularity. Positive and negative charges accumulate on to the powder particles in the presence of gap voltage. Electric charge density was more at the points, which were nearer to the top or bottom and thus discharge breakdown gets started at these points when the electric field density exceeds the breakdown resistant capability thus resulting in enlarged and widened discharge passages. As a result reorganization of electric charges takes place and a series discharge starts between the tool and workpiece thus increasing MRR and surface finish.

Batish and Bhattachrya [2012] performed experiment to study effect of powder mixing in dielectric on surface microhardness and microstructure for H11 and H13 die steels. They conducted experiments using three different types of electrode materials (Cu, W-CU and graphite) and three different dielectric (kerosene, EDM oil and refined mineral oil) wherein four different powders (W, Cu, Al and graphite). Factors that significantly affected micro hardness were addition of powder followed by current and pulse on time. Best increase in microhardness was achieved with the addition of tungsten powder. For good machining and surface improvement kerosene was found to be best choice. The comparative performance of different levels for various factors is shown in Fig. 2.1 and Fig. 2.2.

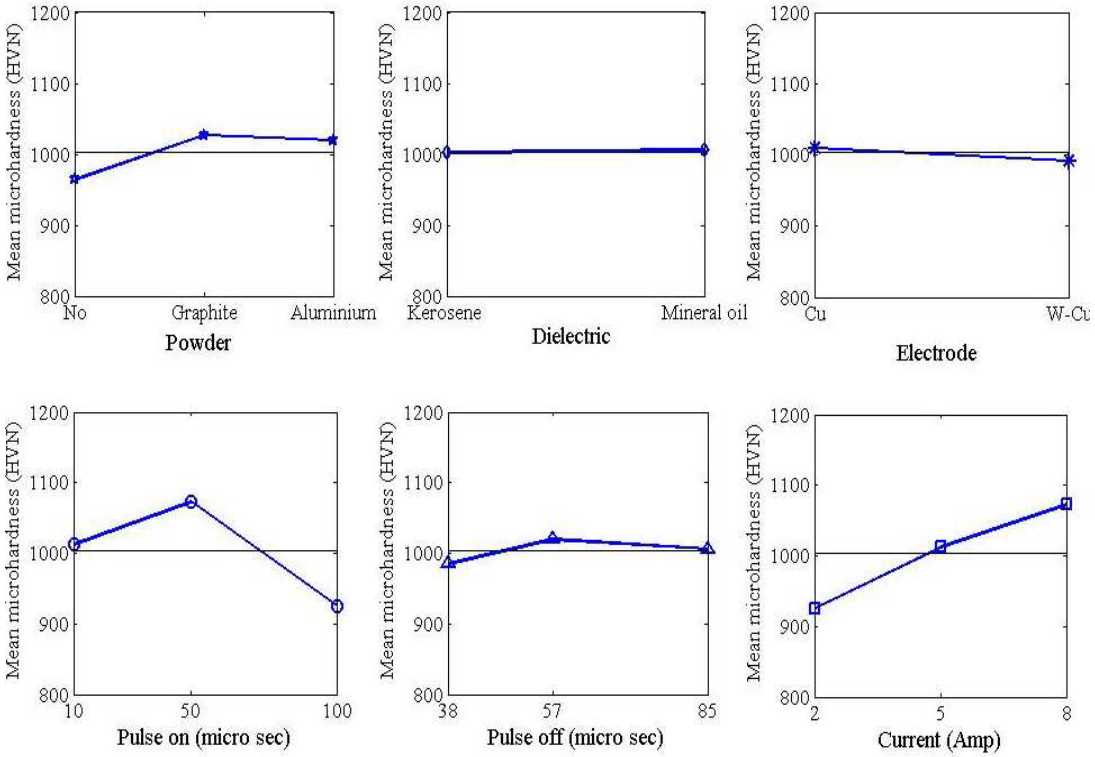

Figure 2.1: Main effect plot for different factors after PMEDM of H11 work piece [Batish and Bhattacharya, 2012]

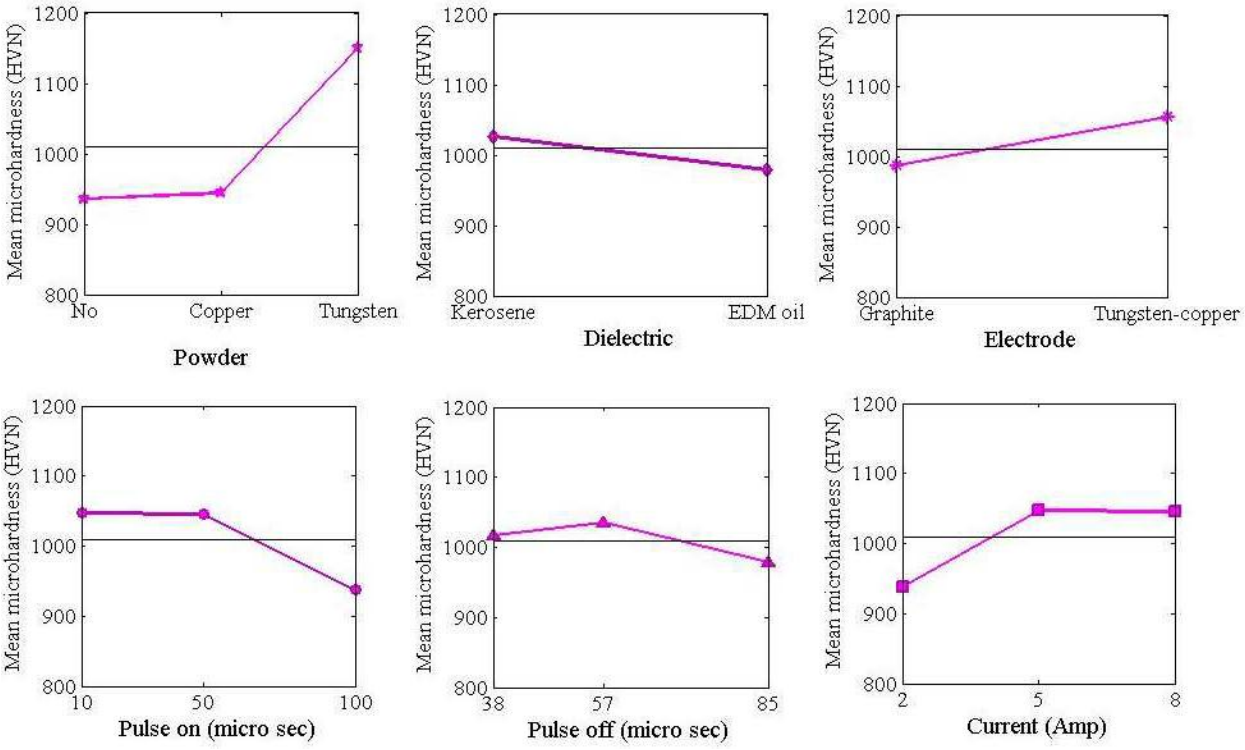

Figure 2.2: Main effect plot for different factors after PMEDM of H13 work piece [Batish and Bhattacharya, 2012]

Bhattacharya et al. [2011] performed experiments to classify the appropriate parameter settings for rough and finish machined surface for EN31, H11, and high carbon high chromium (HCHCr) die steel materials in a powder-mixed electric discharge machining process. A dummy-treated experimental design was used to study effect of seven different process variables. After each trial material removal rate (MRR), tool wear rate, and surface finish were measured. It was observed that EN31 displayed maximum MRR as paralleled to the other two materials at similar process settings. When aluminum was suspended in dielectric with copper electrode it maximized the MRR and caused surface modification. Suspension of graphite powder resulted in lower MRR and enhanced surface finish. Machining of HCHCr with combination of tungsten–Cu electrode and graphite powder requisite higher current and pulse on settings for initiating a machining cut and for giving improved surface finish. Under same machining conditions it was observed that MRR for H11 is less than EN31but significantly higher than HCHCr. It was observed that MRR was dependent upon pulse off and on time and current. Electrode material in combination with suspended powder showed significant effect on MRR but independently had no effect.

Bhattacharya et al. [2012] investigated effect of EDM and process parameters and powder mixed in dielectric on surface properties of three die steel work materials; namely High Carbon High Chromium (HCHCr), EN 31 and Hot Die Steel (HDS).In the study most significant factor affecting micro hardness along powder mixed in dielectric was reported to be tool electrode. Copper-tungsten along with tungsten powder had the best micro hardness among the two electrodes .Samples were analyzed using X-ray Diffraction (XRD) resulys of XRD analysis are shown in Table 1.1 and Scanning Electron Microscope (SEM). Results showed that micro hardness was most affected by the suspended powder material. The micro hardness of the machined surface increased due to deposition of the powder material which was indicator of the modification of surface properties. Increase in micro hardness is found to be greater with tungsten powder than with copper; also it increased with increase in current and was found to be higher when machined with tungsten electrode than with graphite.

Table 2.1: Summary of XRD analysis [Bhattacharya et al., 2012]

Workpiece	Electrode	Powder	Dielectric	Observations
HCHCr	W-Cu	No	EDM oil	• Majority proportion of Cohenite synthetic (Fe_3C). • Improved corrosion resistance and hardenability. • Reduced mechanical stresses at layer boundary.
	W-Cu	Tungsten	Kerosene	• Tungsten content and copper content increased from 0.02 to 1.37% and 0.05 to 0.94% respectively on machined surface • Traces of tungsten carbide, chromium molybdenum seen on surface. • Increased hardness and rigidity. • Expected improvement in toughness and wear resistance
	Graphite	Copper	Kerosene	• Carbon deposit on surface along with Cu and α -Cr. • Chromium reduces stresses and improves corrosion resistance.
EN31	Graphite	Tungsten	Kerosene	• Showed almost equal proportion of chromium iron carbide and iron carbide. • Carbon and tungsten increased from 0.35% to 0.47% and 0.01% to 0.22%. • Improved corrosion resistance. • Reduced mechanical stresses
	Graphite	Copper	Kerosene	• Showed majority carbon deposition as well as $FeCu_4$.
	W-Cu	Copper	EDM oil	• Shows deposition of 2/3rd copper and remaining cementite • Cementite increased the hardness of machined surface • Copper did not form any compound.
HDS	Graphite	Copper	Kerosene	• Showed equal proportion of iron carbide and copper formation. • Iron carbide contributed to increase in hardness of material.
	Graphite	Tungsten	Kerosene	• Showed formation of Chromium carbide compound. • Improved corrosion resistance of materials improves.
	W-Cu	Copper	Kerosene	• Showed formation of Iron carbide and Copper. • Iron carbide increased hardness.

Bhattacharya et al. [2011] performed study to identify parameter settings for uneven and finish machined surface for EN31, H11, and high carbon high chromium (HCHCr) die steel materials in a powder-mixed electric discharge machining process. Parameters obtained showed that EN31 showed extreme MRR as compared to the other two materials at similar process settings. It was found that copper (Cu) electrode with aluminum powder suspension in the dielectricopyimized the MRR. Powder suspension resulted in surface modification. Different effects were observed on suspension of different powders graphite powder displayed a lower MRR but improved the surface finish whereas higher current and pulse on settings were required for starting a machining cut in HCHCr. Under same process conditions MRR for H11 was less than EN31 but higher than HCHCr. MRR was found to be increased with an increase in the current and pulse on time. Two factors that affected TWR were current and powder whereas surface roughness was affected by current, pulse on time, suspended powder, workpiece material, and electrode material. The surface roughness improved by graphite powder suspension .Best surface finish was observed for EN31 and the lowest roughness value was observed during machining of HCHCr with tungsten–copper

electrode at a pulse on time of 10 μs and current set at 2 amp with graphite-mixed powder in dielectric. Conclusion drawn was that EN31 can be machined with good surface finish even at low current and pulse on settings but same was not feasible to machine H11 and HCHCr at these settings.

Kansal et al. [2007] studied effect of silicon powder mixing on machining characteristics of AISI D2 steel. Six process parameters peak current, pulse on time, pulse of time, concentration of powder, gain and nozzle flushing were considered. Studies indicated that all other factors affected MR except nozzle flushing. It was observed that with increase in peak current the MR improved because it had large impact on input energy. Input energy is the energy per pulse in the spark region and thus controls rate of material erosion.
It was concluded that short pulse on time causes less vaporization whereas longer pulse duration makes machining process unstable.

MRR increased considerably on suspension of silicon powder. When conductive powder particles were added MR was mainly attributed to lower breakdown strength of dielectric. At concentration of 4 g/l of silicon powder maximum MR was produced. Optimum process parameters obtained were Peak current =10A, Powder concentration = 4g/l, Pulse-on time =100 μs.

Bhattacharya et al.[2010] studied effect of seven different process parameters on material removal rate (MRR), tool wear rate (TWR) and surface roughness (SR) using Taguchi technique. For high carbon high chromium (HCHCr), EN31 and hot diesteel (HDS) workpiece machining situations that affected the three outputs were recognized and improved. Control factors that identified were the workpiece material, type of dielectric fluid, the electrode material, pulse-off and -on time, current, and type of powder suspended in the dielectric. Seven factors, namely (i) workpiece material, (ii) pulse-on time, (iii) pulse-off time, (iv)current, and (v) powder, were varied at three levels and the remaining two factors dielectric and electrode materials were varied at two levels. Copper powder gave best results and tungsten the worst, thus tungsten powder may be used for roughing operations and copper for finishing. Most significant factors affecting MRR were current, electrode material and pulse on time. Kerosene was better choice than EDM oil for all three materials. For HCHCr and HDS copper powder gave optimal solution.

2.3 Magnetic EDM/PMEDM

Govindan et al. [2013] performed single-spark analysis of removal phenomenon in magnetic field assisted dry EDM by investigating more than 100 single-discharge for dry and liquid EDM trials, with and without magnetic fields at different values of current, voltage, magnetic field, pulse on -time and bi-pulse current. Confinement of plasma due to Lorentz forces is a very important factor in characterizing higher MRR in magnetic field assisted EDM. In case of dry EDM, the magnetic field assistance reduced the diameter of the crater and increased the depth.

Teimouri and Baseri [2012a] studied about the effect of magnetic field and rotary tool on EDM performance with X210Cr12 cold work steel as work piece and copper tool. Experiments were divided in three energy regimes namely low, middle and high depending on the values of peak current, pulse on time and pulse off time. MRR was found to increase with energy (i.e., high current, high pulse on time and high pulse off time situation), while SR was found to increase with the energy.

Teimouri and Baseri [2012b] studied about TWR and overcut in EDM with rotary tool and magnetic field assistance with SPK cold work steel (X210Cr12) as work piece and copper tool at three energy regimes namely low, medium and high. It was observed that the TWR increases with increase in discharge energy but at the high energy regime due to deposition of pyrolytic carbon on the surface of the tool, TWR decreases but TWR was found to increase continuously with increase in rotational speed of electrode which avoids deposition of pyrolytic carbon on the electrode by properly clearing the machining gap.

Heinz et al. [2011] investigated magnetic field assisted material removal in micro-EDM for non-magnetic materials. Micro EDM is used for creating micro sized features irrespective of their hardness. For increasing MRR up to desirable level, i.e., (10 – 15) mm3/h, from current MRR possible from (0.6 – 6) mm3/h; experiments were conducted. In this experiment tungsten wire (100 μm diameter) as electrode, grade 5 titanium as work piece, deionised water as dielectric, gap of 1 μm, gap voltage 100 V, power (100 – 150) W and electromagnets with strength 0.33 T, 0.66 T and 1 T were used. Single spark discharge experiments were chosen to study behaviour of melt pool, while erosion efficiency and volume analysis was done to predict MRR. Plasma temperature, electron density, and debris distribution were used to investigate and explain the mechanisms influencing material removal.

Joshi et al. [2011] discussed about the effect of pulsating magnetic field on dry EDM. Problems like low stability of arc column, arcing and poor surface quality are seen in the case of dry EDM. In order to prevent these types of problems, effect of pulsating magnetic field on this process was studied. Two stainless steel split work pieces were used with copper pipe electrode and oxygen gas with 99.9 % purity as energy transfer media. Pulsating magnetic field was provided using a triangular configuration of electromagnets energized by (0 – 30) V DC (sequential actuation). Rotating magnetic field produced by sequential actuation influenced electric field and deflected electrons at some angle. By this increased collision was observed with reduced mean free path helping in raising ionization and better transfer of thermal energy to work piece, this helped in increasing the MRR. Better geometric accuracy and better machined surface quality, i.e., lower SR was observed

Lin and Lee [2008] discussed about effects of magnetic forces on the EDM process with SKD 61 steel as work piece and copper electrode with positive polarity using dielectric kerosene. Different levels of peak current and pulse duration were used. Magnetic force assisted device consisting of rotating disc, driven by electric motor with two magnets under the complete set up of EDM was established for carrying out the experimentation. Magnetic field used helped in gap cleaning and changing the motion path of electrolyte. It resulted mainly in maintaining regular discharge waveforms at prolonged time duration. Using magnetic field, MRR was increased nearly three times as compared to that of conventional EDM, and SR was also less. MRR was high at high peak current and more pulse duration as well as SR was also lower at longer pulse durations. However, the TWR was slightly higher comparatively, but it reduced to even negative at higher pulse duration due to deposition of pyrolytic carbon generated from kerosene on the electrode surface. It helped in expelling debris leading towards improved machining efficiency with lesser surface cracks. Bhatt [2013]

2.4 Tool Wear in EDM

In EDM the problem of tool wear is very important because the final shape is directly affected by the shape of the tool, also the tool cost is the total cost of manufacture as it consists of raw material cost of tool, number of tools needed for the operation and the production cost of tool . While designing EDM operations tool wear should be thoroughly considered as it contributes 70% of the total operation cost.

Measurement of tool wear- It is expressed in following two ways –

$$Tool\ wear\ rate\ (V_E) = \frac{\text{volumetric removal from the tool}}{\text{per minute machining time}}$$

$$Workpiece\ removal\ rate\ \ (V_W) = \frac{\text{volumetric removal from the workpiece}}{\text{per minute machining time}}$$

$$Relative\ wear(\nu) = \frac{\text{volume of the tool electrode material removed}}{volume\ of\ workpart\ removed}$$

2.4.1 Parameters Affecting Tool Wear

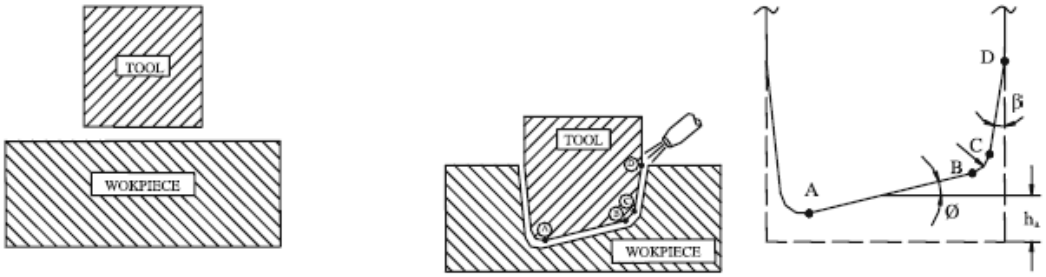

Figure 2.3: Geometrical wear Characteristics [Ozgedik and Cogun , 2006]

Area	Symbol	Wear
AB	Φ, ha	Front Wear
BC	r	Edge Wear
CD	β	Side Wear

- **Discharge Current** – Ozgedik and Cogun [2006] studied that on increasing the discharge current large amount of material melts and evaporates both from the tool and the workpiece as energy of pulse increases with increase in discharge current. Due to this increase in energy large amount of material melts and evaporates from both the tool and the workpiece. Sohani et al. [2009] found that MRR varies linearly with current whereas TWR varies nonlinearly.
- **Pulse Duration** – Chen and Mahdavian [1999] observed that at short pulse durations the increase in pulse duration results in increase in tool wear whereas at long pulse durations reverse results are observed on increasing pulse duration, reason being less spatial current density of the discharge channel and increased time duration of heat transfer from crater to the tool. Sohani et al. [2009] found that more is the pulse on duration more is the MRR but till half of the way but after that it decreases as pulse duration is increased. This happens because input energy increases with high pulse duration which leads to

expansion of plasma channel due to which energy density on workpiece is not enough to melt it. Increasing pulse on duration rapidly decreases the tool wear and remains constant for long durations of pulse on time.

- **Polarity** – Lee SH and Li XP [2001] studied the effect of polarity on tool wear and found that at low to medium discharge current values negative polarity of tool results in less tool wear rate as compared to positive polarity, whereas at high current settings polarity has no effect. Positive polarity reduces relative tool wear significantly with increasing current. At higher values of discharge current there is no effect on relative tool wear for both polarities.
- **Type of dielectric fluid –** Kerosene is more commonly used as compared to other dielectrics like distilled water, glycol, glycerin etc. Different dielectrics have different effects. Kerosene – It was studied by Chen et al.[1999] and Koing et al.[1987] that as compared to other dielectrics on increasing current higher workpiece removal rates are achieved with kerosene. Whereas tool wear rate decreases on increasing current on using other dielectrics but for kerosene it increases. Chen et al. [1999] compared the use of kerosene and distilled water and found that on using kerosene a carbide layer was forms on the surface of the workpiece which possessed higher melting temperature and requires higher pulse energy as compared to the oxide layer formed with the use of distilled water. Distilled water – Jilani and Pandey [1984] compared the use of tap water and distilled water and found that tap water gave higher relative tool wear. They also found that higher relative tool wear was obtained on using copper at positive polarity whereas negative polarity reduced the tool wear for both tap water and distilled water. Chen et al.[1999] discovered that when water is used as a dielectric a layer of oxygen is formed on the workpiece which increases the removal rate.

- **Dielectric Flushing method** – The tool wear as shown in Fig. 2.4 was found low in the case of injection and suction flushing when compared with side flushing. The reason behind this was low temperature, gas volume and dielectric contamination in machining gap at these settings. Tool surface inclination angle is shown in Fig. 2.5.

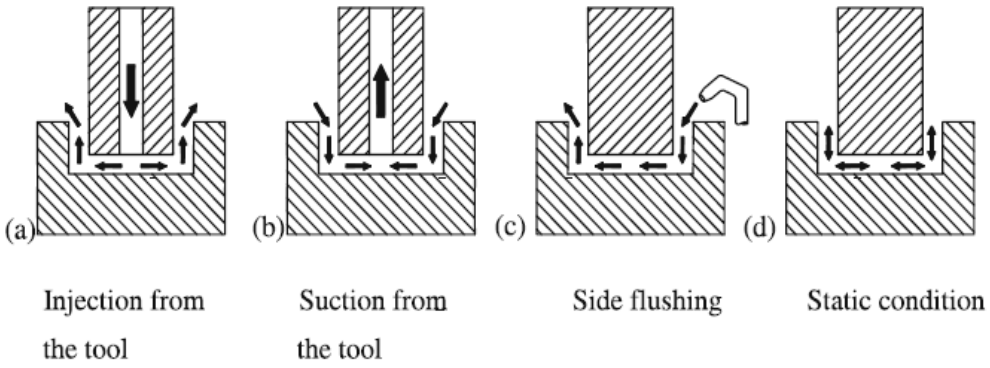

Figure 2.4: Dielectric Flushing Methods [Ozgedik and Cogun, 2006]

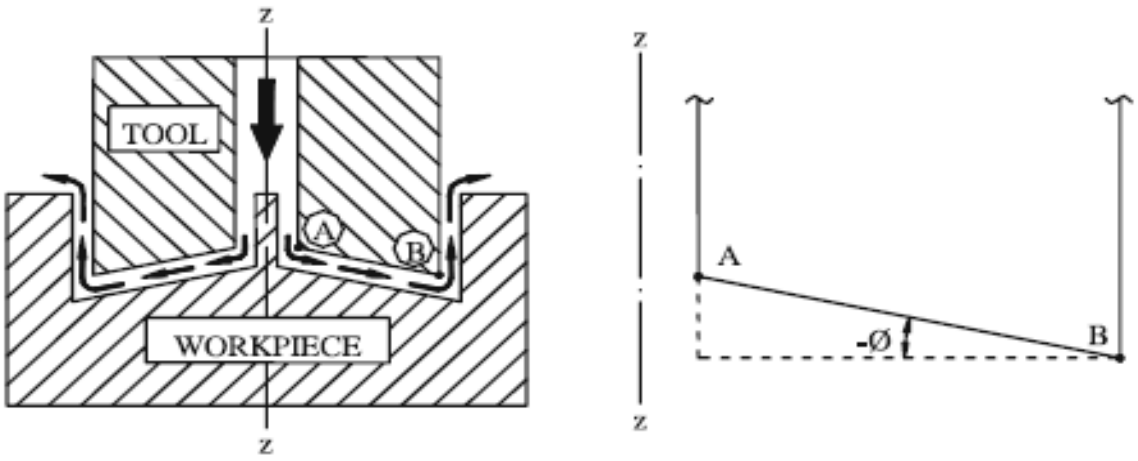

Figure 2.5: Tool front surface inclination angle [Ozgedik and Cogun, 2006]

- **Powder suspended** – Masuzawa and Heuvelman [1983] studied that at reduced concentration of conductive powder the tool wear rate rapidly decreases at low current settings and at high current settings it decreases slowly, whereas at high concentrations high electrode wear occurs. Tzeng and Lee observed that in changing the inter electrode gap copper has least effect whereas aluminum has high effect.
- **Tool and materials** – Samuel and Phillip [1997] observed that for low tool wear, properties of material such as melting point, density, specific heat all should be high. Lee

and Li found that tool materials with low melting temperatures have high relative wear. They also found that graphite and tungsten carbide tools have low value of relative wear compared to copper tools. Lee and Li [2001] revealed that increase in workpiece removal rate is obtained for copper with increase in discharge current whereas graphite tools gave maximum workpiece removal rates.

- **Tool geometry, machining area, vibrating and rotating tools** – Lonardo and Bruzzone [1999] studied that increasing tool area increases work piece removal rates in roughing operations and in finishing operations surface roughness of work piece increases with increase in tool area. Yan and Wang [1999] found that for hollow tools both the tool wear and the work piece wear is maximum and for solid tools surface roughness for the work piece is minimum at normal down feed. Ghoreishi and Atkinson [2002] in an experiment found that in finishing conditions the work piece removal rate increases for high frequency ultrasonic vibration of tool and for low frequency combined with rotation all work piece and tool wear rates as well as surface roughness for work piece is high

2.4.2 Geometrical Tool Wear Characteristics

- **Side wear –** Side wear is represented by tool side surface taper angle, as it is very small angle so it is neglected in most cases. Edge wear and side wear mostly responsible for degeneration of tool shape.
- **Edge wear** – Cogun et al. [2006] found that at the beginning of machining rapid wear is observed at the tool edges and is in the form of rounded edges of tool.. Crookall and Fereday [1973] in an experiment observed that a wear resistant layer is formed at the edges of the tool by the carbon from cracked dielectric kerosene and carbon steel workpiece. At the beginning as the tool edges are sharp it is difficult to attach carbon on them hence fast wear is observed at the beginning. They also conducted experiments for V- shape tools and found that enlargement of radius takes place at the beginning at a fast rate but as the machining continues rounding of the tip slows down. Cogun et al. [2002] through an experimental study found out that the minimum wear at inner and outer radii are observed at static flushing conditions very high flushing conditions should be avoided.
- **Front wear** – Koeing et al. [1977] found that front surface inclination angle depends on the inlet direction of dielectric with respect to machining gap. Front surface inclination angle increase with increasing dielectric flow, discharge current and pulse duration, whereas it decreases as the tool area increases. Front surface inclination angle is always negative in injection flushing and positive in suction flushing.

Mohri et al. [1995] stated that maximum wear of tool happens during initial periods of machining, although a layer of carbon is deposited on the tool due to breaking of EDM oil but it does not help in decreasing its wear. It was observed that on keeping the prolongation for pulse on more than 20μs the tool damage was less.

Yu et al. [1998a] investigated the square shaped tools with sharp corners for 3D micro EDM with tool path correction and achieved uniform wear on tool with programmed X-Y plane path. Square tools were used for finishing parts containing sharp corners. Yu et al. (b)[1998] put forwarded an approach of machining the component layer by layer to obtain consistent wear of tool to control its actual shape during machining in on the subject of cylindrical tools in micro EDM.

Sato et al. [2000] conducted an experimental study on rotating cylindrical electrodes for shallow cuts and proposed a two dimension model to study wear of tool in a steady

condition. Experimental study revealed that the rotating cylindrical tools have added to three sided cuts as forecasted by the model.

Zhao et al. [2003] manufactured an EDM tool by the process of selective laser sintering, the tool was found to be composed of copper encompassing steel. Strong discharge was observed on increasing the value of current and high values of temperature led to absorption of carbon which increased the weight of electrode and protected it. This tool can be used for roughing and semi finishing.

Yoshida and Kunieda [2004] found that the light given off by dielectric cannot be ignored. It was also concluded that process of release of spark in dielectric is similar to that of in air as the channel of plasma in dielectric is enclosed by the gases emitted by the dielectric fluid.

Kunieda and Kobayashi [2004] conducted experimental investigation using copper as tool and work piece material was carbon steel and found that the layer of carbon deposited on the tool upon machining had a linear relation with the pulse on duration, moreover it was found that it did not had any effect on the plasma generation but blocked the deterioration of tool to some extent. On the other hand when the tool was given positive polarity the deposition rate of carbon layer was less and evaporation rate of copper was more consequently more wear of tool occurred.

Luis et al. [2005] carried out experimental study on MRR and TWR of silicon carbide using design factors intensity, pulse time, duty cycle, and open circuit voltage and flushing pressure and found that only voltage and intensity influenced MRR to a confidence level of 95%. In relation to tool wear the most influencing factor was intensity followed by pulse time and flushing pressure, the electrode wear was found to decrease when intensity was increased. MRR was found to be increased when intensity and open circuit voltage were increased.

Zarepour et al. [2007] performed an experimental investigation for testing wear of EDM tool made of copper for machining DIN 1.2714 and found out that main influencing factor was current controlled the wear directly whereas pulse on time affected the tool wear inversely.

Pham et al. [2007] conducted an experimental investigation to study the wear of tool in form of its shape and volume. It was found that the deterioration in the shape of the electrode was because of change of location of concentration of the electric field, as in the beginning the electric field is concentrated on the edge of tip of the tool hence the wear of tip starts in the beginning after that concentration of electric field moves on to the center of the

tool tip .Thus it follows such pattern for distortion of tool shape. Experimental investigations were performed using tool steel, aluminum and brass as workpiece and tool material was tungsten carbide using same values of energy required to generate spark. On using aluminum and brass as work materials a rapid shift in trend of tool wear was observed. The reason was that bigger bits of debris of aluminum and brass were formed initially as they have low melting temperatures which were broken on continuous machining. On machining of tool steel the tool wear was 50% whereas it was only 2% when workpieces of brass and aluminum were machined but the machining of brass and aluminum needs to have a superior system for flushing of debris.

Marafona [2007] conducted an experimental study on machining high carbon steel by tungsten-copper tool and investigated the black layer formed on the tool which increases as the machining time increases. The author concluded that the layer was composed of iron and carbon along with other materials like vanadium, molybdenum and chromium. The deposit of this layer is linked with the used machining conditions and is found to reduce the tool wear.

Pham et al. [2007] put forwarded an approach to calculate volumetric wear ratio established on the analytical knowledge chalked up from the process. Li et al. [2007] put forwarded an approach to calculate the wear of tool during machining time by controlling the gap between workpiece and tool through a servo mechanism. An approach of workpiece vibration backed by scanning 3D micro EDM machine was put forwarded to rectify the process.

Sohani et al. [2009] found that with increase in tool area TWR decreases linearly because ratio of corner wear to tool surface area decreases. Tools having circular cross sectional area have lower TWR and more MRR.

Yan et al. [2009] designed a machine vision system to calculate the wear of tool from front and from corner in the field of micro EDM. By using this system tool wear was measured with an error of 3% in the measurement when correlated with the results obtained by microscope measurement. Further analysis revealed that deepness of the hole and groove were linearly related to length of front wear when machining was being done at a fixed feed rate. This system helped in reducing the machining time by 40% as compared to uniform wear method.

Abdulkareem et al. [2009] carried an experimental work for decreasing the EWR by using liquid nitrogen, titanium alloy (Ti-6Al-4V) was used as workpiece and copper was used as the tool material. It was observed that use of nitrogen as the coolant helped in achieving

about 27% decrease in the EW besides this it also helped in improving the surface roughness, as the liquid nitrogen decreased the temperature and both these outputs are dependent on temperature. These results were found to hold good even when the machining parameters were varied.

Kung et al. [2009] conducted an experimental study on MRR and EWR using cobalt tungsten carbide as work material. Through this study he found that suspending aluminum powder in the dielectric increased the efficiency of the process. On varying the concentration of powder MRR increased with the increased powder but after a certain optimum value it started reducing on the other hand EWR varied inversely to the concentration. On using powder of greater grain size as well as on increment in the values of current and pulse duration the MRR and EWR increased.

He et al. [2009] conducted a study of tubular electrode by injecting pressurized dielectric inbetween the discharge gap for efficient removal of debris. It was found out that in this case there are six factors affecting electrode wear and their sequence in order of increasing influence are : electrode cross sectional area, peak current, dielectric pressure, pulse width, machining depth and pulse interval. A wear prediction model was also layed based on the experimental investigation which precisely controlled error upto 8% .This method was found better than conventionally used neural network as training time for this was less and accuracy was more.

Koshy and Tovey [2011] analysed the performance of textured electrodes and found out that texturing the tool decreased the force to be applied during machining . On comparison of the textures obtained by textured tools to those of non-textured the textured tools were found to give more continuous texture and non-textured were found to give linear texture consisting of grooves.It was found out that for optimum decrease of the force the tool the texturing should be done at away from cutting edge. This type of machining was found to be beneficial for components such as taps, gear cutting tools that is for components which are made up of heat resistant alloy.

Pellicer et al. [2011] studied the effect of process parameters and tool geometry on AISI H13 steel using copper electrodes of square, triangular, circular and rectangular shapes. Results obtained show that MRR and surface roughness increase with discharge current whereas pulse off duration effect on MRR is not linear. Square and rectangular shape tools gave good radial and axial wear ratios hence are the most preferable option.

Aas [2004] and Maradia [2012] found out that graphite being a good electric and heat conductor is a good material to be used as an electrode in EDM since possessing these

properties it distorts or deteriorates very less compared to other common tool materials copper being one of them. But it is suitable mostly for roughing operations only as machining with graphite gives a very high value of surface roughness, also different types of graphite are available which can be used for different purposes depending on the requirement.

Klocke et al. [2013] conducted experimental study using different types of graphite as electrodes and found out that MRR was affected by current settings and pulse on time. On increasing the pulse on time MRR was found to decrease. The reason behind this was found to be that on increasing the pulse on time diameter of plasma canal expanded which reduced the energy of the plasma thus decreasing the MRR. It was also found out that various types of graphite used did not had any effect on MRR. Whereas tool wear was affected by the duration of the pulse, it even had negative values the reason behind it was deposition of material of work piece used these deposits were mainly found on the boundaries of the electrode.

Bhattacharya et al. [2014] studied surface modification and metallurgical characteristics after machining with EDM and PMEDM for three die steels i.e. AISI D2, D3 and H13. It was found that XRD analysis done affirmed the drifting of material of suspended powder the tool material used and the dielectric to the workpiece. It was also found that extraneous magnetic field used helped in reduction of TWR. Under positive conditions the tungsten and titanium carbide was formed which was found to notbly increase the microhardness of the workpiece.

2.5 Literature Summary

By studying the research papers on Electrical discharge machining it is seen that different experimental studies have been carried out in the field of Powder EDM and EDM for increasing MRR , surface finish and reducing tool wear rate. Some of them are:

1. Steel is the best material to be used compared to other soft metals like brass, aluminum for the purpose of short holes as sideways removal of debris is not an issue [Pham et al., 2007].
2. Suspension of tungsten powder and use of kerosene as a dielectric were found to be most suitable for increasing micro hardness and surface finish [Batish and Bhattacharya., 2012].
3. Analysis of black layer deposited on the tool during EDM machining showed that it is composed of iron and carbon and deposition of this helped in reducing the tool wear [Marafona., 2007].
4. Increasing discharge current increases the tool wear rate and material removal rate. Conditions of straight polarity, injection and suction method of removing debris and decreasing the powder suspended in dielectric reduces the tool wear.

   [Ozgedik and Cogun, 2006 ; Cogun, 2002]
5. Among different shapes of tool circular cross section showed best results that is more material removal rate and less tool wear rate succeeded by triangular, rectangular and square. The shapes of the tool have a close impact on MRR and TWR [Sohani et al., 2009].
6. Tool made by the process of selective laser sintering was tested and was found suitable for roughing and semi finishing operations, it was found to soak up carbon and safeguard it against wear [Zhao., 2003].
7. Study of suspension of different powders revealed that their properties like density, size, electrical resistivity etc had an impact on MRR and TWR, with results showing that smallest size of particles gave best results with concentration being fixed. Also it had a close relation with the machining parameters [Wong et al. 1998].
8. TWR was found to decrease with increasing current except when kerosene was used as dielectric. On comparison of tap and distilled water higher TWR was observed tap water also it was found both gave better results with negative polarity [Jilani and Pandey., 1984; Koing et al., 1987 ; Chen et al., 1999].

9. Graphite was found to be good electrode material for roughing purposes , using different grades of graphite did not showed any variance on MRR [Aas., 2004; Maradia., 2012; Klocke et al, 2013].
10. Cryogenic cooling done with coolants like liquid nitrogen helps in optimizing the machining efficiency as well as obtaining a good surface. [Abdulkareem 2009]

2.6 Scope and Objectives

A crater made by single discharge was analyzed made by magnet assisted PMEDM and was found that due to magnetic force an increment in the depth of crater and decrement in its diameter occurred [Govindan et al., 2013]. EDM conducted under the influence of external magnetic field with rotary tool and with ultrasonic vibrations gave desired results i.e. higher MRR and lower TWR [Teimouri and Baseri, 2012]. Higher MRR was achieved when tool was given positive polarity i.e. when reverse polarity was used also surface roughness was found to decrease and MRR was found to increase when machining was conducted under the magnetic field [Lin and Lee, 2008]. Maximum wear of tool was found to occur during early periods of machining whereas it was found to decrease with time due to deposition of carbon layer on tool which was found to have linear relation with pulse-on duration; this black layer was found to be composed of iron and carbon along with molybdenum and chromium [Mohri et al., 1995; Kunieda and Kobayashi., 2004; Marafona., 2007 Fereday., 1973]. Different shapes of tools were investigated and it was found that with increase in tool area the TWR was found to decrease linearly also square tools having sharp corners were reported to have a uniform wear, circular cross sectional area tools were found to have lower MRR and more TWR [Sohani et al, 2009]. Square and rectangular shaped tools were found to give good radial and axial wear ratios and were considered as most preferred option [Yu et al., 1998 a); Pellicer et al., 2011; Sohani et al., 2009; Lonardo and Bruzzone, 1999]. Intensity of current was found to influence MRR directly and TWR inversely [Luis et al, 2005]. TWR was also inversely related to pulse-on duration.Deterioration in the shape of tool was reported to occur due to change of location of concentration of electric field. An approach to calculate volumetric wear ratio, to calculate the wear of tool during machining time by controlling the gap between workpiece and a machine vision system was designed to calculate the wear of tool from front and from corner in the field of micro EDM [Pham et al., 2007; Li et al., 2007; Yan et al., 2009]. Graphite and tungsten carbide tools were found to have low relative wear compared to copper tools also graphite being a good electric and heat conductor is a good

material to be used as an electrode in EDM different grades of graphite did not had any effect on MRR [Samuel and Phillip., 1997; Aas and Maradia., 2012; Klocke et al., 2013]. Literature survey reveals that so far enough work has not been done in studying the tool wear geometrical characteristics in the field of slot cutting.

Based on the above summary, the following objectives are decided for the present work.

1. To study the effect of following process parameters on TWR and MRR during PMEDM for three workpiece materials (H11, H13 and D3) during slot cutting.
    - Current
    - Pulse-on duration
    - Type of powder
    - Powder concentration
    - Effect of magnetic field
    - Tool material
2. To study tool behavior for change in its shape and geometrical tool wear characteristics side wear and corner wear during
    - PMEDM with and without external magnetic field.
    - During machining of slot cutting.
    - While machining 3 different graded die steels (AISI D3, H11 and H13).
3. To study different metallurgical characteristics of slot cutting during PMEDM with and without magnetic field.

.

CHAPTER 3
Design of Study

3.1 Introduction

Literature survey indicated that the variations of machine output parameters such as TWR, MRR were calculated for different roughing and cutting operations, however not much research has been carried out for studying these on slot cutting. This experimental work is aimed at studying the tool behavior during macro and micro EDM during slot cutting with and without magnetic strength. It consists of analysis of tool shape deformation at edges and front in EDM/PMEDM with magnetic field.

3.2 Experimental Design

Designing an experiment is the principle need of any experimentation plan. In present study Taguchi Method is used for preparing experimental design. Main steps of experiment plan are listed below.

- Defining objective function
- Selecting an appropriate OA
  - Selection of factors
  - Pilot Experimentation
  - Finalizing the factors and their levels

3.2.1 Defining Objective Function

The main objective of this experimentation is to study the effect of current, powder concentration, type of powder and magnetic strength on tool behavior during macro and micro EDM, PMEDM during slot cutting to analyze output parameters dimensional and profile accuracy of tool.

3.2.2 Selecting an Appropriate OA

The Taguchi method involves reducing the variation in a process through robust design of experiments by using a selected set of experimentation plan. The overall objective of this method is to determine which factors affect the most with a minimum amount of experimentation, thus saving time and resources. Each factor is assigned column(s) depending on its DOF. Each level of a factor has an equal number of occurrences within each column; and for each level within one column, each level within any other column will occur an equal number of times as well.

3.2.3 Selection of Factors

Selection of factors is an important task which is to be done carefully to prepare the most effective design of experiment. Brainstorming and pilot experimentations are conducted to decide factors and their levels.

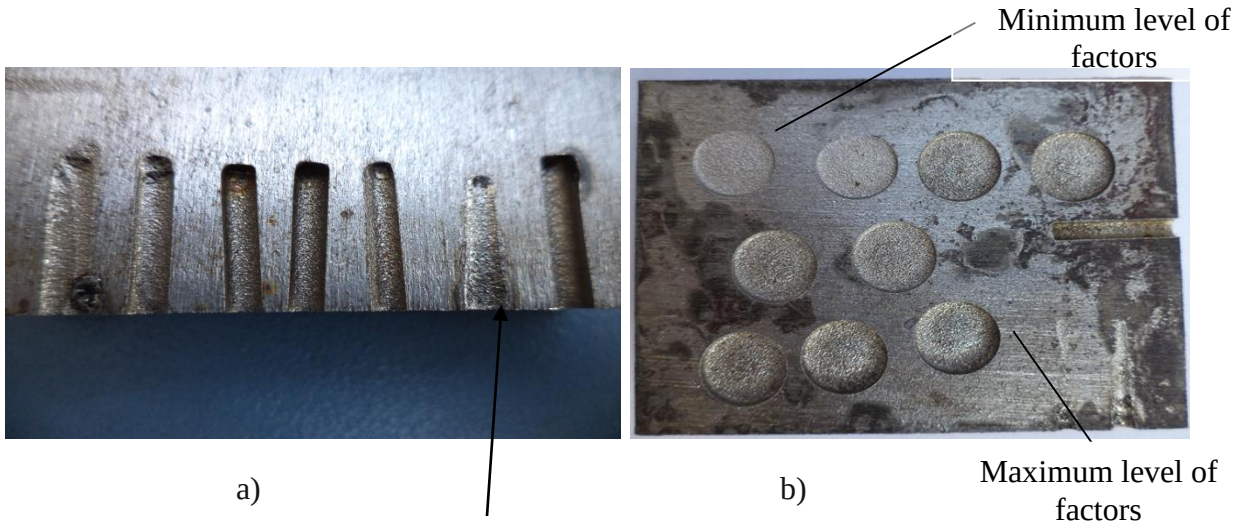

Figure 3.1: Pilot experimentation cuts for deciding levels of factors

3.2.4 Calculation of DOF

DOF denotes the number of the independent comparisons that can be made in any experiment. The number of factors considered for experimentation, their respective levels determine the total degree of freedom required for designing OA. Mathematically, DOF for each factor is calculated as,

DOF= *n*-1, where *n* is the level of each factor

Table 3.1: Factors and Degree of Freedom

S.No.	Factors	Units	Degree of Freedom
1	Current	A	2
2	Magnetic Strength	T	1
3	Tool Material	-	2
4	Powder	-	2
5	Concentration	g/L	2
6	Pulse On	µs	2

3.2.5 Selection of OA for PMEDM

Different factors considered for PEDM experiments and their levels are listed in Table 3.2.

Table 3.2: Factors and their levels for magnetic assisted PMEDM

Factors (unit)	Levels		
	Level 1	Level 2	Level 3
Current (A)	2	4	6
Magnetic field (T)	0.1	No	-
Tool material	Copper	C18000	Tungsten
Powder type	Tungsten	Copper	Titanium
Concentration (g/L)	2	4	6
Pulse-on time (µs)	50	100	200

Table 3.3: L18 OA for PMEDM

S.No	Magnetic strength (T)	Powder	Concentration (g/L)	Current (A)	Tool material	Pulse-on (µs)
1.	0.1	W	2	2	Cu	50
2.	0.1	W	4	4	W	100
3.	0.1	W	6	6	C18000	200
4.	0.1	Ti	2	2	Cu	50
5.	0.1	Ti	4	4	W	100
6.	0.1	Ti	6	6	C18000	200
7.	0.1	Cu	2	2	Cu	50
8.	0.1	Cu	4	4	W	100
9.	0.1	Cu	6	6	C18000	200
10.	No	W	2	2	Cu	50
11.	No	W	4	4	W	100
12.	No	W	6	6	C18000	200
13.	No	Ti	2	2	Cu	50
14.	No	Ti	4	4	W	100
15.	No	Ti	6	6	C18000	200
16.	No	Cu	2	2	Cu	50
17.	No	Cu	4	4	W	100
18.	No	Cu	6	6	C18000	200

Magnetic field in this case is produced by using bar magnets. Tool electrodes namely copper (Cu), tungsten (W) and C18000 alloy (Copper, Chromium, Nickel, Silicon (beryllium free)) of diameter 2.4mm are used. No interaction is considered in this case.

3.2.6 Analysis of Results

Analysis of results will be done by using Analysis of Variance ANOVA. ANOVA is analysis of variance. It is a statistical tool in which statistical models and their procedures are collected.

3.2.7 Response Characteristics

The response variables are listed below in the table

Table 3.4: Response Characteristics

Response Name	Response Type	Units
Material Removal Rate(MRR)	Higher the better	mm^3/min
Tool Wear Rate (TWR)	Lower the better	mm^3/min
Overcut	Lower the better	mm
Dimensional Change in tool	Lower the better	mm

3.3 Experimental Set Up

3.3.1 Machine Set Up

The experimentation work is performed on T-3822 M Electric Discharge Machine of Victory Electromech placed in non-traditional machining lab at Thapar University, Patiala. A separate arrangement is added for performing powder mixed EDM, a mild steel tank with inside dimensions as length 330 mm, breadth 180 mm, height 187 mm and plate thickness 3 mm. Capacity of the used tank is 9 L. A stirrer with the maximum speed of 1400 rpm is used to properly mix the powder in the dielectric medium.

Figure 3.2: Electric Discharge Machine (Courtesy: NTM lab, Thapar University, Patiala)

Figure 3.3: EDM machine with stirrer arrangement

Various input parameters varied on the EDM machine for present study are current and pulse on time. Levels of the input parameters are decided on the basis of pilot experimentation. Some parameters that are kept constant during the study are listed in Table 3.5.

Table 3.5: Constant input parameters

S. No	Parameter	Value
1	Voltage	135±5% V
2	Polarity	Positive
3	Machining time	8min
4	Pulse-off time	57µs
5	Dielectric medium	EDM oil

3.3.2 Workpiece and Tool Electrode Details

For experimentation, die steel material is used as workpiece with three different grades namely AISI D3, AISI H11 and AISI H13 for macro PMEDM. Before machining, workpiece is properly grinded from both the sides for maintain perfect alignment of workpiece with the tool electrode during machining. The chemical composition of the three workpiece used is given in Table 3.6. Three electrode materials used for machining purpose, namely copper,

tungsten and C18000 (alloy (Copper, Chromium, Nickel, Silicon (beryllium free)), all with diameter 2.4mm and 30mm length. The powders to be used are graphite, tungsten and titanium of grit size 320. Workpiece materials before machining and tool electrodes are shown in Fig. 3.4.

Table 3.6: Chemical composition of the workpiece materials

	Workpiece	H11	H13	D3
Percentage of chemical composition	Fe	91.3	89.9	84.4
	C	0.445	0.0741	2.26
	Si	0.923	1.15	0.383
	Mn	0.318	0.0323	0.494
	P	0.0391	0.0250	0.0326
	S	0.0050	0.0050	0.139
	Cr	5.27	5.13	11.9
	Mo	1.31	1.29	0.0100
	Ni	0.104	0.0766	0.129
	Co	0.0138	0.0116	0.0120
	Cu	0.128	0.119	0.0264
	Nb	0.0168	0.0175	0.0050
	Ti	0.0033	0.0084	0.0164
	V	0.0971	0.990	0.01700
	W	0.0547	0.0459	0.0882

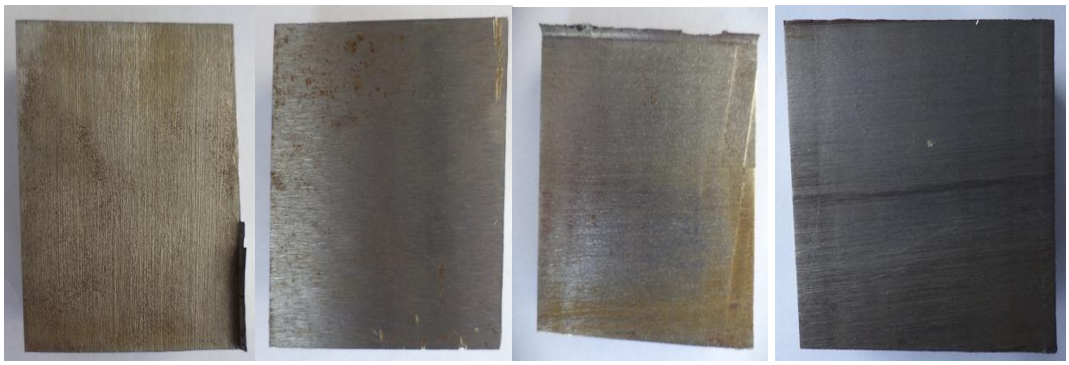

(a) AISID2 (b) AISID3 (c) AISI H11 (d) AISI H13

(i)Tungsten (ii) C18000

(iii)

Figure 3.4: Workpieces and tools to be used

3.3.3 Magnet Configuration and Details

For providing magnetic field bar magnets are used of strength 0.1T dimensions of 5mm x 2.5mm x 1.5mm are used. No separate fixture is designed for placing magnets. Magnets are kept directly on the workpiece material dipped in the dielectric medium.

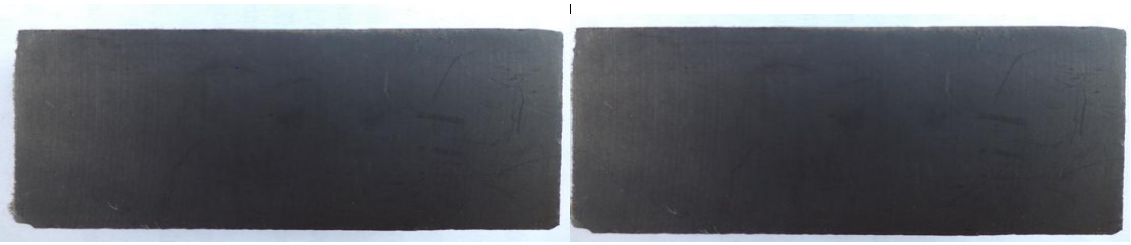

Figure 3.5: Magnets (0.1 T) used for present work

3.4 Measuring Equipment Used

Measuring test and equipment that are used in the present work are:

- Surface Grinder for grinding workpiece material
- Weighing machine with 0.001 g least count for weighing workpiece and tool material during experimentation for MRR and TWR measurement
- Profile Projector
- Metallurgical Microscope
- Optical Emission Spectrometer
- Measuring Microscope

(i) Profile Projector

(ii) Optical Emission Spectrometer

(iii) Metallurgical Microscope

iv) Measuring microscope

Figure 3.6: Instruments used for measurement

3.4.1 Profile Projector

Measurement of front wear and side wear of tool will be done by the Nikon Profile Projector (Model: V -10A) of Japan available in metrology lab of Thapar University of Patiala. Its least count is 0.001 mm.

3.4.2 Optical Emission Spectrometer

Chemical composition of the workpiece base materials and the composition of machined surfaces is measured using Optical Emission Spectrometer (Model: DV-6), Baird, USA. An

accuracy of 0.0001 % is achieved in the measurement. Argon gas is used for composition measurement process.

3.4.3 Metallurgical Microscope

The metallurgical microscope is used to analyze the metallurgical characteristics of the cuts made on the three workpieces used. Maginfication of 10× is used to see the cuts made to analyze their microstructure.

3.4.4 Measuring Microscope

Measuring microscope is used to measure the changes in tool after the machining has been done. It is used to measure side wear of tools used for the three workpieces.

CHAPTER – 4

Results and Analysis

4.1 Introduction

The effect of powder mixed in dielectric, concentration of powder, current, tool material and pulse-on duration is analyzed on MRR and TWR with and without using external magnetic field. Using Taguchi experimental design, L18 orthogonal array is used for the experiments using bar magnets of 0.1 T. Schematic representation of the tool and the workpiece is shown in Fig. 4.1. Tool is made in contact with the workpiece up to 10 mm in length and machining duration is kept 10 minutes.

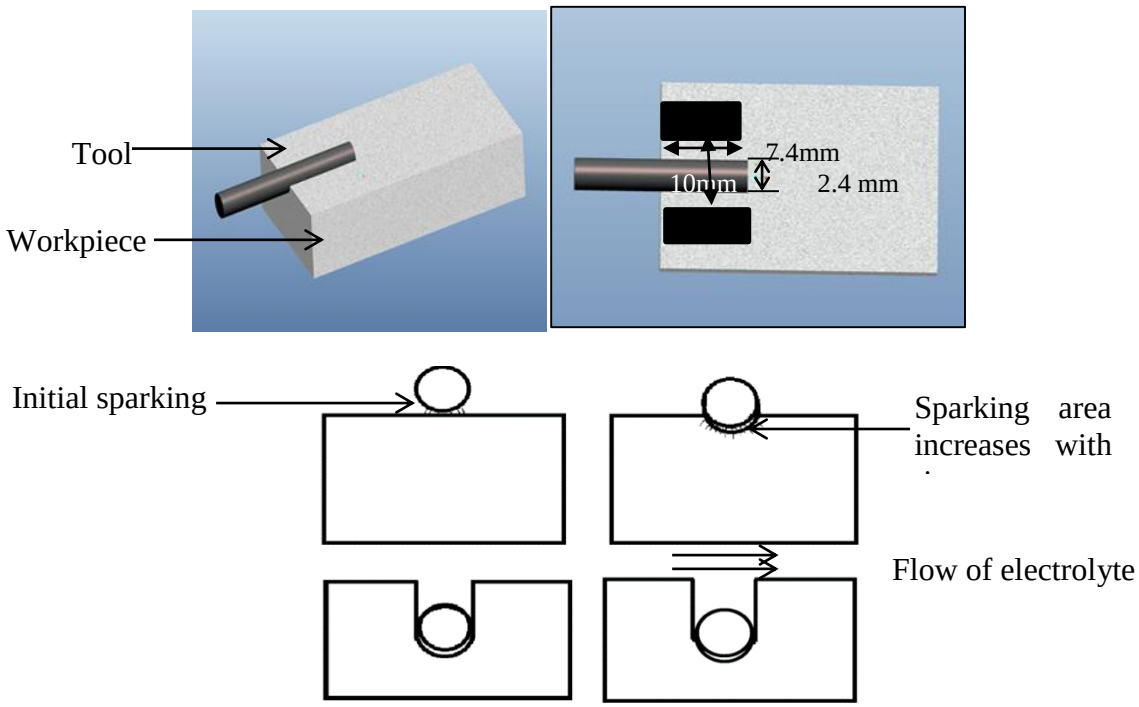

Figure 4.1: Schematic representation of tool and workpiece arrangement

MRR is larger the better type of response variable. MRR is calculated by measuring the initial and final weight of the workpiece using a weighing machine with least count of 0.001 g. For each experiment MRR is calculated using the Eq. (4.1).

$$\text{MRR} = \frac{W_i - W_f}{t} \text{ g/min} \quad (4.1)$$

Where W_i = Initial weight of the workpiece (g)

W_f = Final weight of the workpiece after the experimentation (g)

t = Machining time (min)

4.2 Results and Analysis of MRR

4.2.1 MRR for H11 Workpiece

The results for MRR calculated by the Eq. (4.1) are given in Table 4.1.

Table 4.1: Results of MRR for H11 workpiece

Exp. No	Magnetic strength	Powder	Concentration (g/L)	Current (A)	Tool material	Pulse-on (µs)	MRR (g/min)
1	With	W	2	2	Cu	50	0.05200
2	With	W	4	4	W	100	0.00533
3	With	W	6	6	C18000	200	0.01333
4	With	Ti	2	2	W	100	0.01200
5	With	Ti	4	4	C18000	200	0.02733
6	With	Ti	6	6	Cu	50	0.02000
7	With	Gr	2	4	Cu	200	0.06000
8	With	Gr	4	6	W	50	0.00800
9	With	Gr	6	2	C18000	100	0.01000
10	Without	W	2	6	C18000	100	0.01733
11	Without	W	4	2	Cu	200	0.02533
12	Without	W	6	4	W	50	0.00666
13	Without	Ti	2	4	C18000	50	0.03133
14	Without	Ti	4	6	Cu	100	0.02733
15	Without	Ti	6	2	W	200	0.01200
16	Without	Gr	2	6	W	200	0.00533
17	Without	Gr	4	2	C18000	50	0.02466
18	Without	Gr	6	4	Cu	100	0.05866

The results are analyzed using ANOVA. It helps in identifying the important process parameters affecting the response. Results for mean of MRR calculated at 90% confidence level are given in Table 4.2.

Table 4.2: ANOVA table for MRR of H11workpiece

Parameter	Symbol	DOF	SS	Variance	*F*-value	*p*-value	PC
Magnetic strength (T)	*A*	1	0.00000	0.00000	0.0	0.989	0
Powder	*B*	2	0.000201	0.000101	0.91	0.452	3.822
Concentration (g/L)	*C*	2	0.000383	0.000192	1.73	0.255	7.284
Current (A)	*D*	2	0.000802	0.000401	3.63	0.093	15.252
Tool material	*E*	2	0.003192	0.001596	14.44	0.005	60.707
Pulse-on time (μs)	*F*	2	0.000017	0.000008	0.08	0.927	0.323
Residual error		6	0.000663	0.000111			12.60
Total		17	0.005258				

(Note: For 90% CI, $F_{critical(2,6)} = 3.46$, $F_{critical(1,6)} = 3.78$, PC= percentage contribution)

The principle followed by *F*-test is that, greater is the *F* value for an input parameter the larger is its effect on output parameter. ANOVA (Table 4.2) shows the results of MRR of PMEDM with and without the use of magnetic strength. Under such experimental conditions the two factors i.e. tool material (*F* value 15.56) and current (*F* value 4.27) are found to be significant. The highest MRR is achieved using copper tool followed by C18000 alloy and, the tungsten tool is found to give the least MRR among the three tool materials used as shown in Fig. 4.2. The following pattern is observed due to difference in their electrical conductivities as the electrical conductivity of copper is found to be the highest. Thus MRR achieved by the tungsten is very low due to its poor electrical conductivity. The second significant factor is the current having *F* value as 4.27. Initially the MRR is found to increase with increase in current till the current reaches value of 4 A after that the MRR begins to decrease when current approaches the value of 6 A. The reason behind this may be due to the situation of arcing rather than spark and also due to the fact that as the current increases the downward movement of tool becomes fast as a result there is not enough time for the removal of debris and the suspended powder which of arcing. The next highest value of *F* is for the concentration 1.58 g/L. MRR is found to decrease with concentration because as the amount of powder suspended in the dielectric increases, the circulation of the powder particles is not enough also with increase in concentration above a certain level arcing occurs as the effective gap between the tool and the workpiece decreases with increase in concentration. The performance of factors at various levels is clearly shown in Fig. 4.1. In the Fig. 4.1 abscissa represents levels of various factors and ordinate represents MRR (g/min). The center line represents mean value of the levels.

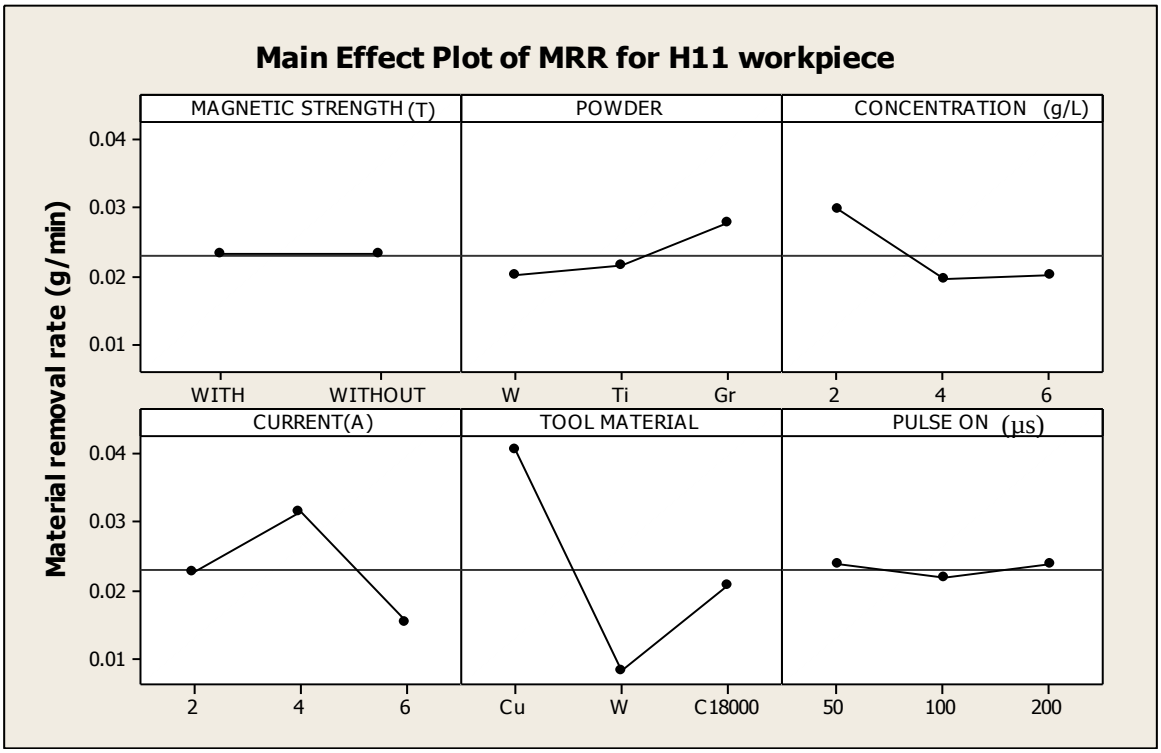

Figure 4.2: Main effects plot of MRR for H11 work piece

The highest MRR is achieved on suspension of graphite powder as its density and electrical resistivity is least among the all three. The MRR obtained by titanium is slightly higher as compared to tungsten but less than graphite as the electrical resistivity and density of titanium is less than tungsten but higher than graphite. Thus less is the density and electrical resistivity of a powder more is the MRR achieved by it till the concentration reaches an optimum level. The effect of pulse on duration and magnetic strength have not been found to be very significant and have been ranked as 5^{th} and 6^{th} respectively based on their *F* values. The MRR is found to increase on increasing the pulse on duration as more melting and vaporization of workpiece will take place when time for which the energy supplied increases. Magnetic strength has least effect on the MRR. The MRR obtained under the influence of magnetic field is slightly less than that obtained without the use of magnets but overall the effect of this factor is negligible. Based on the ANOVA the factors are assigned ranks and are listed in Table 4.3.

Table 4.3: Response table for MRR of H11workpiece

Level	Magnetic strength (T)	Powder	Concentration (g/L)	Current (A)	Tool material	Pulse-on time (µs)
1	0.023110	0.01997	0.029665	0.022665	0.040553	0.023775
2	0.023181	0.021665	0.019663	0.031552	0.008220	0.021775
3		0.027775	0.020108	0.015220	0.020663	0.023887
Delta	0.000071	0.007778	0.010002	0.016332	0.032333	0.002112
Rank	6	4	3	2	1	5

Optimal design

In the experimental study, the mean effect plots (Fig. 4.1.) is used to evaluate the mean MRR at optimal trial conditions. From Table 4.2 considering higher F-value and corresponding percentage contribution two parameters are found to be significant tool material and current. The level of these factors which gives the maximum MRR are noted from main effect plot (Fig. 4.1) and the corresponding MRR for D_2, E_1 is directly obtained from Table 4.3. Maximum value of these parameters is selected because MRR is the higher the better type of response variable. Desired mean in this case is estimated as:

$\mu_{D_2,E_1} = \overline{D_2} + \overline{E_1} - \overline{T}$ = 0.031552 + 0.040553 – 0.0231456 = 0.0489594 g/min

Confidence interval

$$CI = \sqrt{\frac{F_{\alpha,\nu_1,\nu_2} V_e}{n_{eff}}}$$

Where F_{α,ν_1,ν_2} = *F* ratio

α = 0.1 (risk)

Confidence = 1 – α

ν_1 = DOF for mean (always 1)

ν_2 = Total DOF (=17)

$\overline{T}$ = Average of all experimental trials

n_{eff} = Number of tests under that condition using the participating factors

$$n_{eff} = \frac{\mathrm{N}}{1+DOF_{D,E}} = \frac{18}{1+4} = 3.6$$

N is the number of trial in the experiment

V_e = Variance of error

$$CI = \sqrt{\frac{3.03 \times 0.000111}{3.6}} = \pm 0.00966$$

Thus the optimum value of MRR is given by (0.0489594 ± 0.00966) g/min.

The workpiece samples from different views of H11 after each cut is shown in Fig. 4.2. Fig 4.2 (a) shows top view which indicates the length of cut. In Fig. 4.2 (b) shows the side views where depth till which machining has been completed can be seen.

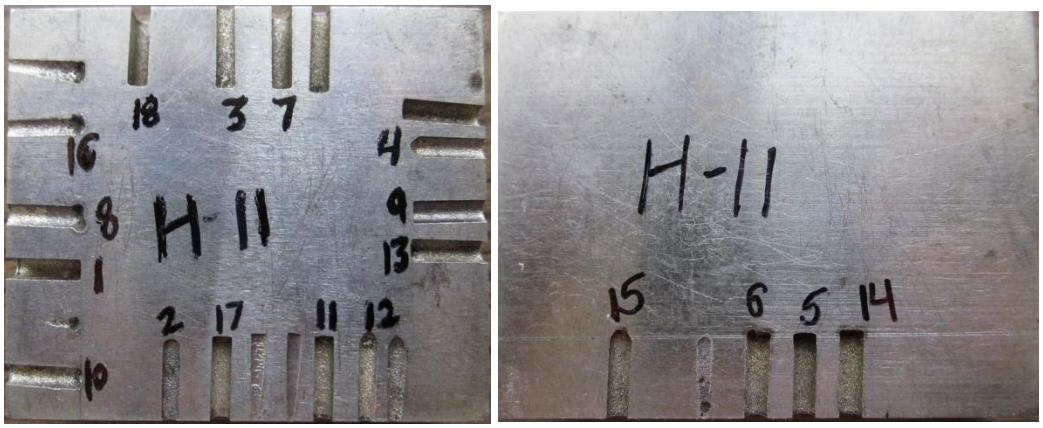

(a)

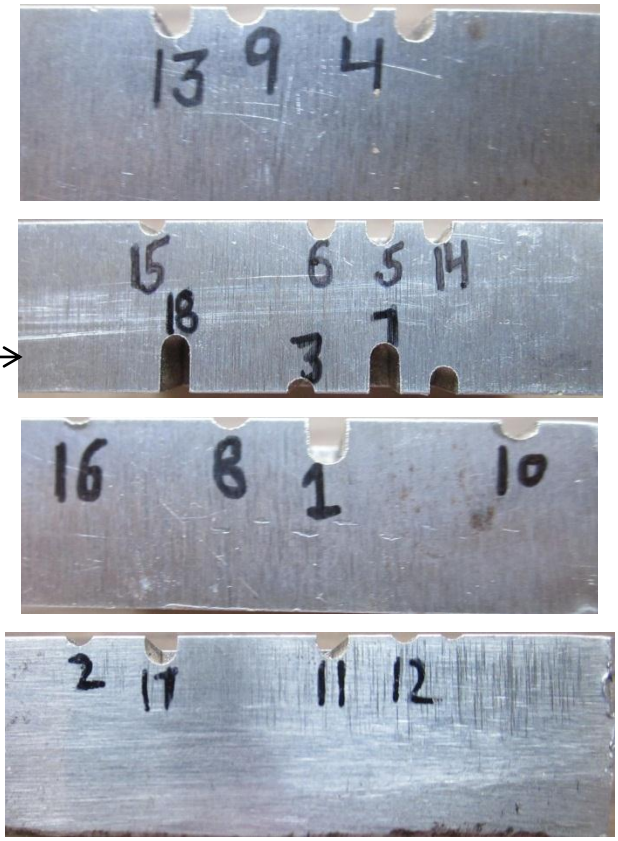

Trial 18 shows maximum depth (W/o magnet, Gr-powder, 6 g/L, 4 A, 100 µs)

(b)

Figure 4.3: (a) Top view of H11 workpiece (b) Side views of H11 workpiece

4.2.2 MRR for H13 Workpiece

The results of MRR for H13 workpiece are calculated and are given in Table 4.4.

Table 4.4: Results of MRR for H13 workpiece

Expt. No	Magnetic strength	Powder	Concentration (g/L)	Current (A)	Tool material	Pulse-on (µs)	MRR (g/min)
1	With	W	2	2	Cu	50	0.062
2	With	W	4	4	W	100	0.007
3	With	W	6	6	C18000	200	0.024
4	With	Ti	2	2	W	100	0.015
5	With	Ti	4	4	C18000	200	0.028
6	With	Ti	6	6	Cu	50	0.040
7	With	Gr	2	4	Cu	200	0.080
8	With	Gr	4	6	W	50	0.040
9	With	Gr	6	2	C18000	100	0.021
10	Without	W	2	6	C18000	100	0.045
11	Without	W	4	2	Cu	200	0.024
12	Without	W	6	4	W	50	0.013
13	Without	Ti	2	4	C18000	50	0.043
14	Without	Ti	4	6	Cu	100	0.050
15	Without	Ti	6	2	W	200	0.005
16	Without	Gr	2	6	W	200	0.060
17	Without	Gr	4	2	C18000	50	0.035
18	Without	Gr	6	4	Cu	100	0.082

These results are analyzed using ANOVA. Results for mean of MRR calculated at 90% confidence level are given in Table 4.5. Based on the results obtained three factors are found to be significant namely the tool material followed by concentration and type of powder respectively.

Table 4.5: ANOVA table for MRR of H13 workpiece

Parameter	Symbol	DOF	SS	Variance	*F*-value	*p*-value	PC
Magnetic strength (T)	*A*	1	0.000012	0.000012	0.17	0.696	0.368
Powder	*B*	2	0.000224	0.000112	1.59	0.280	6.885
Concentration (g/L)	*C*	2	0.000640	0.000320	4.54	0.063	19.674
Current (A)	*D*	2	0.000505	0.000253	3.59	0.095	15.524
Tool material	*E*	2	0.001410	0.000705	10.01	0.012	43.344
Pulse on time (µs)	*F*	2	0.000039	0.000020	0.28	0.766	1.198
Residual error		6	0.000423	0.000070			13.00s
Total		17	0.003253				

(Note: For 90% CI, $F_{critical(2,6)} = 3.46$, $F_{critical(1,6)} = 3.78$, PC= percentage contribution)

Among the three tool materials the highest MRR is achieved by using copper tool followed by C18000 alloy and tungsten. These results are shown in the Fig. 4.3. The order followed is same as the electrical conductivities of the respective materials, with the material having the highest conductivity giving the highest MRR and the one with least value of conductivity giving least MRR. In the category of the powders used, the highest MRR is achieved using graphite powder having highest conductivity and being least dense. The MRR achieved using titanium and tungsten varies slightly, with titanium giving slightly higher MRR. Second significant factor is identified as powder concentration having *F* value as 4.54. MRR is found to decrease with increase in concentration as highest MRR is achieved at concentration of 2 g/L this is probably because of decrease in the gap between the tool electrodes due to increase of amount of powder suspended in the dielectric, MRR at concentrations 4 g/L and 6 g/L are more or less same as shown in Fig. 4.3. In the Fig. 4.3 abscissa represents levels of various factors and ordinate represents MRR (g/min). The center line represents mean value of the levels.

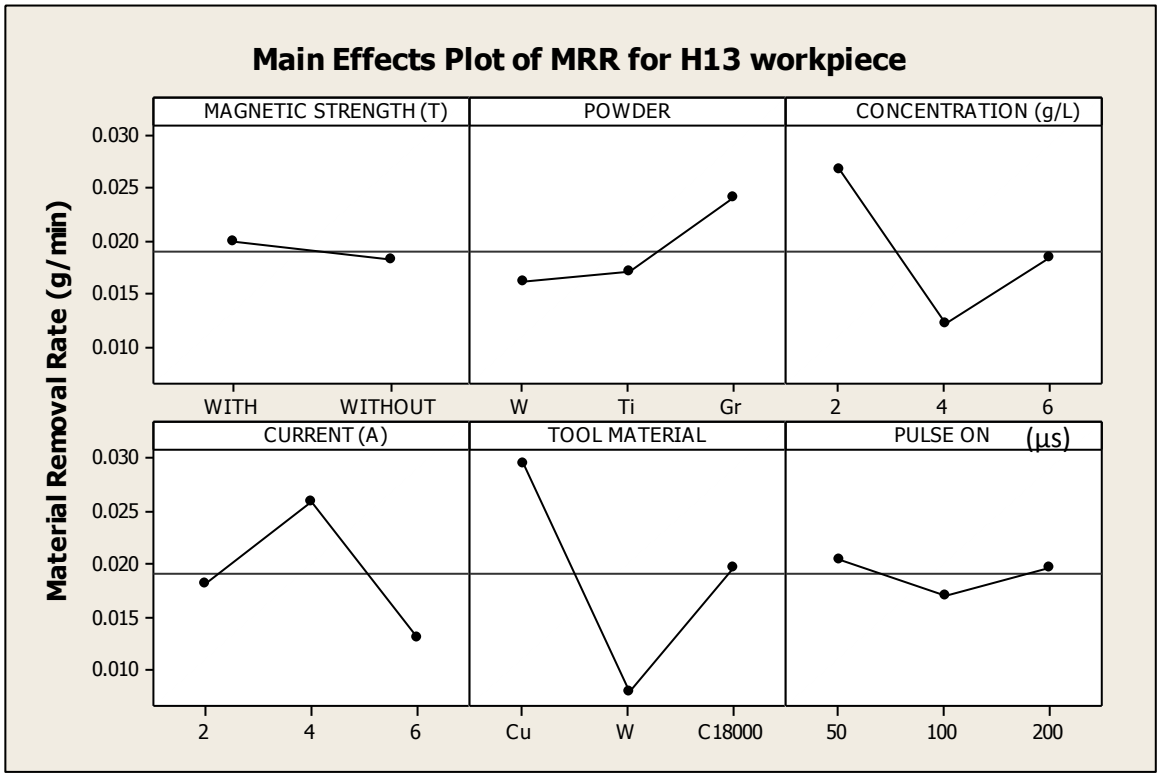

Figure 4.4: Main effects plot of MRR (H13) work piece

The reason behind this may be that higher is the amount of powder in the dielectric more presence of powder and debris in the inter electrode gap thus which increases the chance of arcing and hence decreases the MRR. Third significant factor is the current; MRR is found to increase with increase in current till 4 A after that MRR decreases because probably due to increase in current the movement of tool becomes quick and thus not giving enough time for sufficient removal of debris thus leading to arcing as a result giving less MRR. Magnetic strength and pulse on duration is found to have negligible effect on MRR as depicted by the main plot graphs and also the *F* values. MRR attained at the three pulse on durations are more or less same. Based on their significance of affecting MRR these factors are ranked, and these ranks are given in Table 4.6.

Table 4.6: Response table for MRR of H13workpiece

Level	Magnetic strength (T)	Powder	Concentration (g/L)	Current (A)	Tool material	Pulse-on (µs)
1	0.019849	0.016118	0.026663	0.018220	0.029552	0.020452
2	0.018226	0.016997	0.012105	0.025895	0.007897	0.016997
3		0.023997	0.018343	0.012997	0.019663	0.019663
Delta	0.001623	0.007878	0.014558	0.012898	0.021655	0.003455
Rank	6	4	2	3	1	5

Optimal design

In the experimental study, the mean effect plots (Fig. 4.3. are used to evaluate the mean MRR at optimal trial conditions. From Table 4.5 considering higher F-value and corresponding percentage contribution three parameters are found to be significant tool material followed by concentration and type of powder. The level of these factors which gives the maximum MRR are noted from main effect plot (Fig. 4.3) and the corresponding MRR for C_1, D_2 and E_1 is directly obtained from Table 4.6. Maximum value of these parameters is selected because MRR is the higher the better type of response variable. Desired mean in this case is estimated as:

$\mu_{B_3,C_1,E_1} = \overline{C_1} + \overline{D_2} + \overline{E_1} - \overline{T}$ = 0.023997 + 0.025895 + 0.029552 – 0.037444

= 0.087336 g/min

Confidence interval

$$CI = \sqrt{\frac{F_{\alpha,\nu_1,\nu_2} V_e}{n_{eff}}}$$

Where F_{α,ν_1,ν_2} = *F* ratio

α = 0.1 (risk)

Confidence = 1 – α

ν_1 = DF for mean (always 1)

ν_2 = Total DOF (=17)

$\overline{T}$ = Average of all experimental trials

n_{eff} = Number of tests under that condition using the participating factors

$$n_{eff} = \frac{\text{N}}{1+DOF_{B,C,E}} = \frac{18}{1+6} = 2.571$$

N is the number of trial in the experiment

V_e = Variance of error

$$CI = \sqrt{\frac{3.03 \times 0.000070}{2.571}} = \pm 0.0090827$$

Thus the optimum value of MRR is given by (0.08733± 0.0090827) g/min.

The workpiece samples from different views of H11 after each cut is shown in Fig. 4.4. Fig 4.4 (a) shows top view which indicates the length of cut. In Fig. 4.4 (b) shows the side views where depth till which machining has been completed can be seen.

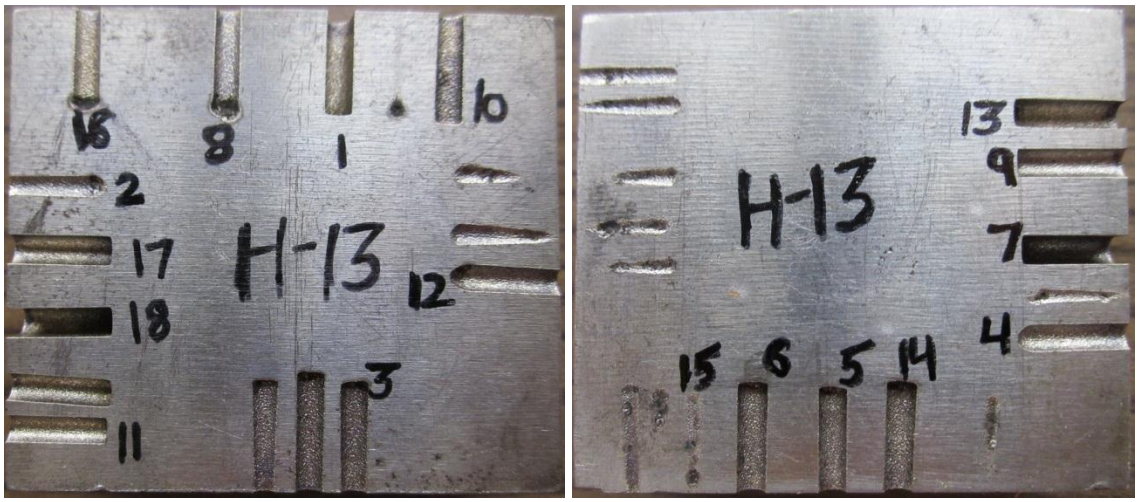

(a)

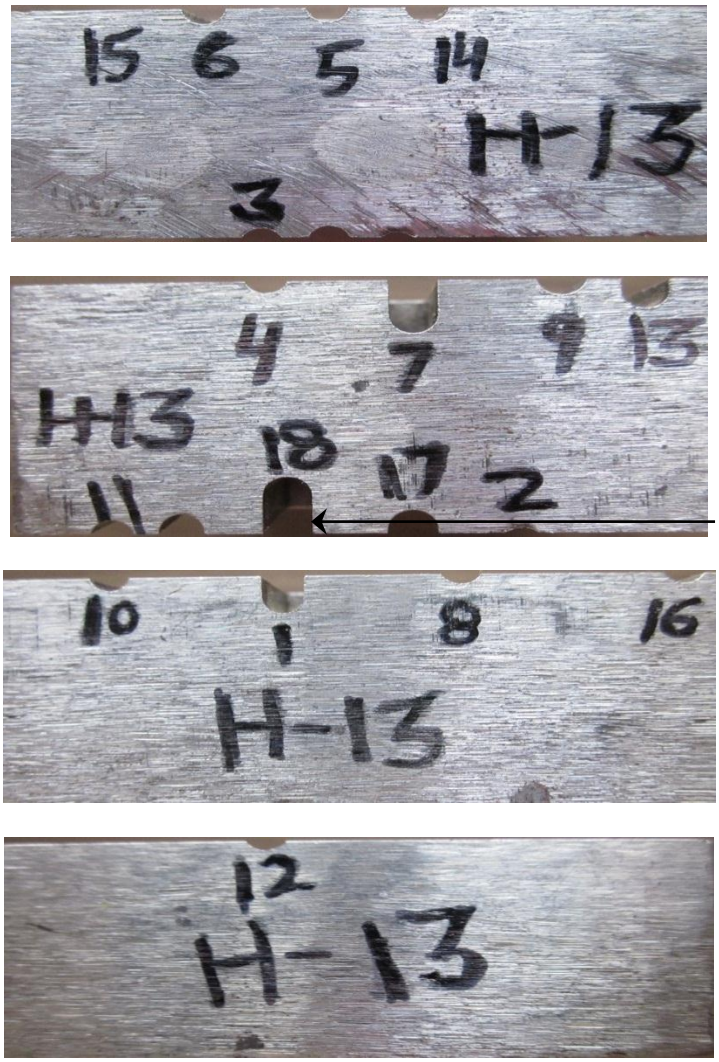

Trial 18 shows maximum depth (W/o magnet, Gr-powder, 6 g/L, 4 A, 100 µs)

(b)

Figure 4.5: (a) Top view of H11 workpiece (b) Side views for H13 workpiece

4.2.3 MRR for D3 Workpiece

Results for MRR for D3 workpiece are given in Table 4.7.

Table 4.7: Results of MRR for D3 workpiece

Expt. No	Magnetic strength	Powder	Concentration (g/L)	Current (A)	Tool material	Pulse-on (µs)	MRR (g/min)
1	With	W	2	2	Cu	50	0.05
2	With	W	4	4	W	100	0.0066
3	With	W	6	6	C18000	200	0.0133
4	With	Ti	2	2	W	100	0.0253
5	With	Ti	4	4	C18000	200	0.028
6	With	Ti	6	6	Cu	50	0.014
7	With	Gr	2	4	Cu	200	0.0613
8	With	Gr	4	6	W	50	0.0113
9	With	Gr	6	2	C18000	100	0.0293
10	Without	W	2	6	C18000	100	0.0113
11	Without	W	4	2	Cu	200	0.008
12	Without	W	6	4	W	50	0.0073
13	Without	Ti	2	4	C18000	50	0.0366
14	Without	Ti	4	6	Cu	100	0.0214
15	Without	Ti	6	2	W	200	0.014
16	Without	Gr	2	6	W	200	0.01
17	Without	Gr	4	2	C18000	50	0.0293
18	Without	Gr	6	4	Cu	100	0.0573

These results are analyzed using ANOVA at 90% confidence level and is given in Table 4.8. Based on the analysis three factors are found to be significant. The most significant factor is found as tool material with *F* value 7.22 and second significant factor is the current.

Table 4.8: ANOVA table for MRR of D3 workpiece

Parameter	Symbol	DOF	SS	Variance	*F*-value	*p*-value	PC
Magnetic strength (T)	*A*	1	0.000107	0.000107	0.98	0.360	2.10
Powder	*B*	2	0.000874	0.000437	4.00	0.079	17.184
Concentration (g/L)	*C*	2	0.000696	0.000348	3.19	0.114	13.684
Current (A)	*D*	2	0.001148	0.000574	5.26	0.048	22.57
Tool material	*E*	2	0.001578	0.000789	7.22	0.025	31.026
Pulse-on time (μs)	*F*	2	0.000026	0.000013	0.12	0.888	0.511
Residual error		6	0.000655	0.000109			12.878
Total		17	0.005086				

(Note: For 90% CI, $F_{critical(2,6)} = 3.46$, $F_{critical(1,6)} = 3.78$, PC= percentage contribution)

The highest MRR is achieved using copper as the tool material as it has highest electrical conductivity and least MRR is given by tungsten having least conductivity. In the case of current initially MRR was found to increase with increase in current till 4 A after that it decreases as the current reaches value of 6 A, this is because as the current increases so does tendency of arcing. Third significant factor is the powder suspended in the dielectric. The variation of MRR with each of the process parameter is shown in Fig. 4.3. In the Fig. 4.5 abscissa represents levels of various factors and ordinate represents MRR (g/min). The center line represents mean value of the levels.

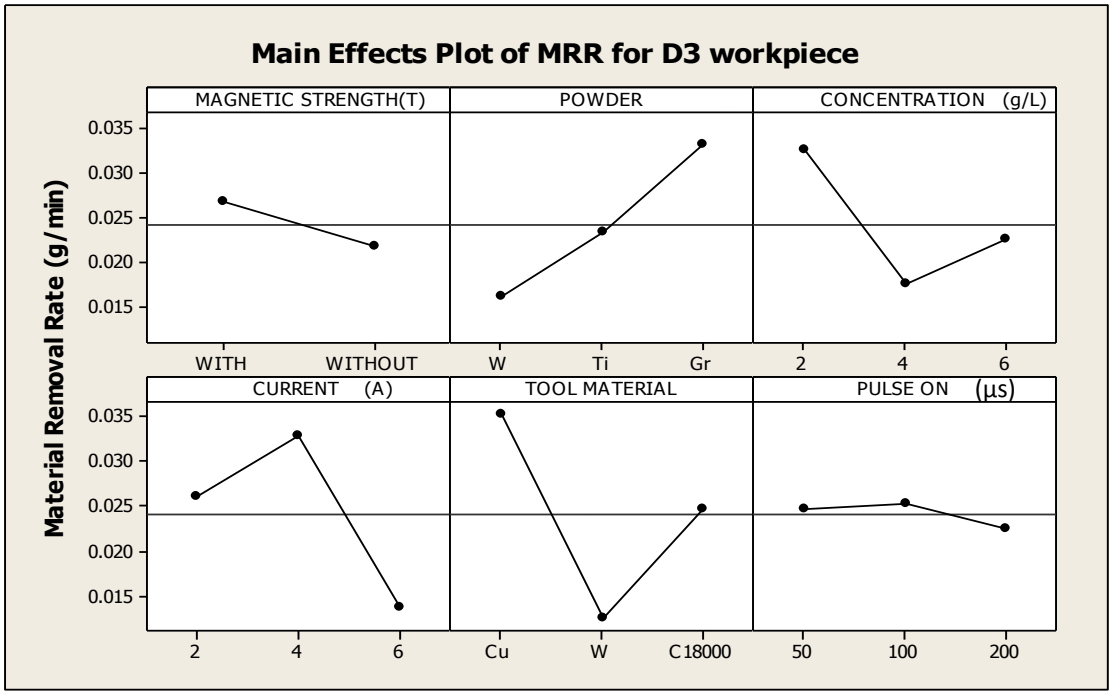

Figure 4.6: Main effects plot of MRR for D3 workpiece

Use of graphite gave the highest MRR as it has highest electrical conductivity compared to other two powders used. Fourth significant is the concentration of the powders. Best results were obtained at concentration of 2 g/L. Magnetic strength and pulse on duration does not have much effect on the MRR however MRR is higher by using external magnetic field compared to those conducted without magnetic field this could be due to the application of external magnetic strength that helps in easy removal of debris. Based on their significance these factors are assigned rank and these ranks are listed in Table 4.9.

Table 4.9: Response table for MRR of D3 workpiece

Level	Magnetic strength (T)	Powder	Concentration (g/L)	Current (A)	Tool material	Pulse-on (µs)
1	0.02657	0.01608	0.03242	0.02598	0.03533	0.02475
2	0.02169	0.02322	0.01743	0.03285	0.01242	0.02520
3		0.03308	0.02253	0.01355	0.02463	0.02243
Delta	0.00488	0.01700	0.01498	0.01930	0.02292	0.00277
Rank	5	3	4	2	1	6

Optimal design

In the experimental study, the mean effect plots (Fig. 4.5.) are used to evaluate the mean MRR at optimal trial conditions. From Table 4.8 considering higher F-value and corresponding percentage contribution three parameters are found to be significant tool material followed by current and type of powder. The level of these factors which gives the maximum MRR are noted from main effect plot (Fig. 4.3) and the corresponding MRR for B_3, D_2 and E_1 is directly obtained from Table 4.9. Maximum value of these parameters is selected because MRR is the higher the better type of response variable. Desired mean in this case is estimated as:

$\mu_{B_3,D_2,E_1} = \overline{B_3} + \overline{D_2} + \overline{E_1} - \overline{T}$ = 0.03308 + 0.03285 + 0.03533 – 0.024123

= 0.077137 g/min

Confidence interval

$$CI = \sqrt{\frac{F_{\alpha,\nu_1,\nu_2} V_e}{n_{eff}}}$$

Where F_{α,ν_1,ν_2} = *F* ratio

α = 0.1 (risk)

Confidence = 1 – α

ν_1 = DF for mean (always 1)

ν_2 = Total DOF (=17)

$\overline{T}$ = Average of all experimental trials

n_{eff} = Number of tests under that condition using the participating factors

$$n_{eff} = \frac{N}{1+DOF_{B,D,E}} = \frac{18}{1+6} = 2.571$$

N is the number of trial in the experiment

V_e = Variance of error

$$CI = \sqrt{\frac{3.03 \times 0.000109}{2.571}} = \pm 0.011340$$

Thus the optimum value of MRR is given by (0.077137 ± 0.011340) g/min.

The workpiece samples from different views of D3 after each cut is shown in Fig. 4.6. Fig 4.6 (a) shows top view which indicates the length of cut. In Fig. 4.6 (b) shows the side views where depth till which machining has been completed can be seen.

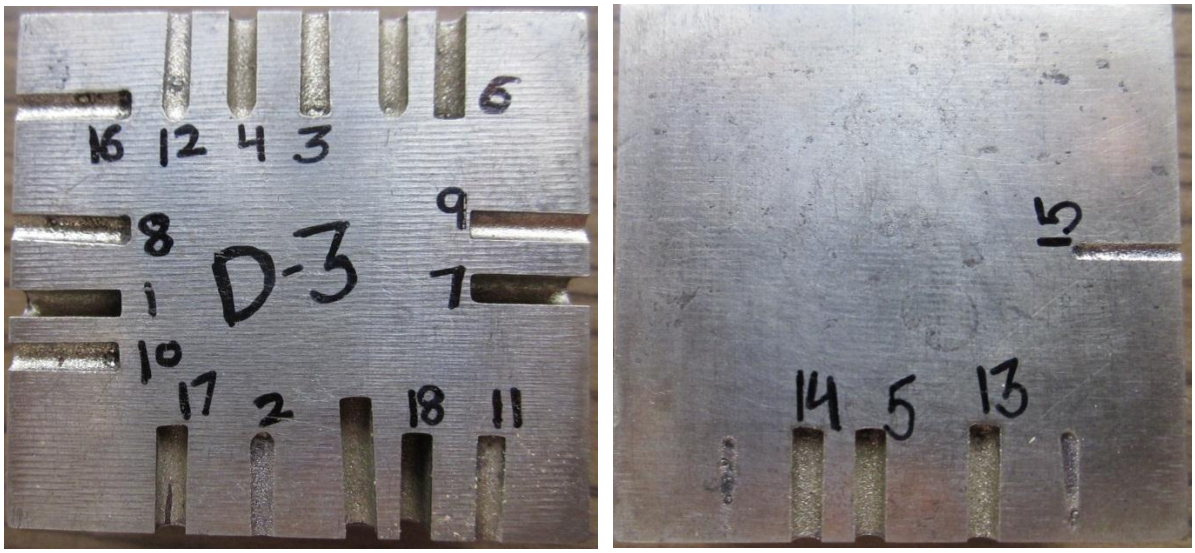

(a)

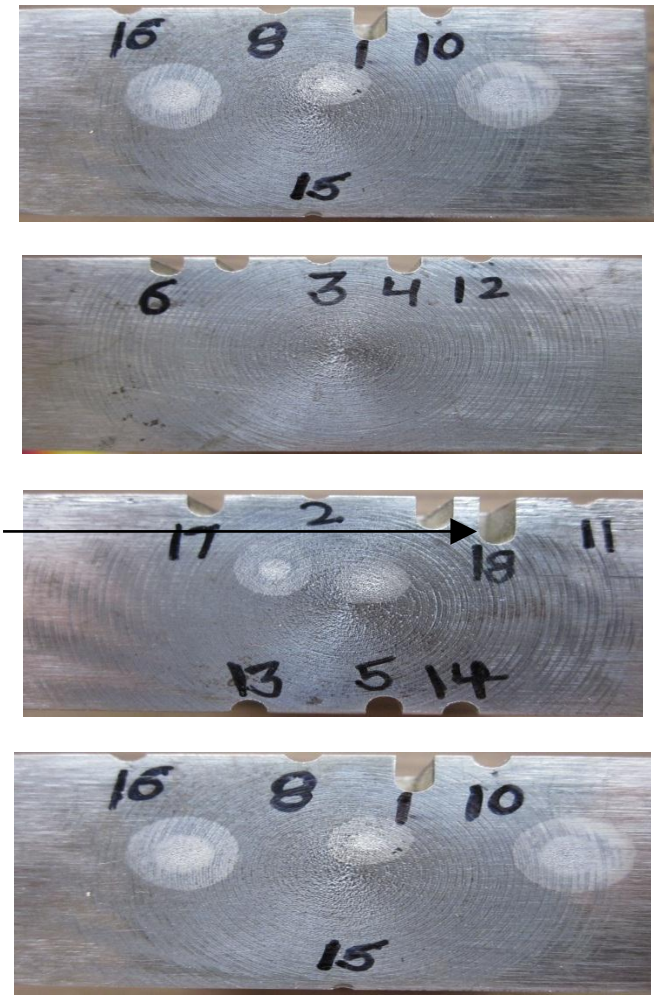

Trial 18 shows maximum depth (W/o magnet, Gr-powder, 6 g/L, 4 A, 100 µs)

Figure 4.7: (a) Top view of D3 workpiece (b) Side views for D3 workpiec

4.3 Results and Analysis of TWR

The effect of powder mixed in dielectric, concentration of powder, current, tool material and pulse on duration on tool wear rate is analyzed with and without using external magnetic field on tool wear rate, using Taguchi experimental design. L18 orthogonal array is used for the experiments using bar magnets of 0.1 T. It is smaller the better type of response variable. TWR is calculated by measuring the initial and final weight of the tool using a weighing machine with least count of 0.001 g. For each experiment TWR is calculated using the following Eq. (4.2)

$$\text{TWR}= \frac{W_{i-}W_f}{t} \text{ g/min} \quad (4.2)$$

Where W_i = Initial weight of the workpiece (g)

W_f = Final weight of the workpiece after the experimentation (g)

t = Machining time (min)

4.3.1 TWR for H11 workpiece

Results for mean TWR for H11 workpiece are given in Table 4.10

Table 4.10: Results of TWR for H11 workpiece

Expt. No	Magnetic strength (T)	Powder	Concentration (g/L)	Current (A)	Tool material	Pulse-on (µs)	TWR (g/min)
1	With	W	2	2	Cu	50	0.00067
2	With	W	4	4	W	100	0.00006
3	With	W	6	6	C18000	200	0.00066
4	With	Ti	2	2	W	100	0.00006
5	With	Ti	4	4	C18000	200	0.00067
6	With	Ti	6	6	Cu	50	0.00067
7	With	Gr	2	4	Cu	200	0.00060
8	With	Gr	4	6	W	50	0.00067
9	With	Gr	6	2	C18000	100	0.00670
10	Without	W	2	6	C18000	100	0.00133
11	Without	W	4	2	Cu	200	0.00067
12	Without	W	6	4	W	50	0.00006
13	Without	Ti	2	4	C18000	50	0.00200
14	Without	Ti	4	6	Cu	100	0.00067
15	Without	Ti	6	2	W	200	0.00006
16	Without	Gr	2	6	W	200	0.00067
17	Without	Gr	4	2	C18000	50	0.00067
18	Without	Gr	6	4	Cu	100	0.00133

These results of TWR are analyzed using ANOVA at 90% confidence level and result is given in Table 4.11.

Table 4.11: ANOVA table for TWR of H11 workpiece

Parameter	Symbol	DOF	SS	Variance	*F* -value	PC
Magnetic strength (T)	*A*	1	0.00000036	0.00000036	0.18	0.914
Powder	*B*	2	0.000004	0.000002	1	10.162
Concentration (g/L)	*C*	2	0.000004	0.000002	0.87	10.162
Current (A)	*D*	2	0.000002	0.000001	0.51	5.081
Tool material	*E*	2	0.000011	0.000005	2.42	27.947
Pulse-on time (µs)	*F*	2	0.000005	0.000002	1.06	12.703
Residual error		6	0.000013	0.000002		33.028
Total		17	0.00003936			

(Note: For 90% CI, $F_{critical(2,6)} = 3.46$, $F_{critical(1,6)} = 3.78$, PC= percentage contribution)

Based on this analysis conducted, most significant factor is tool material. The highest tool wear is observed with C18000 alloy followed by copper tool. Tungsten tool has been found to give the least tool wear. This is because of difference in the melting points of the tool materials. Thoriated tungsten having 2% thorium has the highest melting point 3695 K hence it gives the lowest tool wear whereas there is not much difference in the melting points of opper and C18000 alloy the melting point of pure copper is approximately 1357 K and C18000 is 1311 K approx. Thus the tool wear of C18000 is slightly higher than that of copper. Tool wear of a particular material also depends on the density of that material; the density of copper is 8.75 g/cm^3 of alloy C18000 is 8.81 g/cm^3 whereas the density of the thoriated tungsten is almost double of them hence tool wear observed in the tungsten used is almost negligible. Thermal conductivity of copper at 100 ºC is about 400 W/m-K and of alloy C18000 is 208 W/m K and that of tungsten is 173 W/m-K although tool wear is found to decrease with increase in thermal conductivity but in this case it is not a dominating factor. Pulse on duration is the second factor affecting the tool wear rate after the tool material. Tool wear rate increases with pulse on duration till 100 µs after that tool wear rate begins to decrease as the level reaches tool 200 µs, the reason behind this may be that as the pulse on durations increase the layer of carbon deposited on the tool due to decomposition of dielectric and from melting if workpiece also increases as a result it protects the tool from wear. Concentration is the third factor affecting the tool wear rate. The tool wear rate decreases with increase in concentration. This may be because as the amount of powder is increased in the dielectric the spark is diffused homogenously and also it widens the plasma channel. The fourth factor affecting the tool wear rate is the type of powder suspended in the dielectric, maximum tool wear is observed when the graphite is suspended in the dielectric as it has maximum conductivity whereas titanium and tungsten powder suspension gives almost the

same tool wear rate. The next factor affecting the tool wear rate is current, the tool wear rate is found to decrease with increase in current the reason behind this may be combined effect of current and magnetic field as the current increases to 6 A the magnetic field produced increases and copper particles being diamagnetic are repelled more strongly thus decreasing the tool wear. The variation of tool wear with different process parameters are shown in Fig. 4.7. In the Fig. 4.7 abscissa represents levels of various factors and ordinate represents TWR (g/min). The center line represents mean value of the levels.

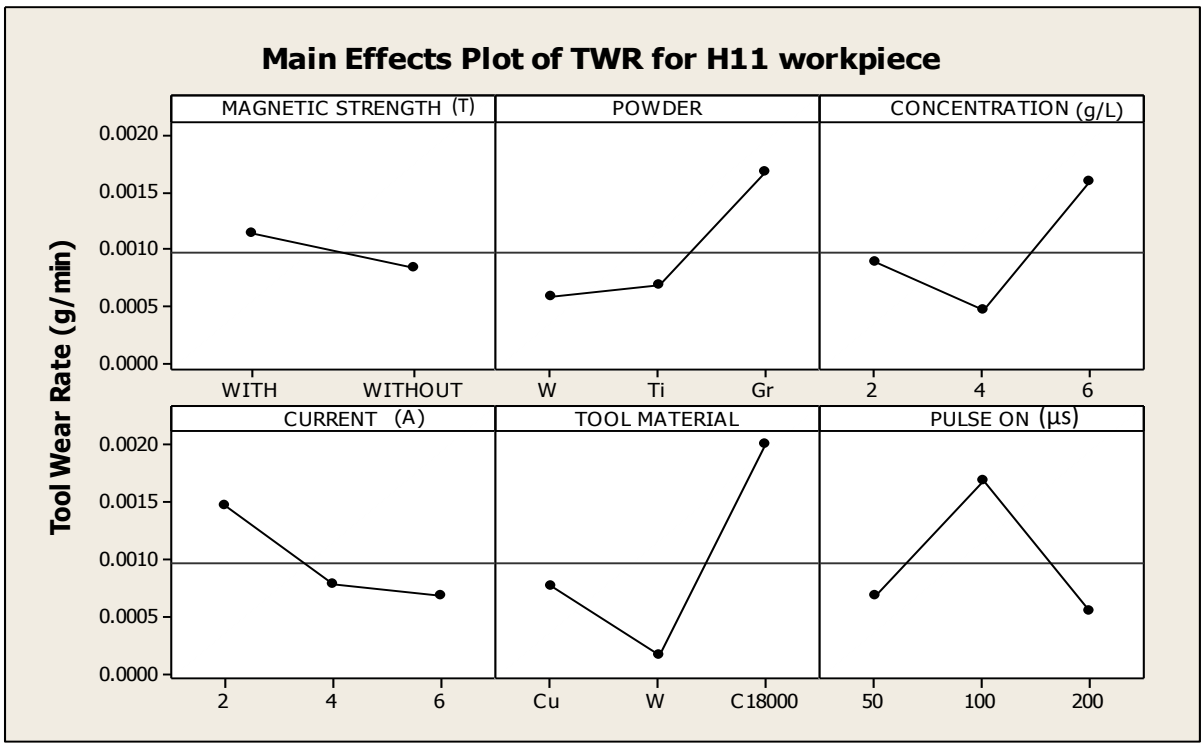

Figure 4.8: Main effect plots of TWR for H11 workpiece

Based on the analysis the factors are ranked according to their significance of affecting tool wear rate, shown in table 4.12.

Table 4.12: Response table of TWR for H11 workpiece

Level	Magnetic strength (T)	Powder	Concentration (g/L)	Current (A)	Tool material	Pulse-on (µs)
1	0.001128	0.000575	0.000888	0.001472	0.000768	0.000688
2	0.000829	0.000688	0.000467	0.000787	0.000162	0.001692
3		0.001672	0.001580	0.000677	0.002005	0.000555
Delta	0.000299	0.001097	0.001113	0.000795	0.001843	0.001137
Rank	6	4	3	5	1	2

Optimal design

In the experimental study, the mean effect plots (Fig. 4.7. are used to evaluate the mean TWR at optimal trial conditions. From Table 4.11 considering higher F-value and corresponding percentage contribution three parameters are found to be significant tool material followed by current and type of powder. The level of these factors which gives the minimum TWR are noted from main effect plot (Fig. 4.7) and the corresponding TWR for E_2 and F_3 is directly obtained from Table 4.12. Minimum value of these parameters is selected because TWR is the lower the better type of response variable. Desired mean in this case is estimated as:

$\mu_{E_2} = \overline{E_2} + \overline{F_3} - \overline{T}$ = 0.000162 + 0.000555 – 0.0010122

= -0.0002952 ≡ 0

The optimal calculation for population mean (µ) gives negative value. This situation may appear for responses which are lower the better type and where the optimum/target value is zero. For such case negative value of µ may not have any physical significance and is to be considered as zero.

Confidence interval

$$CI = \sqrt{\frac{F_{\alpha,\nu_1,\nu_2} V_e}{n_{eff}}}$$

Where F_{α,ν_1,ν_2} = F ratio

α = 0.1 (risk)

Confidence = 1 – α

ν_1 = DF for mean (always 1)

ν_2 = Total DOF (=17)

$\overline{T}$ = Average of all experimental trials

n_{eff} = Number of tests under that condition using the participating factors

$$n_{eff} = \frac{\text{N}}{1+DOF_{E,F}} = \frac{18}{1+4} = 3.6$$

N is the number of trial in the experiment

V_e = Variance of error

$$CI = \sqrt{\frac{3.03 \times 0.000002}{3.6}} = \pm 0.001297$$

Thus the optimum value of TWR is given by (0 ± 0.001297) g/min.

4.3.2 TWR for H13 workpiece.

Results for mean TWR for H13 workpiece are given in table 4.13.

Table 4.13: TWR results of H13 workpiece

Expt. No	Magnetic strength (T)	Powder	Concentration (g/L)	Current (A)	Tool material	Pulse-on (µs)	TWR (g/min)
1	With	W	2	2	Cu	50	0.00060
2	With	W	4	4	W	100	0.00006
3	With	W	6	6	C18000	200	0.00066
4	With	Ti	2	2	W	100	0.00006
5	With	Ti	4	4	C18000	200	0.00067
6	With	Ti	6	6	Cu	50	0.00067
7	With	Gr	2	4	Cu	200	0.00060
8	With	Gr	4	6	W	50	0.00006
9	With	Gr	6	2	C18000	100	0.00067
10	Without	W	2	6	C18000	100	0.00067
11	Without	W	4	2	Cu	200	0.00067
12	Without	W	6	4	W	50	0.00006
13	Without	Ti	2	4	C18000	50	0.00200
14	Without	Ti	4	6	Cu	100	0.00067
15	Without	Ti	6	2	W	200	0.00006
16	Without	Gr	2	6	W	200	0.00200
17	Without	Gr	4	2	C18000	50	0.00200
18	Without	Gr	6	4	Cu	100	0.00133

The results of TWR are analyzed using ANOVA at 90% confidence level and are listed in table 4.14.

Table 4.14: ANOVA table for TWR of H13 workpiece

Parameter	Symbol	DOF	SS	Variance	*F*-value	PC
Magnetic strength (T)	*A*	1	0.000002	0.000002	4.79	24.027
Powder	*B*	2	0.000001	0.000001	1.96	12.013
Concentration (g/L)	*C*	2	0.000001	0.0000000243	0.81	12.013
Current (A)	*D*	2	0.000000042	0.000000021	0.07	0.505
Tool material	*E*	2	0.000002	0.000001	2.34	24.027
Pulse-on time (µs)	*F*	2	0.000000282	0.000000141	0.47	3.388
Residual error		6	0.000002	0.0000003		24.027
Total		17	0.000007			

(Note: For 90% CI, $F_{critical(2,6)} = 3.46$, $F_{critical(1,6)} = 3.78$, PC= percentage contribution)

Based on the analysis magnetic strength conducted is identified as the most significant factor. The comparative performance of various factors on TWR is shown in Fig. 4.8. In the

Fig. 4.8 abscissa represents levels of various factors and ordinate represents TWR (g/min). The center line represents mean value of the levels.

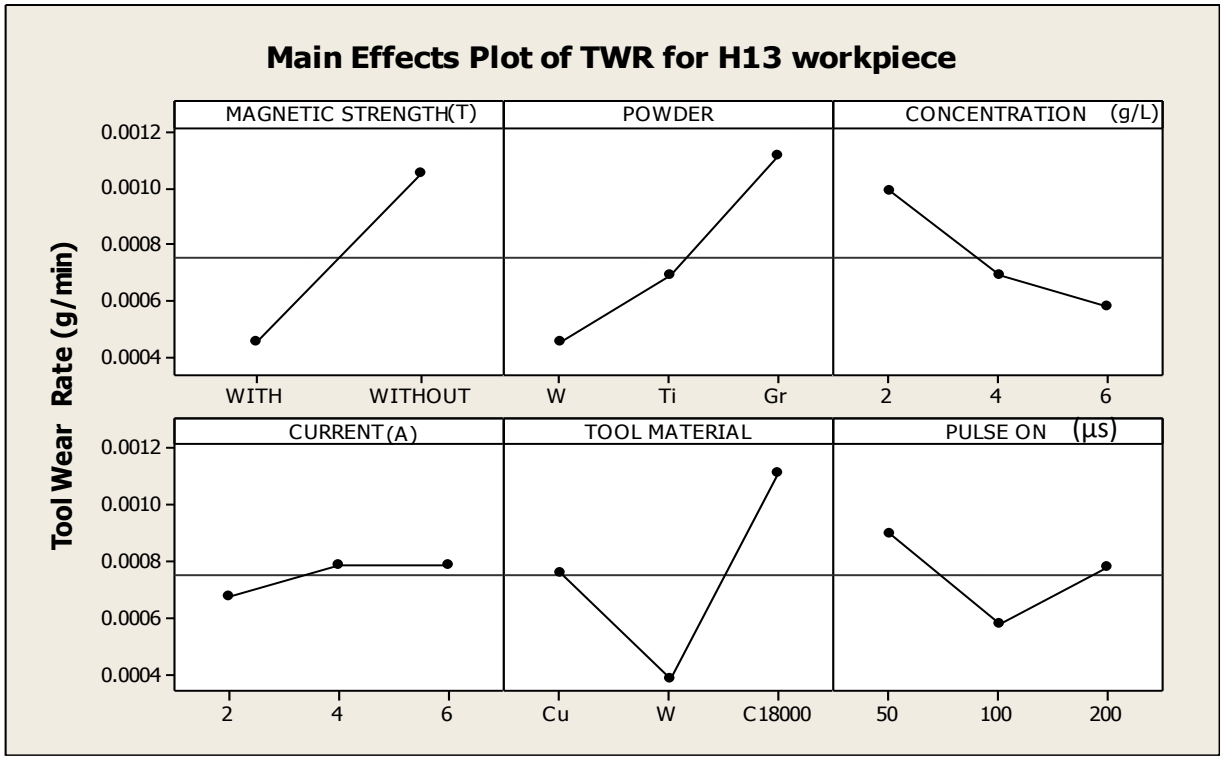

Figure 4.9: Main effect plots of TWR for H13 workpiece

A significant decrease has been found in tool wear rate under the influence of magnetic field. The reason behind this may be diamagnetism effect of copper tool materials and its alloy C18000 but tungsten being paramagnetic does not have much influence of external magnetic field. Second factor affecting the tool wear rate in H13 workpiece is the tool material, with C18000 alloy giving the maximum tool wear followed by copper and least tool wear is observed in tungsten, reason behind this may be the melting points and densities of the respective alloys. Third factor affecting the tool wear is the powder suspended in the dielectric, maximum tool wear is obtained with the use of graphite powder having maximum electrical conductivity. Forth factor affecting the tool wear is the concentration, tool wear decreases with increase in the concentration of powder as the increase in concentration of powder above a certain value results in arcing due to restriction of gap between tool and workpiece. Pulse on duration and current has negligible effect on tool wear rate. Based on this analysis the various factors are ranked in Table 4.15.

Table 4.15: Response Table of TWR for H13 workpiece

Level	Magnetic strength (T)	Powder	Concentration (g/L)	Current (A)	Tool material	Pulse-on (µs)
1	0.000450	0.000453	0.000988	0.000677	0.000757	0.000898
2	0.001051	0.000688	0.000688	0.000787	0.000383	0.000577
3		0.001110	0.000575	0.000788	0.001112	0.000777
Delta	0.000601	0.000657	0.000413	0.000112	0.000728	0.000322
Rank	3	2	4	6	1	5

Optimal design

In the experimental study, the mean effect plots (Fig. 4.8. are used to evaluate the mean TWR at optimal trial conditions. From Table 4.14 considering higher F-value and corresponding percentage contribution two parameters are found to be significant magnetic strength followed by tool material. The level of these factors which gives the minimum TWR are noted from main effect plot (Fig. 4.8) and the corresponding TWR for A_1 and E_2 is directly obtained from Table 4.15. Minimum value of these parameters is selected because TWR is the lower the better type of response variable. Desired mean in this case is estimated as:

$\mu_{E_2} = \overline{A_1} + \overline{E_2} - \overline{T}$ = 0.000450 + 0.000383 – 0.000713

= 0.00012

Confidence interval

$$CI = \sqrt{\frac{F_{\alpha,\nu_1,\nu_2} V_e}{n_{eff}}}$$

Where Fα, ν_1, ν_2 = *F* ratio

α = 0.1 (risk)

Confidence = 1 – α

ν_1 = DF for mean (always 1)

ν_2 = = Total DOF (=17)

$\overline{T}$ = Average of all experimental trials

n_{eff} = Number of tests under that condition using the participating factors

$$n_{eff} = \frac{N}{1+DOF_{A,E}} = \frac{18}{1+4} = 3.6$$

N is the number of trial in the experiment

V_e = *Variance* (error)

$$CI = \sqrt{\frac{3.03 \times 0.0000003}{3.6}} = \pm 0.001589$$

Thus the optimum value of MRR is given by =0.00012 ±0.001589 g/min.

4.3.3 TWR for D3 workpiece.

Results for mean TWR for D3 workpiece are given in Table 4.16.

Table 4.16: TWR results of D3 workpiece

Expt. No	Magnetic strength (T)	Powder	Concentration (g/L)	Current (A)	Tool material	Pulse-on (µs)	TWR (g/min)
1	With	W	2	2	Cu	50	0.00067
2	With	W	4	4	W	100	0.00007
3	With	W	6	6	C18000	200	0.00067
4	With	Ti	2	2	W	100	0.00007
5	With	Ti	4	4	C18000	200	0.00067
6	With	Ti	6	6	Cu	50	0.00200
7	With	Gr	2	4	Cu	200	0.00067
8	With	Gr	4	6	W	50	0.00007
9	With	Gr	6	2	C18000	100	0.00067
10	Without	W	2	6	C18000	100	0.00067
11	Without	W	4	2	Cu	200	0.00270
12	Without	W	6	4	W	50	0.00007
13	Without	Ti	2	4	C18000	50	0.00270
14	Without	Ti	4	6	Cu	100	0.00067
15	Without	Ti	6	2	W	200	0.00007
16	Without	Gr	2	6	W	200	0.00007
17	Without	Gr	4	2	C18000	50	0.00134
18	Without	Gr	6	4	Cu	100	0.00067

These results are analyzed using ANOVA at 90% confidence level and are listed in Table 4.17.

Table 4.17: ANOVA table for TWR of D3 workpiece

Parameter	Symbol	DOF	SS	Variance	*F*- value	PC
Magnetic strength (T)	*A*	1	0.000001	0.000001	0.87	8.038
Powder	*B*	2	0.000001	0.00000041	0.41	8.038
Concentration (g/L)	*C*	2	0.00000022	0.00000011	0.11	1.768
Current (A)	*D*	2	0.00000022	0.00000011	0.11	1.768
Tool material	*E*	2	0.000005	0.000002	3.32	40.192
Pulse-on time (µs)	*F*	2	0.000001	0.000001	0.91	8.038
Residual error		6	0.000004	0.000001		32.154
Total		17	0.00001244			

(Note: For 90% CI, $F_{critical(2,6)} = 3.46$, $F_{critical(1,6)} = 3.78$, PC= percentage contribution)

Based on the analysis conducted most significant factor is again the tool material with *F* value 3.32. In the case of D3 tool material the copper and C18000 tool materials show almost the same wear but tool wear of tungsten tool is very less as compared to these two. The second factor affecting the tool wear rate is the pulse on duration having *F* value 0.91. The third significant factor is the magnetic strength with *F* value 0.87, the tool wear rate is found to decrease with external influence of magnetic field, as two of the tool materials copper and C18000 alloy are diamagnetic hence the repulsion offered by the externally applied magnetic field helps in decreasing the tool wear rate whereas it does not have much effect on tungsten as it is paramagnetic. The other 3 factors type of powder, current and concentration does not have much effect on tool wear in the case of D3 die steel as workpiece material. In the Fig. 4.9 abscissa represents levels of various factors and ordinate represents TWR (g/min). The center line represents mean value of the levels.

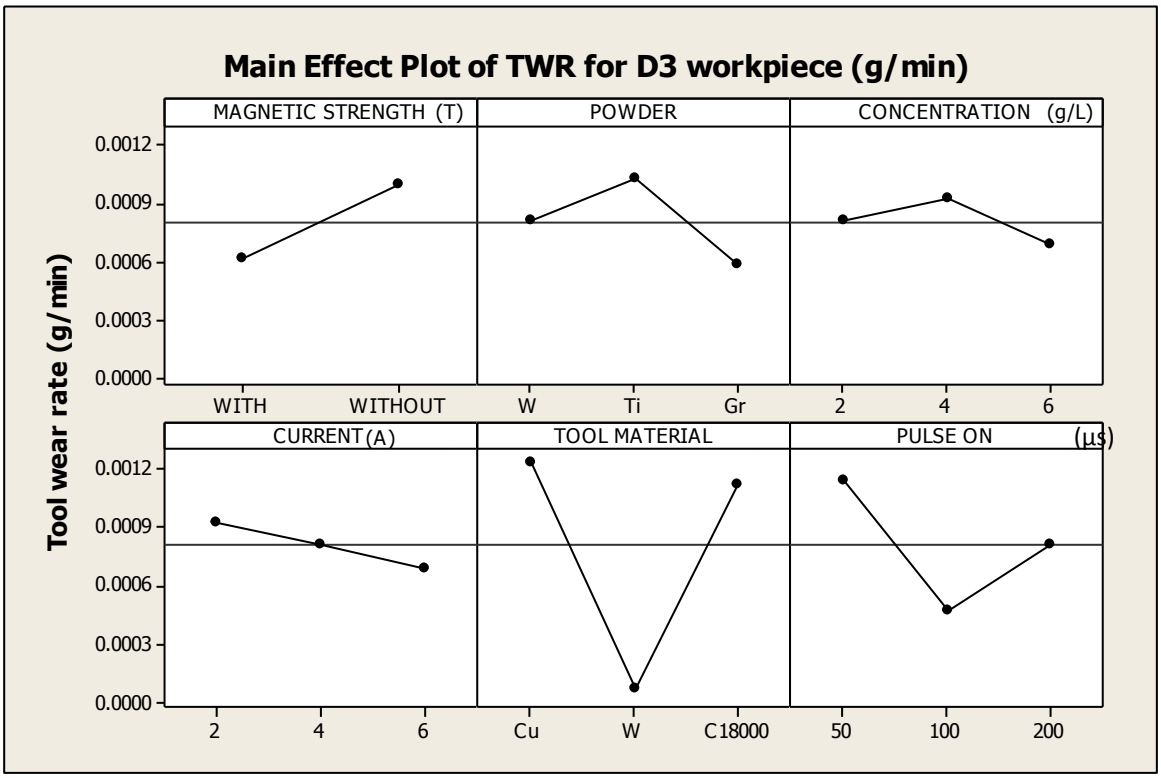

Figure 4.10: Main effect plots of TWR for D3 workpiece

Based on the above observations the factors are ranked in order of their significance in affecting tool wear rate is given in Table 4.18.

Table 4.18: Response Table of TWR for D3 workpiece

Level	Magnetic strength (T)	Powder	Concentration (g/L)	Current (A)	Tool material	Pulse-on (µs)
1	0.000618	0.000808	0.000808	0.000920	0.001230	0.001142
2	0.000996	0.001030	0.000920	0.000808	0.000070	0.000470
3		0.000582	0.000692	0.000692	0.001120	0.000808
Delta	0.000378	0.000448	0.000228	0.000228	0.001160	0.000672
Rank	4	3	5.5	5.5	1	2

Optimal design

In the experimental study, the mean effect plots (Fig. 4.8) are used to evaluate the mean TWR at optimal trial conditions. TWR is the lower the better type of response variable. Desired mean in this case is estimated as:

$\mu_{E_2} = \overline{E_2}$= 0.000070

= 0.000070

Confidence interval

$$CI = \sqrt{\frac{F_{\alpha,v_1,v_2} V_e}{n_{eff}}}$$

Where Fα, v_1, v_2 = *F* ratio

α = 0.1 (risk)

Confidence = 1 – α

v_1= DF for mean (always 1)

v_2 = DF for total (=17)

$\overline{T}$ = Average of all experimental trials

n_{eff} = Number of tests under that condition using the participating factors

$$n_{eff} = \frac{\mathrm{N}}{1+DOF_E} = \frac{18}{1+2} = 6$$

N is the number of trial in the experiment

V_e = Variance of error

$$CI = \sqrt{\frac{3.03 \times 0.000001}{6}} = \pm 7.10633$$

Thus the optimum value of MRR is given by (0.000070±7.10633) g/min.

4.4 Analysis of Tool Profile for Edge and Corner Wear

Wear of tool and their profiles after machining are studied with the help of a measuring microscope (Make: Carl Zeiss, model Axio-Scope A1) having accuracy of 1 µm at 100X magnification. The different profiles showing edge wear and corner wear of tools used for the three workpieces H11, H13 and D3 are observed. The profiles of tool wear showing corner wear and its comparison with ideal profiles for H11, H13 and D3 workpiece are given in Table 4.19, 4.20 and 4.21 respectively. The maximum wear for all the profiles are also indicated for each of the experimental trial conditions.

Tool profiles of the three tool materials copper, C18000 and tungsten are analyzed for all the trails and the snaps are given in Table 4.19 showing the corner wear. The edges were sharp before the trial and after the trial as shown by snaps the edges are slightly round. The coordinates of the tool wear measured using the Nikon profile projector (Model: V-10A) and the CAD profiles are drawn using the same. The CAD profiles show the comparison of the tool profiles before and after the experiments were conducted.

4.4.1 Tool profiles for H11 workpiece

The maximum tool wear readings listed in Table 4.19 depict that in the case of machining of H11 die steel workpiece the maximum wear is observed when the tool material is C18000, followed by copper and tungsten. Photographic view and CAD profiles of regions A and B is shown in Table 4.19. For C18000 tool maximum wear is observed at low values of current i.e. in trial number 9 and 17 where the current is 2 A followed by the trials conducted at 4 A and 6 A respectively. For copper tool the maximum wear is observed at the setting of 4 A current which is shown in trial 7, 18 followed by the trials conducted at 6 A and 2 A. The least tool wear is observed in the case of tungsten tool material. For tungsten the maximum tool wear is observed at the highest current setting i.e. 6 A shown by the trials 8 and 16, followed by the trials conducted at 4 A and 2 A respectively. Of the three tool materials the maximum wear is shown by the C18000 alloy followed by copper and tungsten. This difference in wear behavior for the three tool materials is due to difference in their melting point and thermal conductivities.

Photographic view for side wear of regions C and D for machining of H11 workpiece is shown in Table 4.20 with average wear listed for each trial. Five readings are taken at a distance of 2 mm and average of these readings is listed in the Table. From the analysis it is found that maximum side wear is observed in the trial number 10 i.e. maximum side wear is shown by the tool material C18000. But overall maximum side wear shown by the trials using tungsten as the tool material followed by C18000 alloy and copper. For some trials side wear is found to be negative this is due to deposition of a black layer on the tool due to decomposition of the dielectric. Photographic view of these tools is shown in Fig. 4.11.

Figure 4.11: Tools showing negative wear for H11 workpiece

Table 4.19: Tool corner wear during PMEDM of H11 workpiece

Exp. No	Trial conditions (Magnetic strength, powder, concentration, current, tool material, pulse-on)	Corner wear (photographic view)	Comparison between ideal and measured tool profile (Legend: red dotted line: ideal; blue solid line: measured)
			A B
1	0.1 T, W, 2 g/L, 2 A, Cu, 50 µs	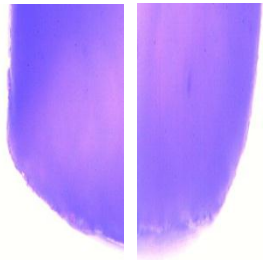	 Maximum wear = 0.135 mm
2	0.1 T, W, 4 g/L, 4 A, W, 100 µs	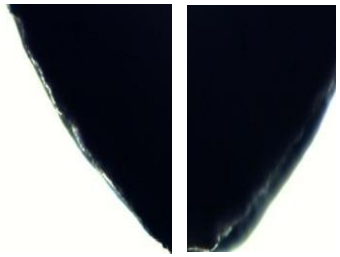	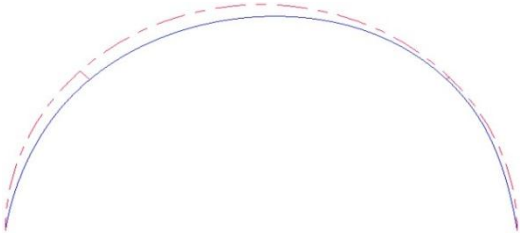 Maximum wear = 0.045 mm
3	0.1 T, W, 6 g/L, 6 A, C18000, 200 µs	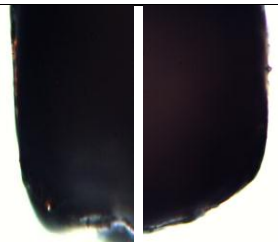	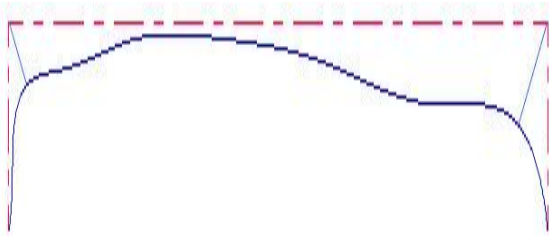 Maximum wear = 0.145 mm

4	0.1 T, Ti, 2 g/L, 2 A, W, 100 µs	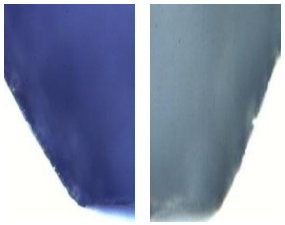	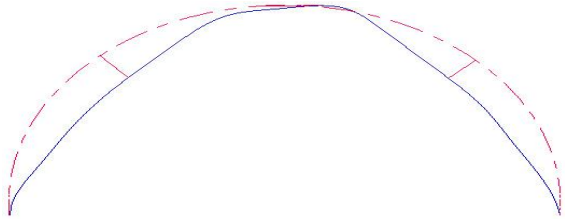 Maximum wear = 0.17 mm
5	0.1 T, Ti, 4 g/L, 4 A, C18000, 200 µs	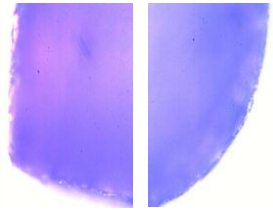	 Maximum wear =0.175 mm
6	0.1 T, Ti, 6 g/L, 6 A, Cu, 50 µs	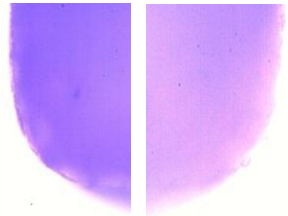	 Maximum wear = 0.165 mm
7	0.1 T, Gr, 2 g/L, 4 A, Cu, 200 µs	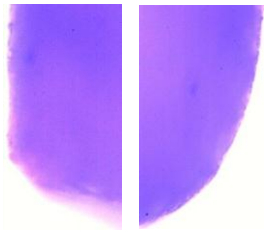	 Maximum wear = 0.195 mm

8	0.1 T, Gr, 4 g/L, 6 A, W, 50 µs	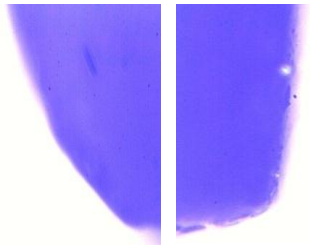	 Maximum wear = 0.194 mm
9	0.1 T, Gr, 6 g/L, 2 A, C18000, 100 µs	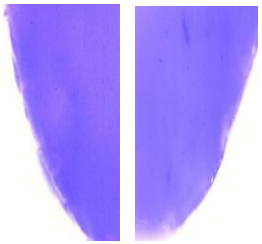	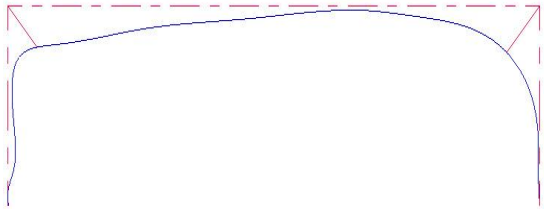 Maximum wear = 0.2 mm
10	0 T, W, 2 g/L, 6 A, C18000, 100 µs	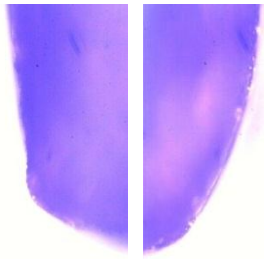	 Maximum wear = 0.18 mm
11	0 T, W, 4 g/L, 2 A, Cu, 200 µs	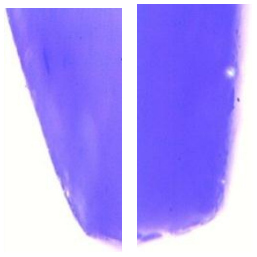	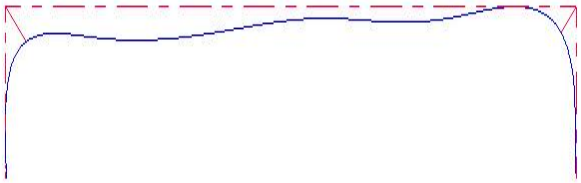 Maximum wear = 0.115 mm

12	0 T, W, 6 g/L, 4 A, W, 50 µs	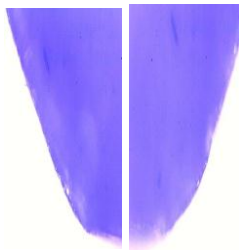	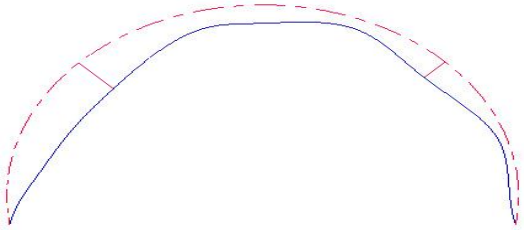 Maximum wear = 0.185 mm
13	0 T, Ti, 2 g/L, 4 A, C18000, 50 µs	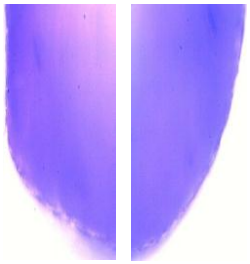	 Maximum wear = 0.2 mm
14	0 T, Ti, 4 g/L, 6 A, Cu, 100 µs	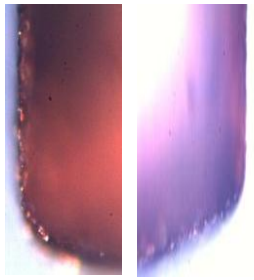	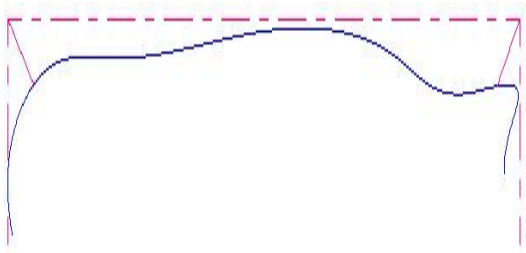 Maximum wear = 0.175 mm
15	0 T, Ti, 6 g/L, 2 A, W, 200 µs	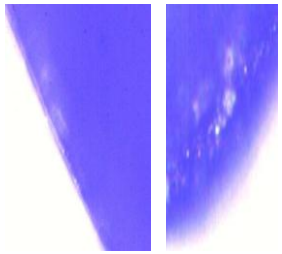	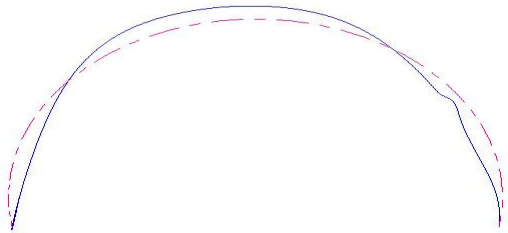 Maximum wear = 0.025 mm

16	0 T, Gr, 2 g/L, 6 A, W, 200 µs	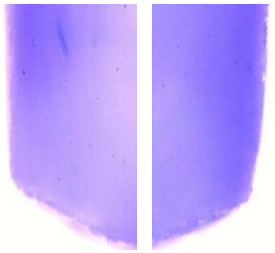	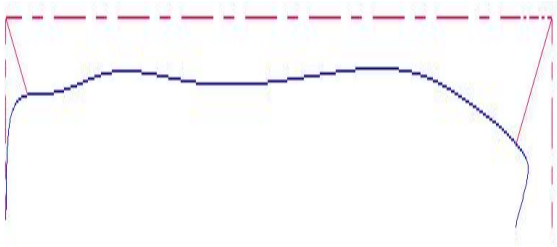 Maximum wear = 0.175 mm
17	0 T, Gr, 4 g/L, 2 A, C18000, 50 µs	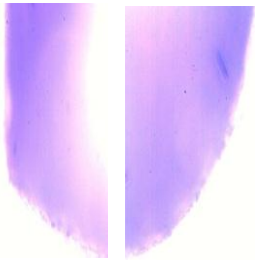	 Maximum wear = 0.245 mm
18	0 T, Gr, 6 g/L, 4 A, Cu, 100µs	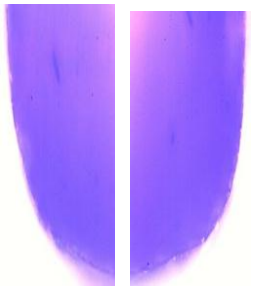	 Maximum wear = 0.18 mm

Table 4.20: Tool side wear during PMEDM of H11 workpiece

Exp. No	Trial conditions (Magnetic strength, powder, concentration, current, tool material pulse-on)	Side wear (photographic view)
		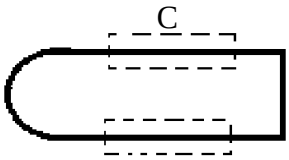
1	0.1 T, W, 2 g/L, 2 A, Cu, 50 µs	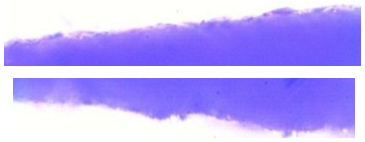 Maximum wear = 0.03 mm
2	0.1 T, W, 4 g/L, 4 A, W, 100 µs	 Maximum wear = 0.0428 mm
3	0.1 T, W, 6 g/L, 6 A, C18000, 200 µs	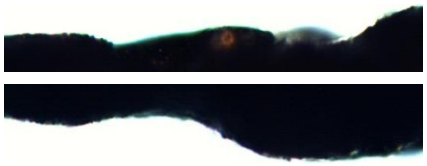 Maximum wear = -0.0424 mm
4	0.1 T, Ti, 2 g/L, 2 A, W, 100 µs	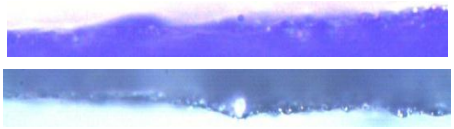 Maximum wear = 0.023 mm
5	0.1 T, Ti, 4 g/L, 4 A, C18000, 200 µs	 Maximum wear = -0.0058 mm

6	0.1 T, Ti, 6 g/L, 6 A, Cu, 50 µs	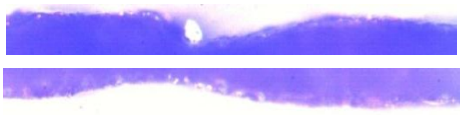 Maximum wear = 0.028 mm
7	0.1 T, Gr, 2 g/L, 4 A, Cu, 200 µs	 Maximum wear = -0.0328 mm
8	0.1 T, Gr, 4 g/L, 6 A, W, 50 µs	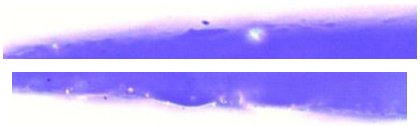 Maximum wear = 0.0362 mm
9	0.1 T, Gr, 6 g/L, 2 A, C18000, 100 µs	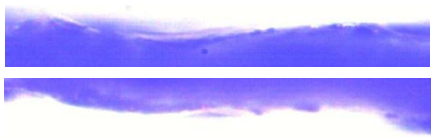 Maximum wear = 0.0628 mm
10	0 T, W, 2 g/L, 6 A, C18000, 100 µs	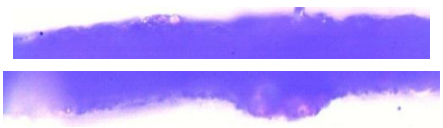 Maximum wear = 0.1408 mm
11	0 T, W, 4 g/L, 2 A, Cu, 200 µs	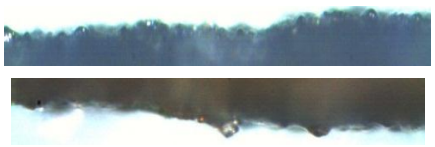 Maximum wear = 0.0360 mm
12	0 T, W, 6 g/L, 4 A, W, 50 µs	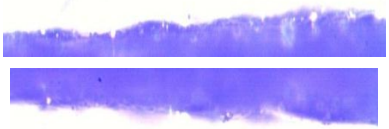 Maximum wear = 0.0222 mm
13	0 T, Ti, 2 g/L, 4 A, C18000, 50 µs	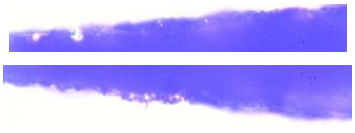 Maximum wear = 0.032 mm

14	0 T, Ti, 4 g/L, 6 A, Cu, 100 µs	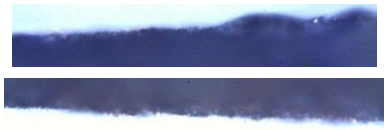 Maximum wear = -0.084 mm
15	0 T, Ti, 6 g/L, 2 A, W, 200 µs	 Maximum wear = 0.0318 mm
16	0 T, Gr, 2 g/L, 6 A, W, 200 µs	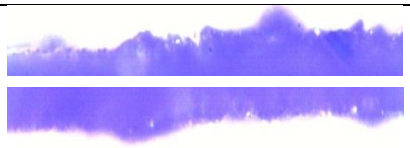 Maximum wear = 0.0414 mm
17	0 T, Gr, 4 g/L, 2 A, C18000, 50 µs	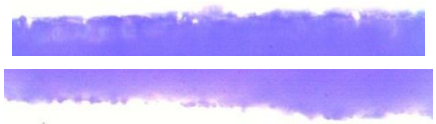 Maximum wear = 0.0072 mm
18	0 T, Gr, 6 g/L, 4 A, Cu, 100µs	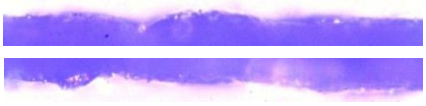 Maximum wear = -0.0172 mm

4.4.2 Tool profiles for H13 workpiece

Tool profiles of the three tool materials copper, C18000 and tungsten are analyzed for H13 workpiece and are given in Table 4.21. The photographic view of regions A and B is shown in Table 4.21. The edges were sharp before the trial and after the trial as shown by snaps the edges are slightly round. The coordinates of the tool wear measured using the Nikon profile projector (Model: V-10A) and the CAD profiles are drawn using the same.

In the case of H13 die steel as listed in Table 4.21 the workpiece the maximum tool wear is observed for the C18000 alloy showing slight variation with the three current settings. The second highest wear is shown by the copper tool material maximum wear being observed at the 4 A as shown by the trials 7 and 18 followed by the trial conducted at 4 A and 6 A. The least tool wear is observed in the case of tungsten tool material showing maximum wear at the highest current setting i.e. 6 A followed by 4 A and 2 A. Of all the values maximum wear is observed at 4 A and 6 A. The reason behind this tool wear behavior may be electrical conductivity of the tool materials and of the powders suspended in the dielectric as a significant tool wear is observed when graphite powder having maximum conductivity of the three powders is being used as indicated by the trials 7, 8, 9, 16, 17 and 18.

Photographic view for side wear of regions C and D for machining of H13 workpiece is shown in Table 4.22 with average wear listed for each trial. Five readings are taken at a distance of 2 mm and average of these readings is listed in the Table. 4.22. For H13 workpiece maximum decrease in diameter of the tool is observed for the trials using tungsten as the tool material followed by C18000 alloy and copper. In some of the trials using C18000 and copper as the tool material the side wear of the tool is observed to be negative due more deposition of the black layer on the tool as compared to the tool material evaporated. Photographic view of such tools is shown in Fig 4.12.

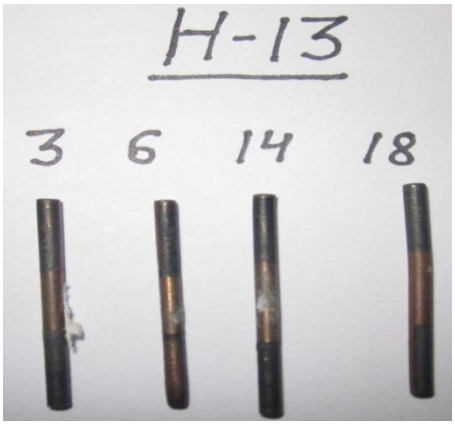

Figure 4.12: Tools showing negative wear for H13 workpiece

Table 4.21: Tool corner wear during PMEDM of H13 workpiece

Exp. No	Trial conditions (Magnetic strength, powder, concentration, current, tool material, pulse-on)	Corner wear (photographic view)	Comparison between ideal and measured tool profile (Legend: red dotted line: ideal; blue solid line: measured)
			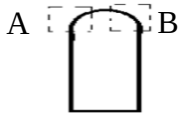
1	0.1 T, W, 2 g/L, 2 A, Cu, 50 µs	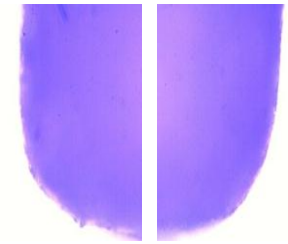	 Maximum wear = 0.145 mm
2	0.1 T, W, 4 g/L, 4 A, W, 100 µs	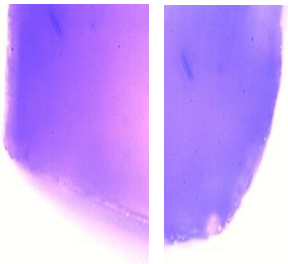	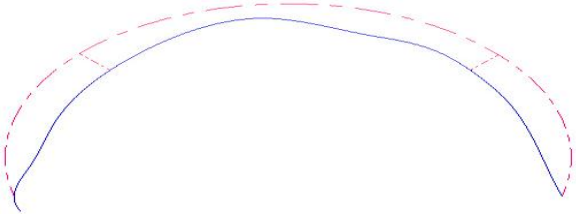 Maximum wear = 0.175 mm
3	0.1 T, W, 6 g/L, 6 A, C18000, 200 µs	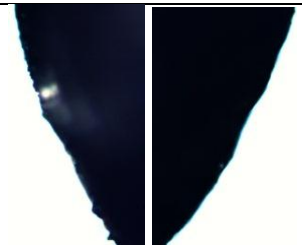	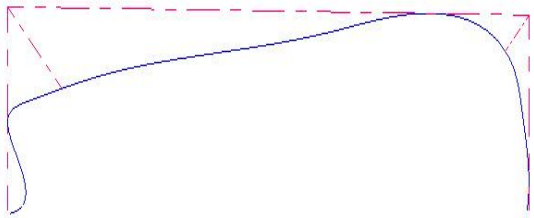 Maximum wear = 0.26 mm

4	0.1 T, Ti, 2 g/L, 2 A, W, 100 µs	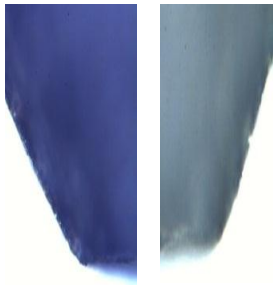	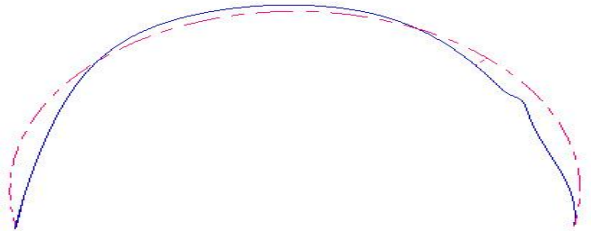 Maximum wear = 0.07 mm
5	0.1 T, Ti, 4 g/L, 4 A, C18000, 200 µs	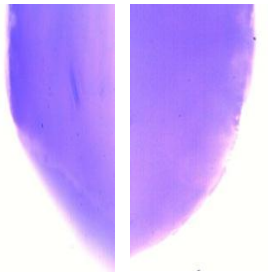	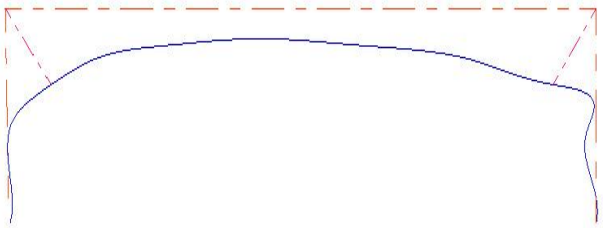 Maximum wear = 0.225 mm
6	0.1 T, Ti, 6 g/L, 6 A, Cu, 50 µs	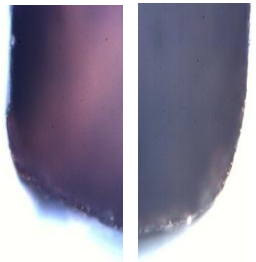	 Maximum wear = 0.14 mm
7	0.1 T, Gr, 2 g/L, 4 A, Cu, 200 µs	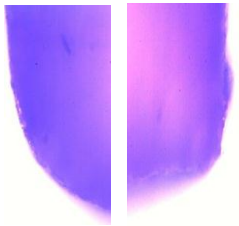	 Maximum wear = 0.205 mm

8	0.1 T, Gr, 4 g/L, 6 A, W, 50 µs	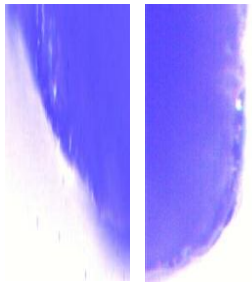	 Maximum wear = 0.285 mm
9	0.1 T, Gr, 6 g/L, 2 A, C18000, 100 µs	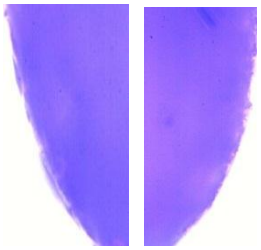	 Maximum wear = 0.27 mm
10	0 T, W, 2 g/L, 6 A, C18000, 100 µs	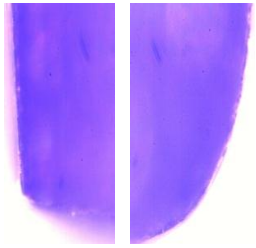	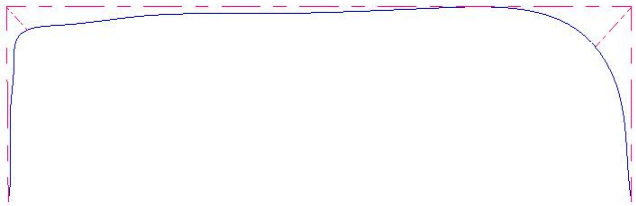 Maximum wear = 0.15 mm
11	0 T, W, 4 g/L, 2 A, Cu, 200 µs	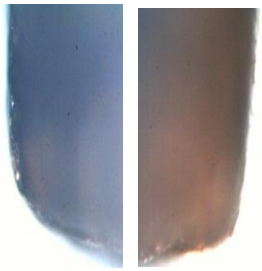	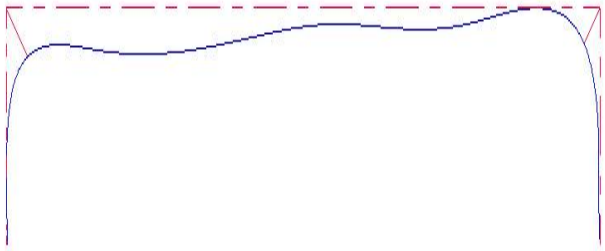 Maximum wear = 0.105 mm

12	0 T, W, 6 g/L, 4 A, W, 50 µs	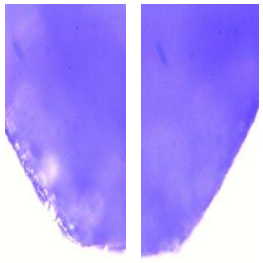	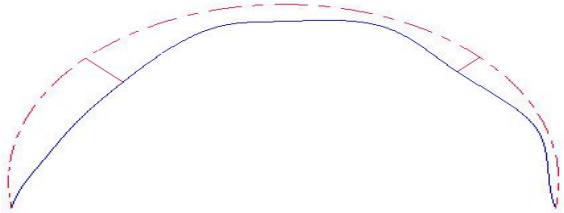 Maximum wear = 0.172 mm
13	0 T, Ti, 2 g/L, 4 A, C18000, 50 µs	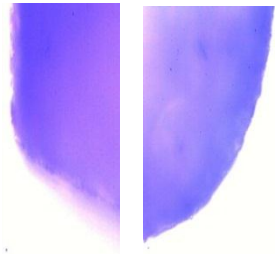	 Maximum wear = 0.18 mm
14	0 T, Ti, 4 g/L, 6 A, Cu, 100 µs		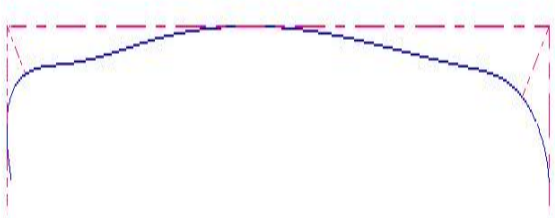 Maximum wear = 0.15 mm
15	0 T, Ti, 6 g/L, 2 A, W, 200 µs	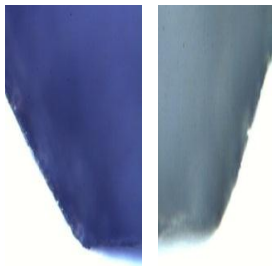	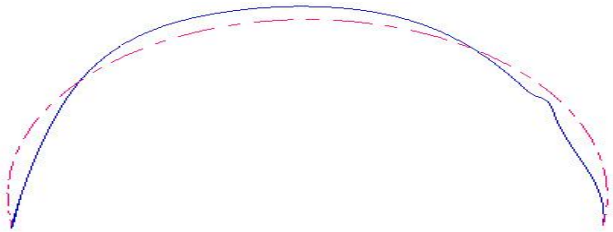 Maximum wear = 0.17 mm

16	0 T, Gr, 2 g/L, 6 A, W, 200 µs	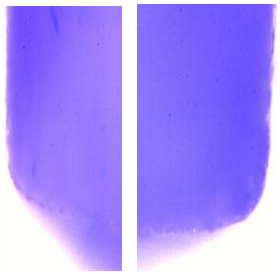	 Maximum wear = 0.21 mm
17	0 T, Gr, 4 g/L, 2 A, C18000, 50 µs	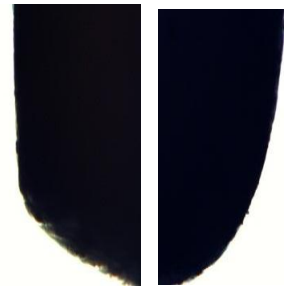	 Maximum wear = 0.225 mm
18	0 T, Gr, 6 g/L, 4 A, Cu, 100µs	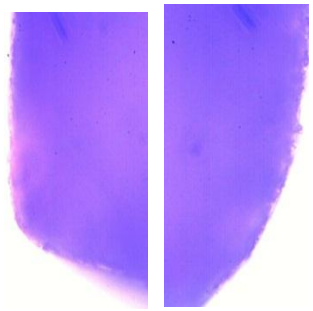	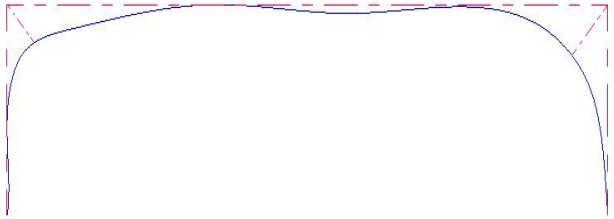 Maximum wear = 0.20 mm

Table: 4.22 Tool side wear during PMEDM of H13 workpiece

Exp. No	Trial conditions (Magnetic strength, powder, concentration, current, tool material, pulse-on)	Side wear (photographic view) 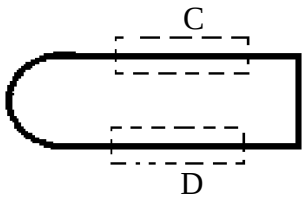
1	0.1 T, W, 2 g/L, 2 A, Cu, 50 µs	 Maximum wear = 0.0402 mm
2	0.1 T, W, 4 g/L, 4 A, W, 100 µs	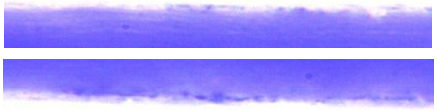 Maximum wear = 0.0284 mm
3	0.1 T, W, 6 g/L, 6 A, C18000, 200 µs	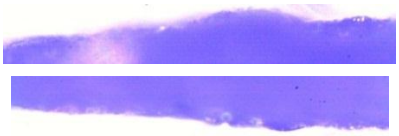 Maximum wear = -0.0532 mm
4	0.1 T, Ti, 2 g/L, 2 A, W, 100 µs	 Maximum wear = 0.0224 mm
5	0.1 T, Ti, 4 g/L, 4 A, C18000, 200 µs	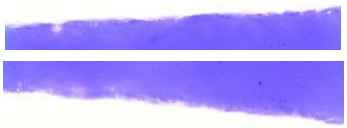 Maximum wear = 0.0128 mm
6	0.1 T, Ti, 6 g/L, 6 A, Cu, 50 µs	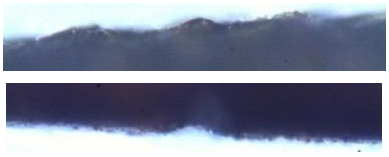 Maximum wear = -0.1004 mm

7	0.1 T, Gr, 2 g/L, 4 A, Cu, 200 µs	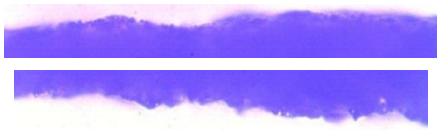 Maximum wear = 0.079 mm
8	0.1 T, Gr, 4 g/L, 6 A, W, 50 µs	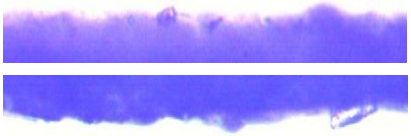 Maximum wear = 0.045 mm
9	0.1 T, Gr, 6 g/L, 2 A, C18000, 100 µs	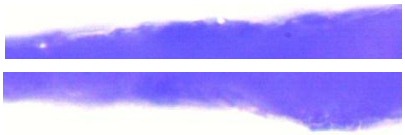 Maximum wear = 0.0616 mm
10	0 T, W, 2 g/L, 6 A, C18000, 100 µs	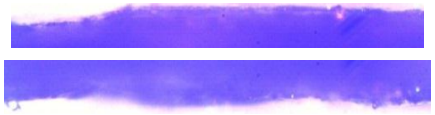 Maximum wear = 0.073 mm
11	0 T, W, 4 g/L, 2 A, Cu, 200 µs	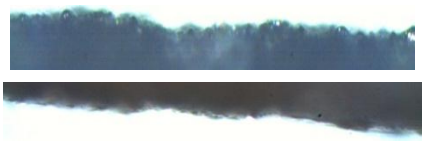 Maximum wear = 0.0124 mm
12	0 T, W, 6 g/L, 4 A, W, 50 µs	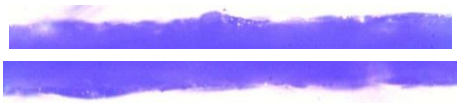 Maximum wear = 0.0104 mm
13	0 T, Ti, 2 g/L, 4 A, C18000, 50 µs	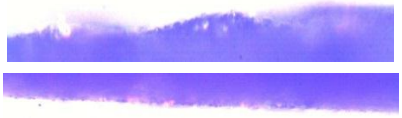 Maximum wear = 0.0572 mm
14	0 T, Ti, 4 g/L, 6 A, Cu, 100 µs	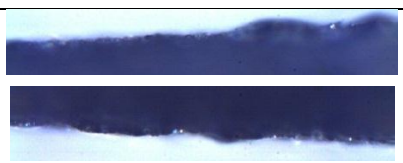 Maximum wear = -0.028 mm

15	0 T, Ti, 6 g/L, 2 A, W, 200 µs	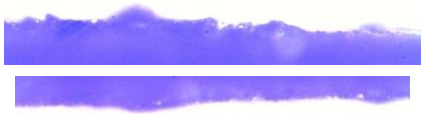 Maximum wear = 0.0309 mm
16	0 T, Gr, 2 g/L, 6 A, W, 200 µs	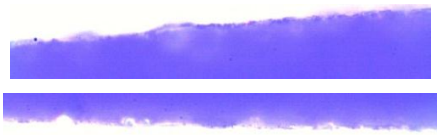 Maximum wear = 0.0224 mm
17	0 T, Gr, 4 g/L, 2 A, C18000, 50 µs	 Maximum wear = 0.0414 mm
18	0 T, Gr, 6 g/L, 4 A, Cu, 100µs	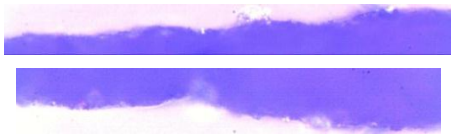 Maximum wear = -0.001222 mm

4.4.3 Tool profiles for D3 workpiece

Tool profiles of the three tool materials copper, C18000 and tungsten are analyzed for D3 workpiece and are given in Table 4.23. The photographic view of regions A and B of corner wear is shown in Table 4.23. The edges wear sharp before the trial and after the trial as shown by snaps the edges are slightly round. The coordinates of the tool wear measured using the Nikon profile projector (Model: V-10A) and the CAD profiles are drawn using the same. The analysis of the profiles is done based on their trial conditions.

For D3 workpiece different behavior is observed for the tool wear as compared to the H11 and H13 workpiece. For D3 workpiece as listed in Table 4.23. Maximum tool wear is observed in the trials conducted using copper with very slight increase compared to those conducted with C18000 alloy with current having negligible effect on the wear. The reason for this behavior is the material properties of the tool materials as well as the magnetic strength as the trials 1-9 show less wear compared to the 10-18.

Photographic view for side wear of regions C and D for machining of D3 workpiece is shown in Table 4.24 with average wear listed for each trial. Five readings are taken at a distance of 2 mm and average of these readings is listed in the Table. 4.24. For D3 workpiece again maximum side wear is observed for the tungsten tool material followed by copper and C18000 alloy. Due to deposition of black layer side wear is observed to be negative for some trials using C18000 and copper as the tool material. Photographic view of such trials is shown in Fig. 4.13.

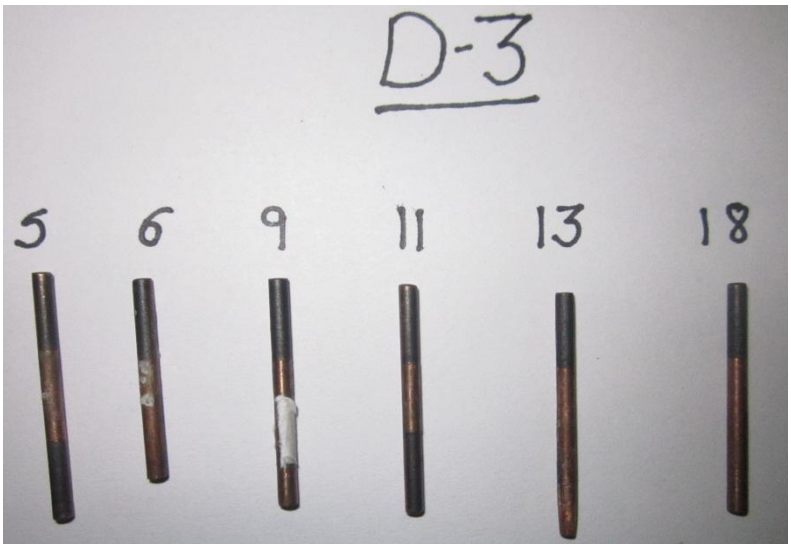

Figure 4.13: Tools showing negative wear for D3 workpiece

Table 4.23: Tool corner wear during PMEDM of D3 workpiece

Exp. No	Trial conditions (Magnetic strength, powder, concentration, current, tool material, pulse-on)	Corner wear (photographic view)	Comparison between ideal and measured tool profile (Legend: red dotted line: ideal; blue solid line: measured)
			A B
1	0.1 T, W, 2 g/L, 2 A, Cu, 50 µs	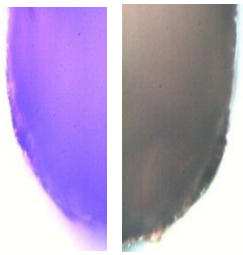	 Maximum wear = 0.135 mm
2	0.1 T, W, 4 g/L, 4 A, W, 100 µs	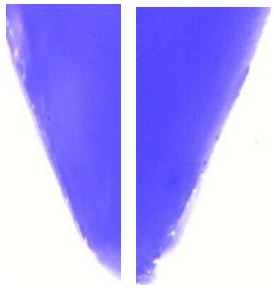	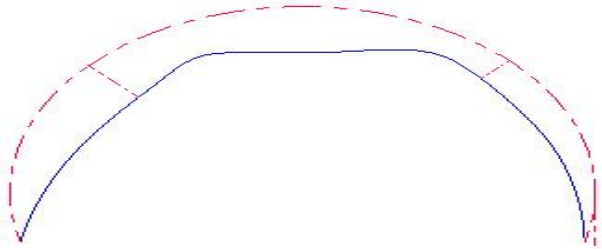 Maximum wear = 0.225 mm

3	0.1 T, W, 6 g/L, 6 A, C18000, 200 µs	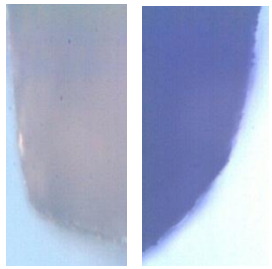	 Maximum wear = 0.25 mm
4	0.1 T, Ti, 2 g/L, 2 A, W, 100 µs	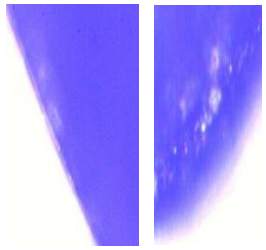	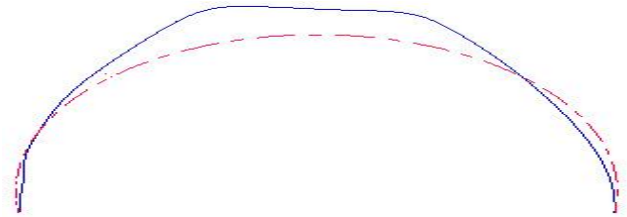 Maximum Wear = 0.07 mm
5	0.1 T, Ti, 4 g/L, 4 A, C18000, 200 µs	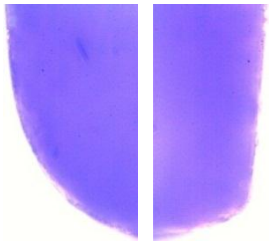	 Maximum wear = 0.165 mm
6	0.1 T, Ti, 6 g/L, 6 A, Cu, 50 µs	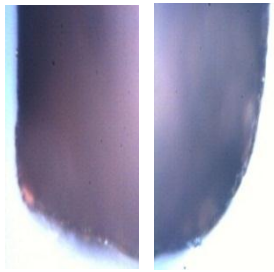	 Maximum wear = 0.16 mm

7	0.1 T, Gr, 2 g/L, 4 A, Cu, 200 µs	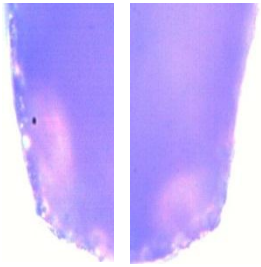	 Maximum wear = 0.27 mm
8	0.1 T, Gr, 4 g/L, 6 A, W, 50 µs	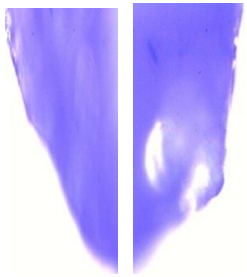	 Maximum wear = 0.205 mm
9	0.1 T, Gr, 6 g/L, 2 A, C18000, 100 µs		 Maximum wear = 0.13 mm

10	0 T, W, 2 g/L, 6 A, C18000, 100 µs	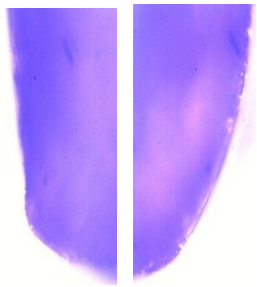	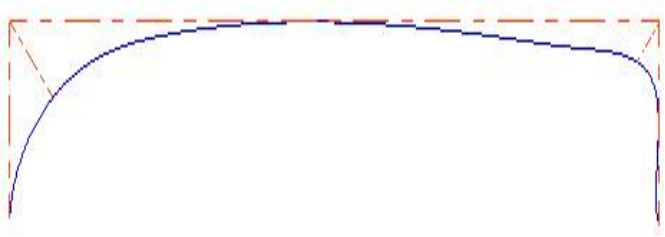 Maximum wear = 0.17 mm
11	0 T, W, 4 g/L, 2 A, Cu, 200 µs	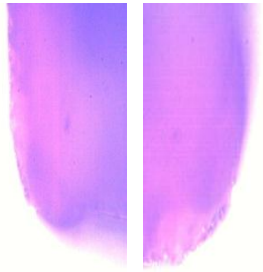	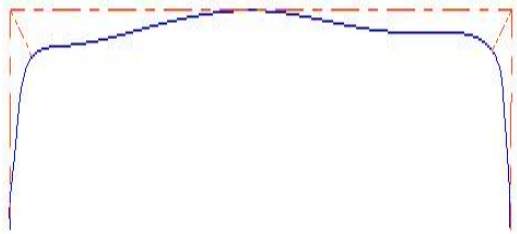 Maximum wear = 0.135 mm
12	0 T, W, 6 g/L, 4 A, W, 50 µs	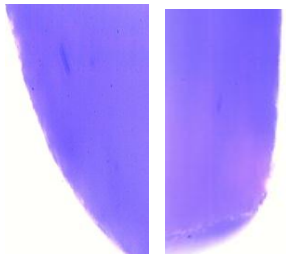	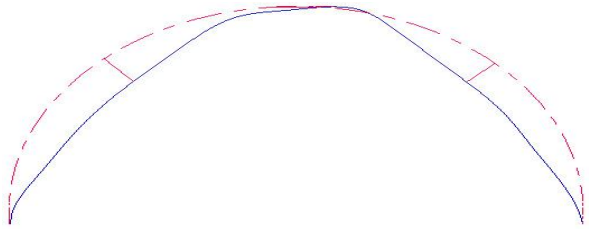 Maximum wear = 0.15 mm
13	0 T, Ti, 2 g/L, 4 A, C18000, 50 µs	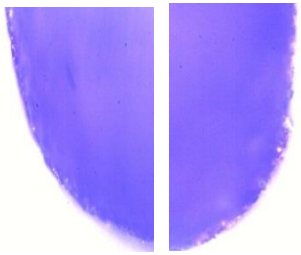	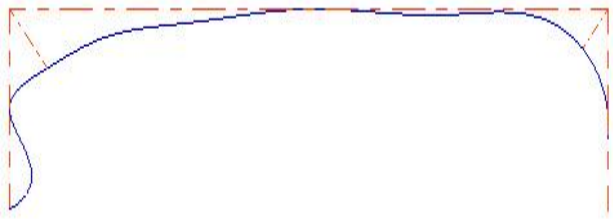 Maximum wear = 0.185 mm

14	0 T, Ti, 4 g/L, 6 A, Cu, 100 µs	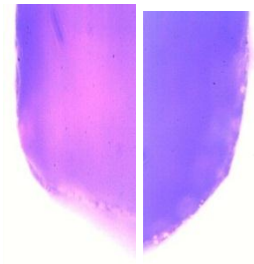	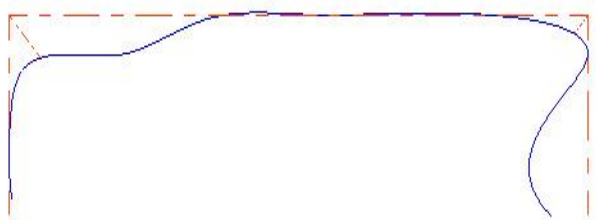 Maximum wear = 0.135 mm
15	0 T, Ti, 6 g/L, 2 A, W, 200 µs	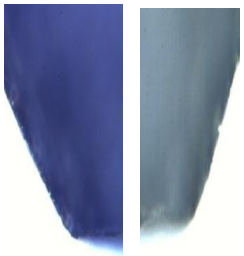	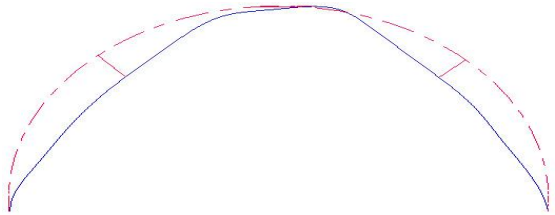 Maximum wear = 0.09 mm
16	0 T, Gr, 2 g/L, 6 A, W, 200 µs	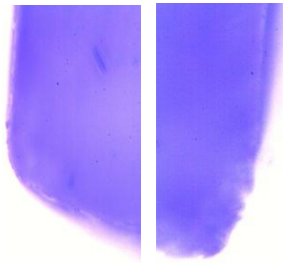	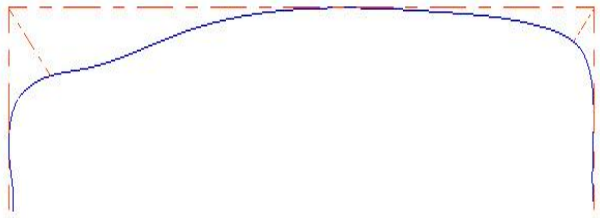 Maximum wear = 0.18 mm
17	0 T, Gr, 4 g/L, 2 A, C18000, 50 µs	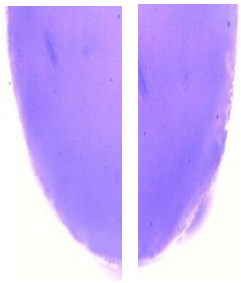	 Maximum wear = 0.16 mm

18	0 T, Gr, 6 g/L, 4 A, Cu, 100µs	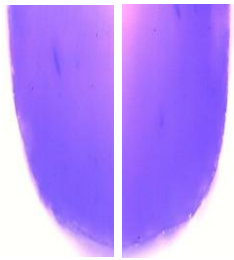	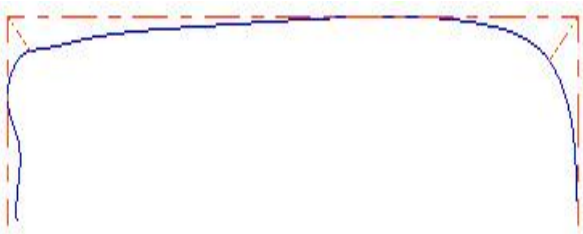 Maximum wear = 0.15 mm

Table 4.24: Tool side wear during PMEDM of D3 workpiece

Exp. No	Trial conditions (Magnetic strength, powder, concentration, current, tool material, pulse-on)	Side wear (photographic view) 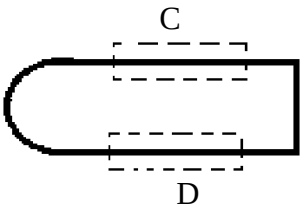
1	0.1 T, W, 2 g/L, 2 A, Cu, 50 µs	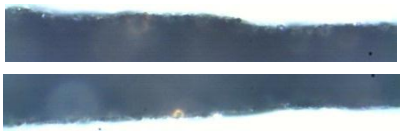 Maximum wear = 0.01925 mm
2	0.1 T, W, 4 g/L, 4 A, W, 100 µs	 Maximum wear = 0.0502 mm
3	0.1 T, W, 6 g/L, 6 A, C18000, 200 µs	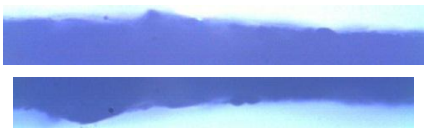 Maximum wear = 0.045 mm
4	0.1 T, Ti, 2 g/L, 2 A, W, 100 µs	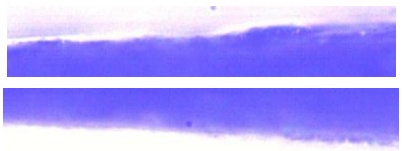 Maximum wear = 0.0208 mm
5	0.1 T, Ti, 4 g/L, 4 A, C18000, 200 µs	 Maximum wear = -0.0428 mm
6	0.1 T, Ti, 6 g/L, 6 A, Cu, 50 µs	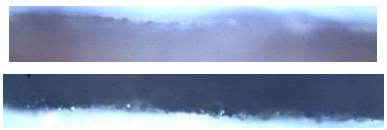 Maximum wear = -0.0852 mm
7	0.1 T, Gr, 2 g/L, 4 A, Cu, 200 µs	 Maximum wear = 0.0198 mm

8	0.1 T, Gr, 4 g/L, 6 A, W, 50 µs	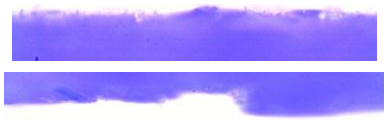 Maximum wear = 0.0368 mm
9	0.1 T, Gr, 6 g/L, 2 A, C18000, 100 µs	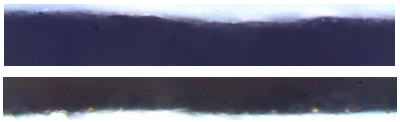 Maximum wear = -0.0732 mm
10	0 T, W, 2 g/L, 6 A, C18000, 100 µs	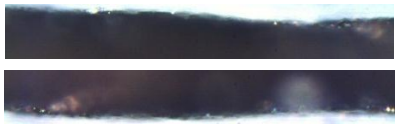 Maximum wear = 0.0698 mm
11	0 T, W, 4 g/L, 2 A, Cu, 200 µs	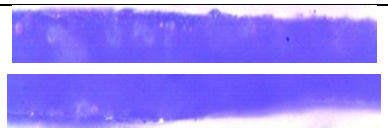 Maximum wear = -0.0598 mm
12	0 T, W, 6 g/L, 4 A, W, 50 µs	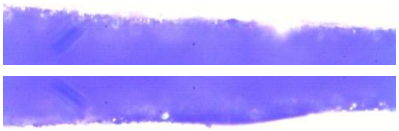 Maximum wear = 0.0278 mm
13	0 T, Ti, 2 g/L, 4 A, C18000, 50 µs	 Maximum wear = -0.0368 mm
14	0 T, Ti, 4 g/L, 6 A, Cu, 100 µs	 Maximum wear = 0.0528 mm
15	0 T, Ti, 6 g/L, 2 A, W, 200 µs	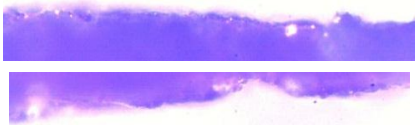 Maximum wear = 0.03135 mm

16	0 T, Gr, 2 g/L, 6 A, W, 200 µs	 Maximum wear = 0.0132 mm
17	0 T, Gr, 4 g/L, 2 A, C18000, 50 µs	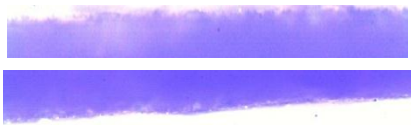 Maximum wear = 0.0042 mm
18	0 T, Gr, 6 g/L, 4 A, Cu, 100µs	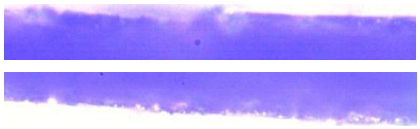 Maximum wear = -0.01039 mm

4.5 Results and Analysis of Overcut

Overcut (OC) is the measure of the amount by which the dimensions of the cut exceed the dimensions of the tool electrode diameter. This measurement was made using Nikon profile projector (Model V10-A). The overcut is measured at five locations as shown in Fig. 4.8. The average of these five readings is calculated and listed in Table 4.22, 4.23 and 4.24 for workpiece H11, H13 and D3 respectively.

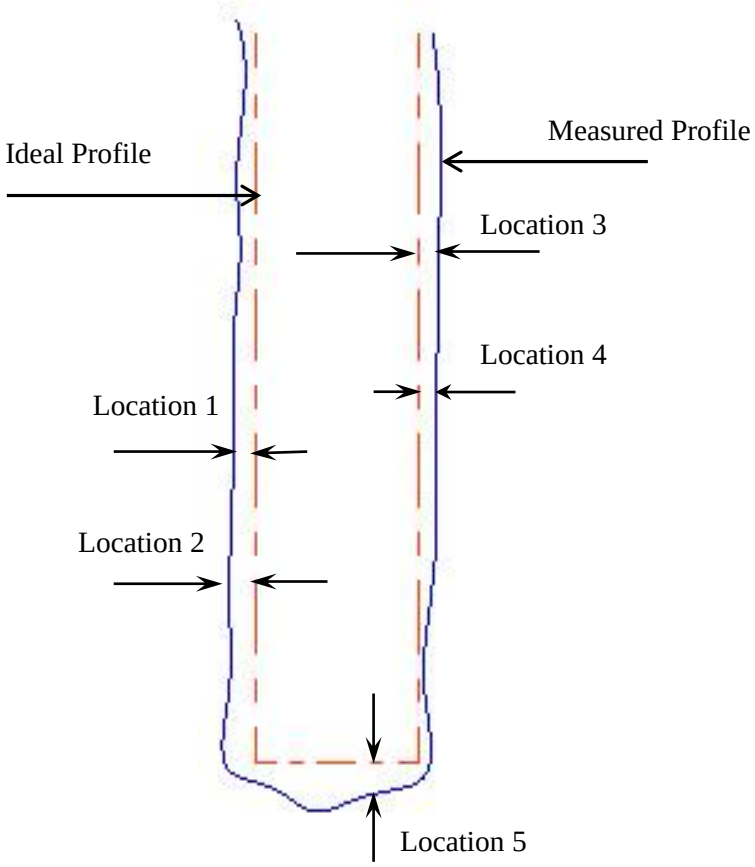

Figure 4.14: Schematic representation location of overcut measurement

4.5.1 Analysis of overcut for H11 workpiece

The overcut for all the 18 trials is calculated for the H11 workpiece. The average of five readings measured at different locations is calculated and listed in Table 4.22 along with the average depth measured for each trial. Comparison of the ideal and measured profiles is also made for the length as well as for the depth of the cuts.

For H11 workpiece the maximum overcut is observed in the trials conducted at 4 A of current settings i.e. in the trial numbers 2, 5, 7, 12, 13 and 18 (refer Table 4.25) which are also the trials for maximum MRR (refer Fig. 4.2) whereas the overcut observed in the case of 2 A and 6 A vary slightly. In the case of tool materials the maximum overcut is observed for the C18000 alloy followed by tungsten and copper respectively whereas maximum MRR was achieved using copper followed by C18000 and tungsten. Overcut is found to decrease with increase in pulse-on duration i.e. trial number 1, 6, 8, 12, 13 conducted at pulse-on duration of 50 µs have shown higher overcut compared to the trials conducted at 100 µs and 200 µs. Similar pattern is followed by the concentration of the powder suspended with lowest concentration of 2 g/L showing the highest overcut followed by the 6 g/L and 4 g/L. The overcut for the trials conducted in presence of magnetic field was less compared to those conducted without any external magnetic field. In the case of type of powder used maximum overcut was observed in the case of graphite with very slight difference in rest of the two powders been used. Maximum depth is achieved using copper tool followed by C18000 alloy and tungsten as shown by the trials 7 and 18 (refer Fig. 4.1). In the case of current the pattern followed is 4 A giving the maximum depth followed by the trials conducted at 2 A and 6 A, the reason behind this may be the occurrence of arcing at 6 A. The depth of the cut is found to be maximum at the concentration of 2g/L followed by the concentration of 6 g/L and 4 g/L having slight difference between them. Rest of the factors pulse-on duration, magnetic strength and type of powder has negligible effect.

Table 4.25: Overcut profiles for H11 workpiece

Trial No	Trial Conditions (Magnetic strength, powder, concentration, current, tool material, pulse-on)	Top view Comparison between ideal and measured tool profile (Legend: red dotted line: ideal; blue solid line: measured	Side view Comparison between ideal and measured tool profile (Legend: red dotted line: ideal; blue solid line: measured w
1	0.1 T, W, 2 g/L, 2 A, Cu, 50 µs	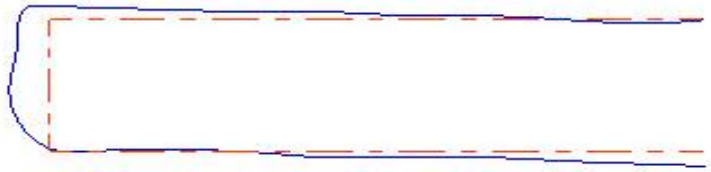 Average overcut = 0.242 mm	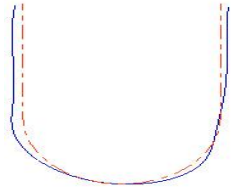 Average depth = 3.365 mm
2	0.1 T, W, 4 g/L, 4 A, W, 100 µs	 Average overcut = 0.162 mm	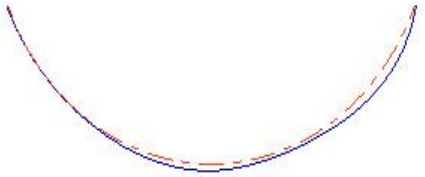 Average depth = 0.836 mm
3	0.1 T, W, 6 g/L, 6 A, C18000, 200 µs	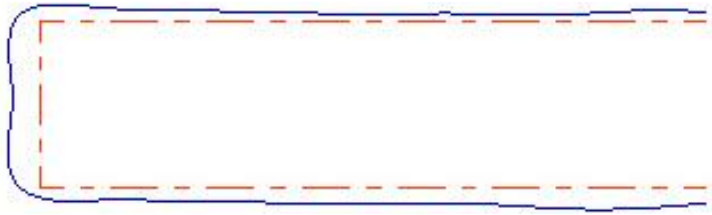 Average overcut = 0.228 mm	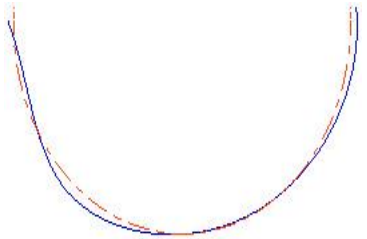 Average depth = 1.271 mm

4	0.1 T, Ti, 2 g/L, 2 A, W, 100 µs	 Average overcut = 0.222 mm	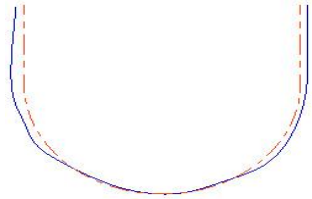 Average depth = 0.832 mm
5	0.1 T, Ti, 4 g/L, 4 A, C18000, 200 µs	 Average overcut = 0.224 mm	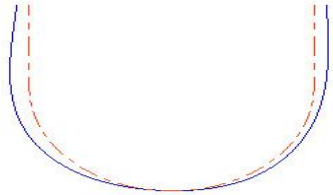 Average depth = 2.155 mm
6	0.1 T, Ti, 6 g/L, 6 A, Cu, 50 µs	 Average overcut = 0.23 mm	 Average depth = 1.670 mm
7	0.1 T, Gr, 2 g/L, 4 A, Cu, 200 µs	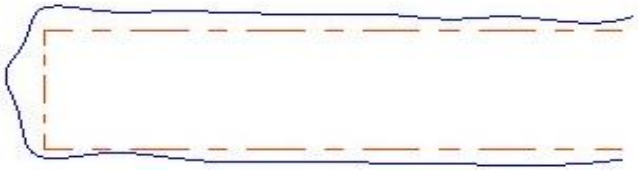 Average overcut = 0.382 mm	 Average depth = 4.924mm

8	0.1 T, Gr, 4 g/L, 6 A, W, 50 µs	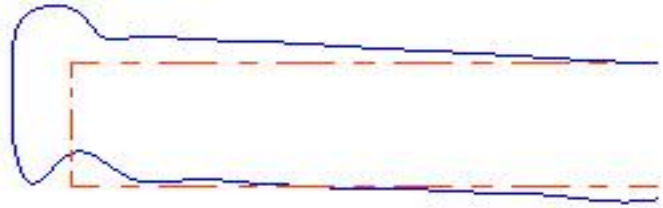 Average overcut = 0.494 mm	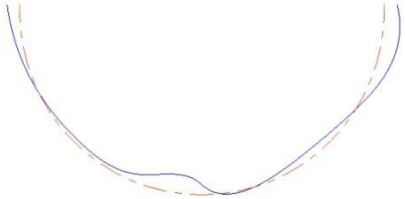 Average depth = 0.796 mm
9	0.1 T, Gr, 6 g/L, 2 A, C18000, 100 µs	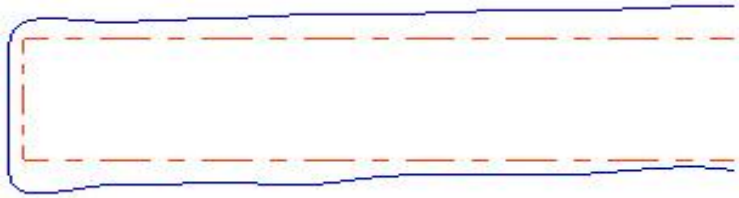 Average overcut = 0.384 mm	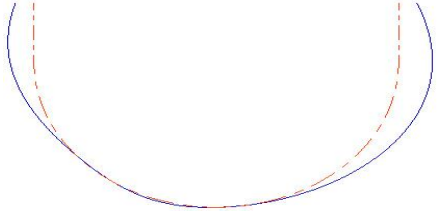 Average depth = 1.068 mm
10	0 T, W, 2 g/L, 6 A, C18000, 100 µs	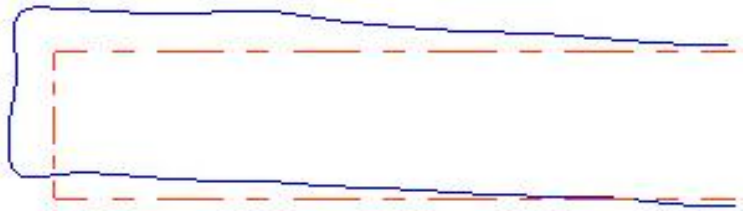 Average overcut = 0.288 mm	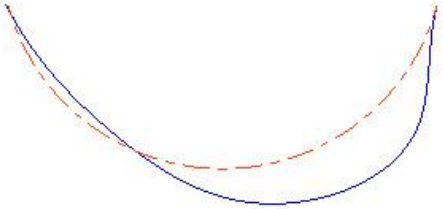 Average depth = 0.931 mm
11	0 T, W, 4 g/L, 2 A, Cu, 200 µs	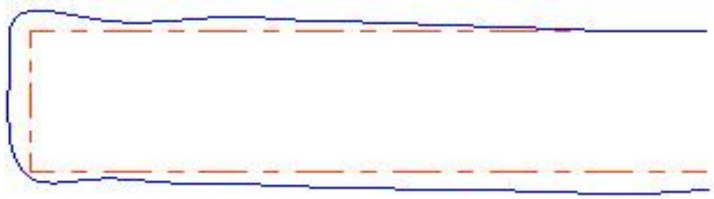 Average overcut = 0.286 mm	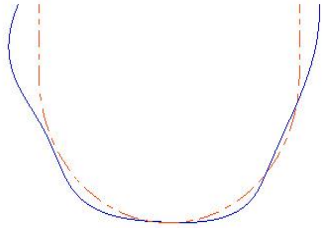 Average depth = 1.748 mm

12	0 T, W, 6 g/L, 4 A, W, 50 µs	 Average overcut = 0.4 mm	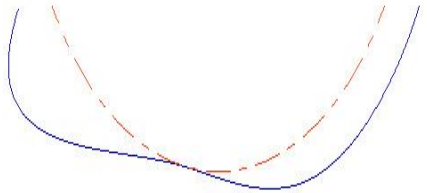 Average depth = 0.665 mm
13	0 T, Ti, 2 g/L, 4 A, C18000, 50 µs	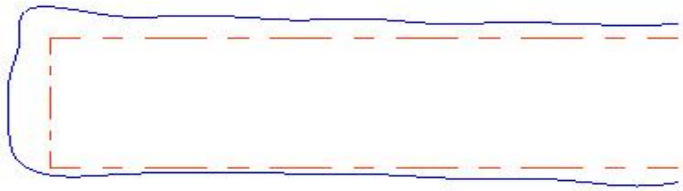 Average overcut = 0.402 mm	 Average depth = 1.917 mm
14	0 T, Ti, 4 g/L, 6 A, Cu, 100 µs	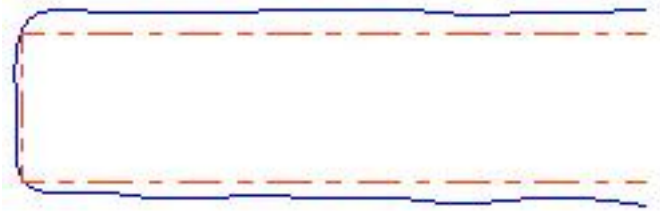 Average overcut = 0.258 mm	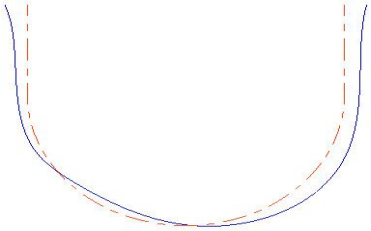 Average depth = 2.051 mm
15	0 T, Ti, 6 g/L, 2 A, W, 200 µs	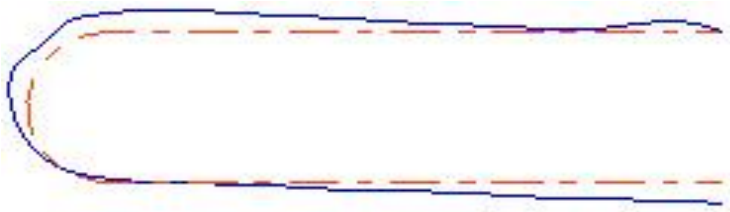 Average overcut = 0.292 mm	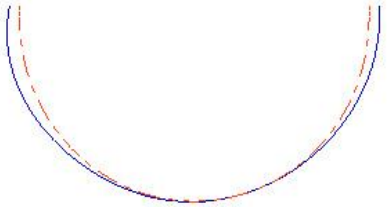 Average depth = 1.285 mm

16	0 T, Gr, 2 g/L, 6 A, W, 200 µs	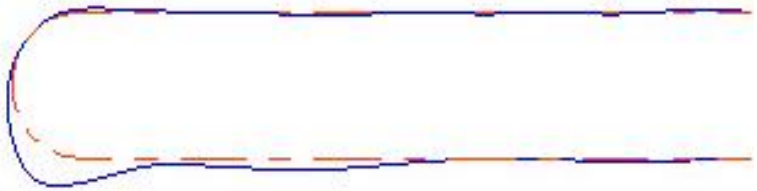 Average overcut = 0.202 mm	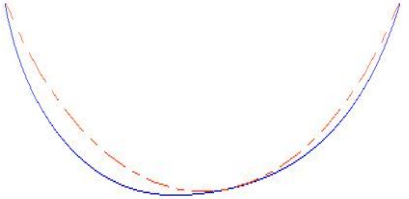 Average depth = 0.838 mm
17	0 T, Gr, 4 g/L, 2 A, C18000, 50 µs	 Average overcut = 0.36 mm	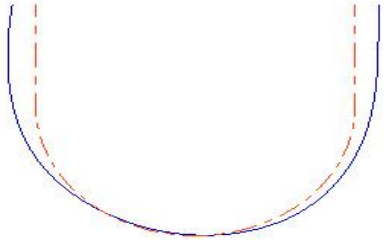 Average depth = 2.126 mm
18	0 T, Gr, 6 g/L, 4 A, Cu, 100µs	 Average overcut = 0.294 mm	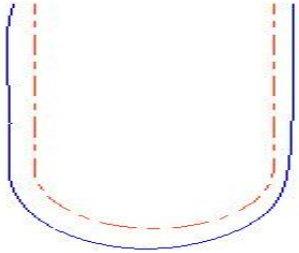 Average depth = 4.287 mm

4.5.2 Analysis of Overcut for H13 Workpiece

The overcut for all the 18 trials is calculated for the H13 workpiece. The average of five readings measured at different locations is calculated and listed in Table 4.26 along with the average depth measured for each trial. Comparison of the ideal and measured profiles is also made for the length as well as for the depth of the cuts.

On use of H13 die steel as the workpiece material maximum overcut is observed in the trials using C18000 alloy as the tool material followed by the copper and tungsten respectively (refer Table 4.23). Overcut is found to decrease with increase in pulse-on duration as the trials 1, 6, 8, 12, 13 and 17 conducted at pulse-on duration of 50 µs have shown higher overcut compared to the trials conducted at pulse-on durations of 100 µs and 200 µs. However overcut observed at 100 µs and 200 µs show very less variation. Trials conducted under the influence of external magnetic field i.e. trials 1-9 have shown less overcut compared to those conducted in the absence of the magnetic field, reason behind this may be the diamagnetic nature of the tool materials and proper removal of debris under influence of magnetic field. Type of powder suspended, concentration of the powder and current are found to have negligible effect on the overcut. Maximum depth is achieved in the trials 1, 6, 7, 11, 14 and 18 (refer Fig. 4.4) i.e. using copper tool followed by C18000 alloy and tungsten. Depth achieved is found to increase with increase in current up to 4 A whereas after that it is found to decrease probably due to occurrence of arcing. In the case of concentration of the powder suspended in the dielectric maximum depth is achieved at the concentration level of 2 g/L i.e. in the trials 1, 4, 7, 10, 13 and 16. Depth achieved at other two levels of concentration vary slightly the reason behind this may be that the debris as well as the powder suspended were not efficiently circulated at the higher concentration levels. Magnetic strength, pulse-on duration and the type of powder suspended in the dielectric have negligible effect on the depth achieved when H13 die steel is used as workpiece material.

Table 4.26: Overcut profiles for H13 workpiece

Trial No.	Trial Conditions (Magnetic strength, powder, concentration, current, tool material, pulse-on)	Top view Comparison between ideal and measured tool profile (Legend: red dotted line: ideal; blue solid line: measured	Side view Comparison between ideal and measured tool profile (Legend: red dotted line: ideal; blue solid line: measured
1	0.1 T, W, 2 g/L, 2 A, Cu, 50 µs	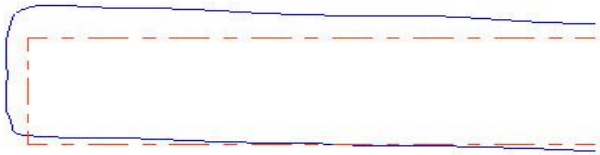 Average overcut = 0.336 mm	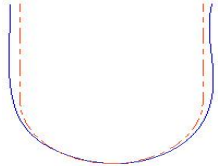 Average depth = 3.019 mm
2	0.1 T, W, 4 g/L, 4 A, W, 100 µs	 Average overcut = 0.226 mm	 Average depth = 1.784 mm
3	0.1 T, W, 6 g/L, 6 A, C18000, 200 µs	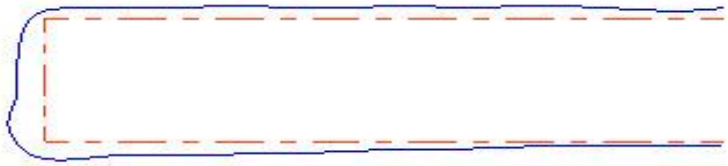 Average overcut = 0.246 mm	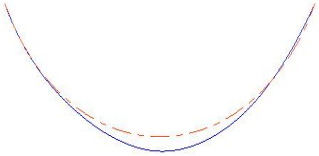 Average depth = 0.849 mm

4	0.1 T, Ti, 2 g/L, 2 A, W, 100 µs	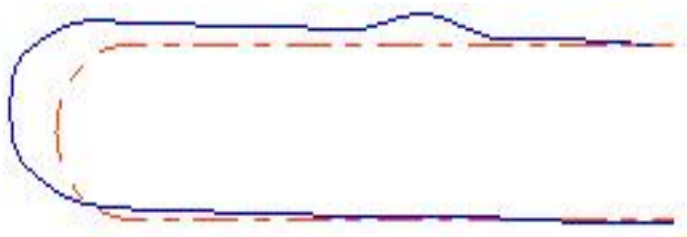 Average overcut = 0.346 mm	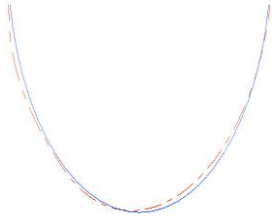 Average depth = 0.957 mm
5	0.1 T, Ti, 4 g/L, 4 A, C18000, 200 µs	 Average overcut = 0.348 mm	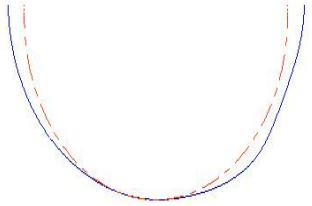 Average depth = 1.189mm
6	0.1 T, Ti, 6 g/L, 6 A, Cu, 50 µs	 Average overcut = 0.406 mm	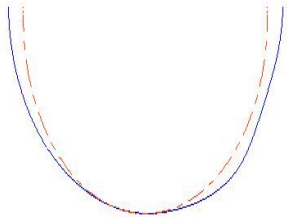 Average depth = 1.312 mm
7	0.1 T, Gr, 2 g/L, 4 A, Cu, 200 µs	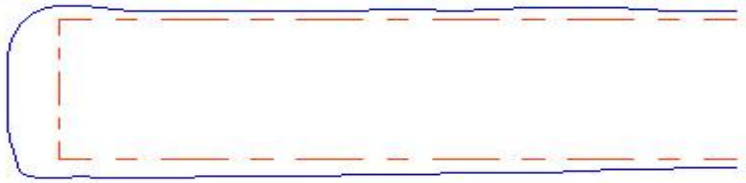 Average overcut = 0.214 mm	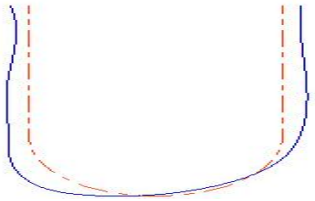 Average depth = 4.021 mm

8	0.1 T, Gr, 4 g/L, 6 A, W, 50 µs	 Average overcut = 0.34 mm	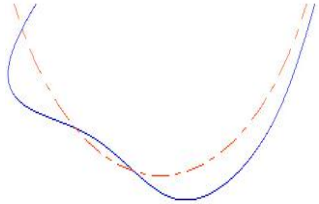 Average depth = 0.848 mm
9	0.1 T, Gr, 6 g/L, 2 A, C18000, 100 µs	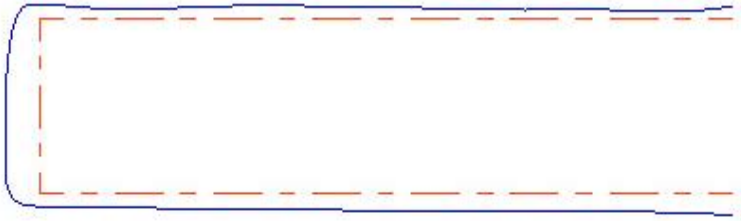 Average overcut = 0.254 mm	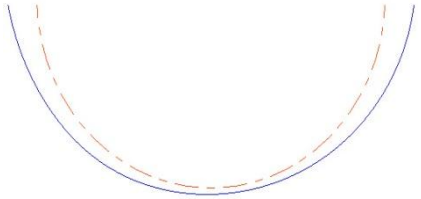 Average depth = 1.199 mm
10	0 T, W, 2 g/L, 6 A, C18000, 100 µs	 Average overcut = 0.346 mm	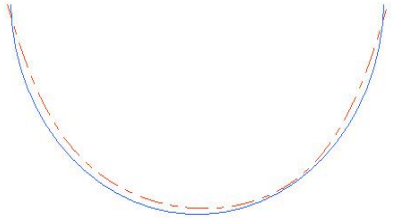 Average depth = 1.124 mm
11	0 T, W, 4 g/L, 2 A, Cu, 200 µs	 Average overcut = 0.358 mm	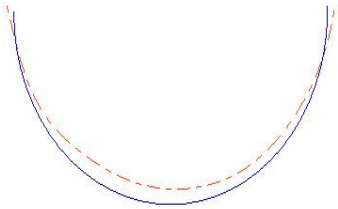 Average depth = 1.139 mm

12	0 T, W, 6 g/L, 4 A, W, 50 µs	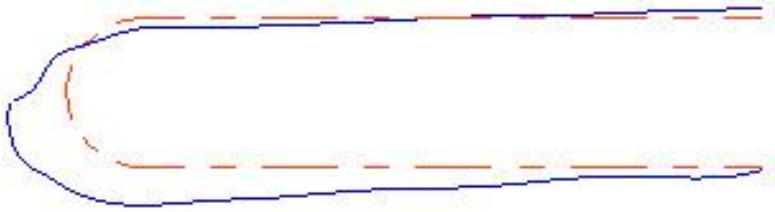 Average overcut = 0.346 mm	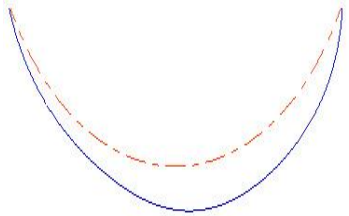 Average depth = 0.875 mm
13	0 T, Ti, 2 g/L, 4 A, C18000, 50 µs	 Average overcut = 0.49 mm	 Average depth = 2.257 mm
14	0 T, Ti, 4 g/L, 6 A, Cu, 100 µs	 Average overcut = 0.364 mm	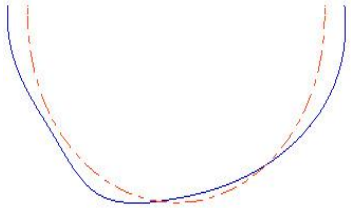 Average depth = 1.326 mm
15	0 T, Ti, 6 g/L, 2 A, W, 200 µs	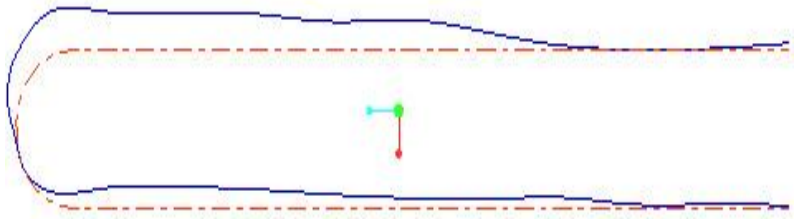 Average overcut = 0.206 mm	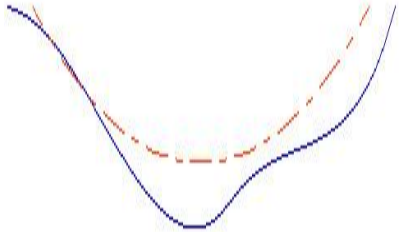 Average depth = 0.178 mm

16	0 T, Gr, 2 g/L, 6 A, W, 200 µs	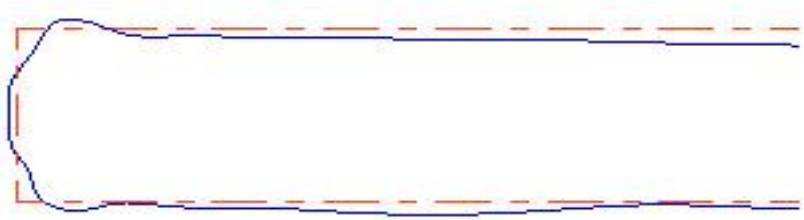 Average overcut = 0.132 mm	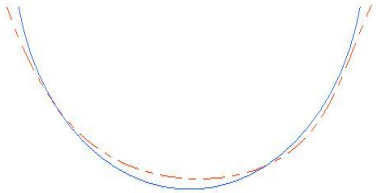 Average depth = 0.859 mm
17	0 T, Gr, 4 g/L, 2 A, C18000, 50 µs	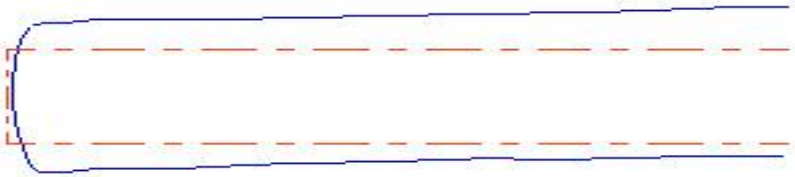 Average overcut = 0.444 mm	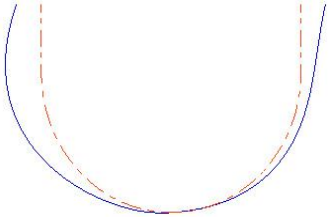 Average depth = 1.796 mm
18	0 T, Gr, 6 g/L, 4 A, Cu, 100µs	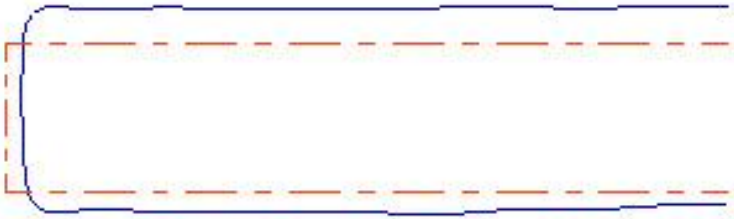 Average overcut = 0.34 mm	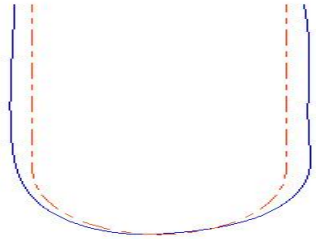 Average depth = 4.321 mm

4.5.3 Analysis of Overcut for D3 Workpiece

The overcut for all the 18 trials is calculated for the D3 workpiece. The average of five readings measured at different locations is calculated and listed in Table 4.27 along with the average depth measured for each trial. Comparison of the ideal and measured profiles is also made for the length as well as for the depth of the cuts.

When die steel D3 is used as the workpiece material maximum overcut is observed in the trials using tungsten as the tool material followed by copper and C18000 alloy (refer table 4.24). The overcut is found to increase with increase in current values with maximum overcut being observed at the current setting of 6 A. Similar pattern is observed in the case of pulse-on duration i.e. overcut is found to increase with increase in pulse-on duration showing maximum overcut at the pulse-on settings of 200 µs. Magnetic strength, type of powder suspended and the concentration of powder being used have negligible effect on the overcut observed. Maximum depth for D3 workpiece material is observed in the trials conducted using copper as the tool material followed by the C18000 alloy and tungsten. In the case of current depth is found to increase with increase in current up to 4 A but after that it is found to decrease this may be due to occurrence of arcing. In the case of concentration maximum depth is observed at the concentration level of 2 g/L whereas there is slight difference in the achieved depths in the trials conducted at 4 g/L and 6 g/L (refer Fig. 4.5 and 4.6). Depth achieved under the influence of external magnetic field is greater than that achieved without the external magnetic field probably due to easy expulsion of debris in the presence of magnetic field. Type of powder suspended in the dielectric and its concentration are found to have negligible effect on the depth achieved.

Table 4.27: Overcut profiles for D3 workpiece

Trial No.	Trial Conditions (Magnetic strength, powder, concentration, current, tool material, pulse-on)	Top view Comparison between ideal and measured tool profile (Legend: red dotted line: ideal; blue solid line: measured	Side view Comparison between ideal and measured tool profile (Legend: red dotted line: ideal; blue solid line: measured
1	0.1 T, W, 2 g/L, 2 A, Cu, 50 µs	 Average overcut = 0.156 mm	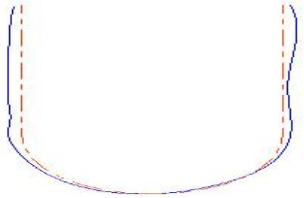 Average depth = 3.800 mm
2	0.1 T, W, 4 g/L, 4 A, W, 100 µs	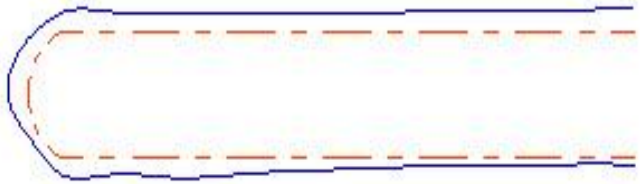 Average overcut = 0.25 mm	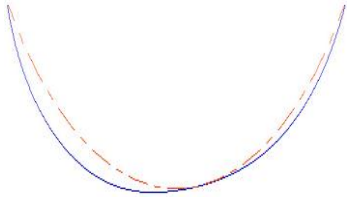 Average depth = 0.496 mm
3	0.1 T, W, 6 g/L, 6 A, C18000, 200 µs	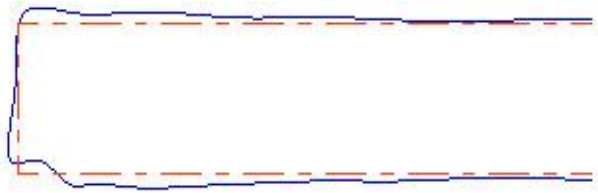 Average overcut = 0.168 mm	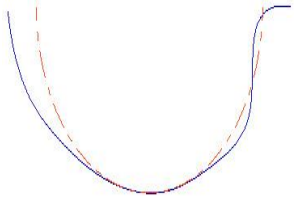 Average depth = 0.949 mm

4	0.1 T, Ti, 2 g/L, 2 A, W, 100 µs	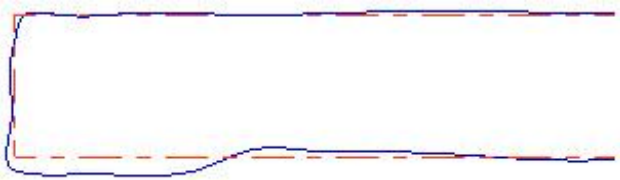 Average overcut = 0.152 mm	 Average depth = 2.054 mm
5	0.1 T, Ti, 4 g/L, 4 A, C18000, 200 µs	 Average overcut = 0.216 mm	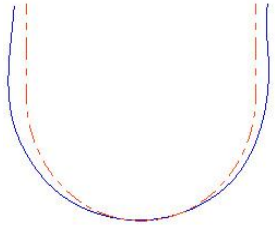 Average depth = 2.073 mm
6	0.1 T, Ti, 6 g/L, 6 A, Cu, 50 µs	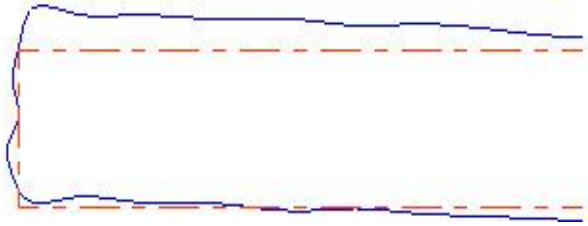 Average overcut = 0.266 mm	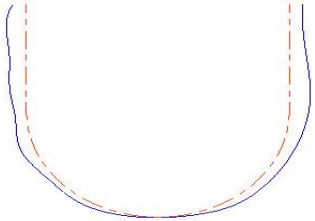 Average depth = 2.392 mm
7	0.1 T, Gr, 2 g/L, 4 A, Cu, 200 µs	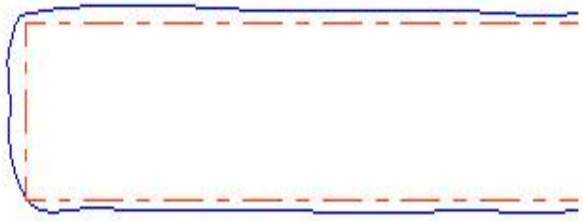 Average overcut = 0.198 mm	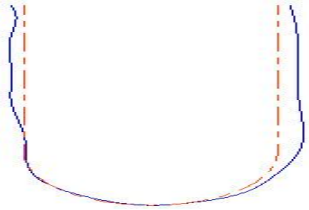 Average depth = 4.604 mm

8	0.1 T, Gr, 4 g/L, 6 A, W, 50 µs	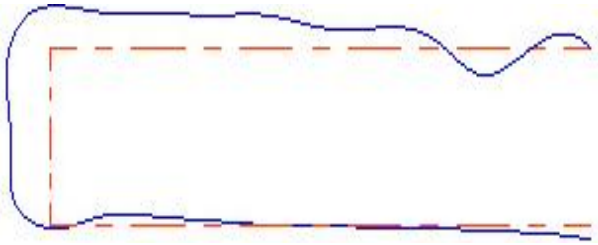 Average overcut = 0.4 mm	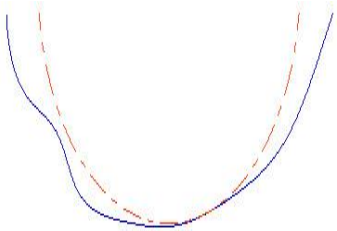 Average depth = 0.863mm
9	0.1 T, Gr, 6 g/L, 2 A, C18000, 100 µs	 Average overcut = 0.248 mm	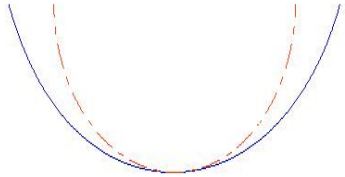 Average depth = 0.928 mm
10	0 T, W, 2 g/L, 6 A, C18000, 100 µs	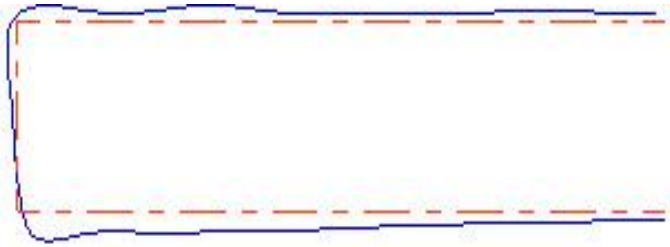 Average overcut = 0.23 mm	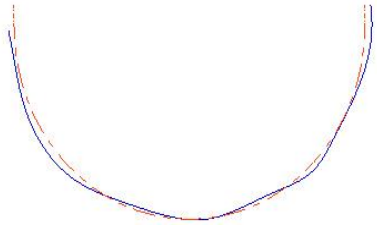 Average depth = 1.298 mm
11	0 T, W, 4 g/L, 2 A, Cu, 200 µs	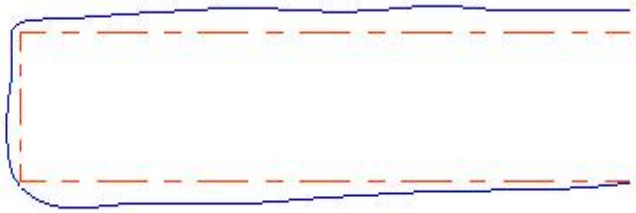 Average overcut = 0.31 mm	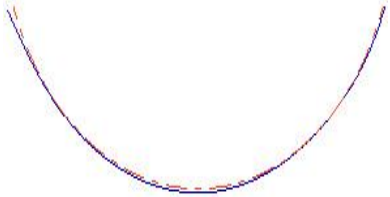 Average depth = 0.790 mm

12	0 T, W, 6 g/L, 4 A, W, 50 µs	 Average overcut = 0.192 mm	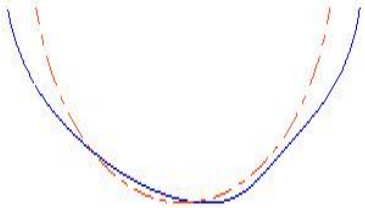 Average depth = 0.724 mm
13	0 T, Ti, 2 g/L, 4 A, C18000, 50 µs	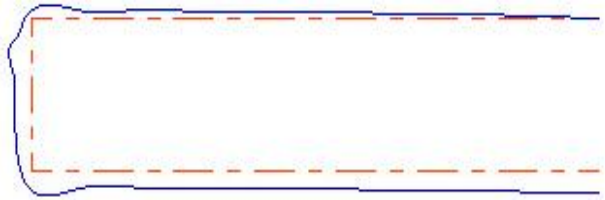 Average overcut = 0.26 mm	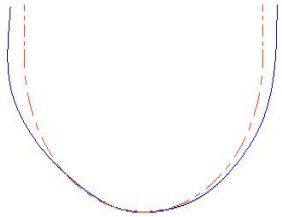 Average depth = 1.640 mm
14	0 T, Ti, 4 g/L, 6 A, Cu, 100 µs	 Average overcut = 0.204 mm	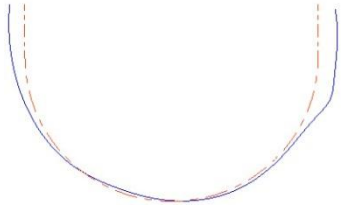 Average depth = 1.628 mm
15	0 T, Ti, 6 g/L, 2 A, W, 200 µs	 Average overcut = 0.17 mm	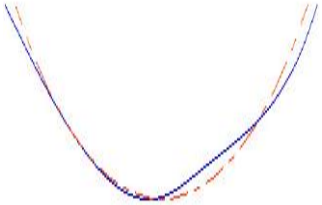 Average depth = 0.280 mm

16	0 T, Gr, 2 g/L, 6 A, W, 200 µs	 Average overcut = 0.292 mm	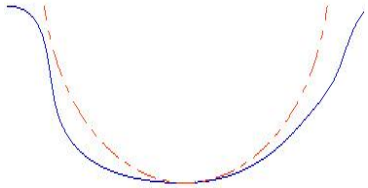 Average depth = 0.810 mm
17	0 T, Gr, 4 g/L, 2 A, C18000, 50 µs	 Average overcut = 0.174 mm	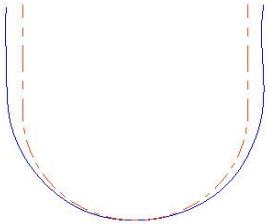 Average depth = 2.375 mm
18	0 T, Gr, 6 g/L, 4 A, Cu, 100µs	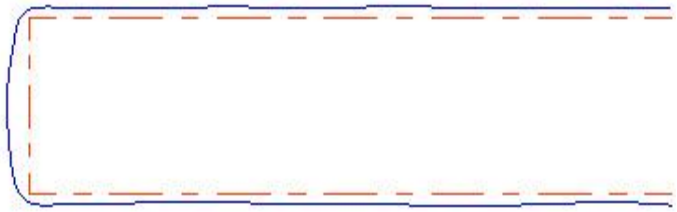 Average overcut = 0.172	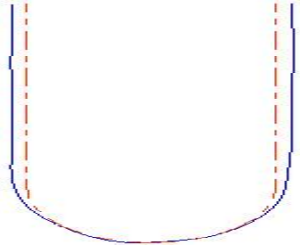 Average depth = 5.234

4.6 Microstructure Analysis

Microstructure analysis was carried out using metallurgical microscope and the cuts made on three different workpieces were viewed at the magnification of 100X.

4.6.1 Microstructure Analysis for H11 Workpiece

The photographic view for the boundaries of the cuts is shown in Fig. 4.9 and Fig 4.10. Fig. 4.9 shows the trials having less amount of resolidified layer. It has been found that trials conducted using copper and C18000 alloy at current setting of 4 A or 6 A and using tungsten tool irrespective of the current setting, show ragged and uneven profile also the resolidified layer is uneven and its thickness is more in these profiles compared to the trials conducted using copper and C18000 as tool material as shown in Fig. 4.10. Fig. 4.11 and Fig. 4.12 show the microstructure for inner profiles of cuts. It shows that the trials conducted at low current settings or at less pulse-on duration i.e. till 100 µs show less area of craters formed this may be because less sparks have occurred compared to the trials conducted at high current settings or at pulse on duration of 200 µs. Also trials conducted using copper as the tool material irrespective of the current settings used also show large amount of craters formed.

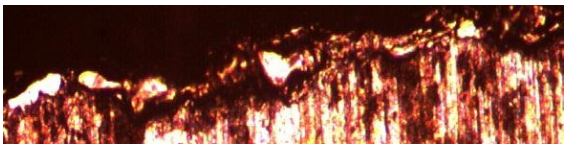

(a)Trial 5 (With magnetic strength 0.1 T, Ti powder, 4 g/L concentration, 4 A current, C18000 tool, 100 µs pulse-on duration)

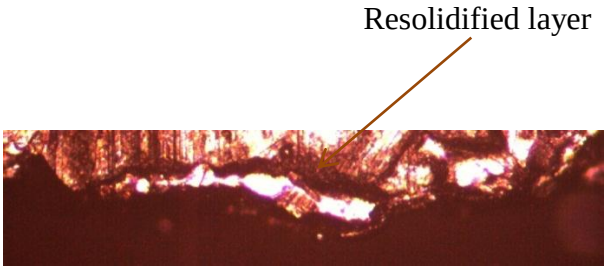

(b)Trial 6 (With magnetic strength 0.1 T, Ti powder, 6 g/L concentration, 6 A current, Cu tool, 50 µs pulse-on duration)

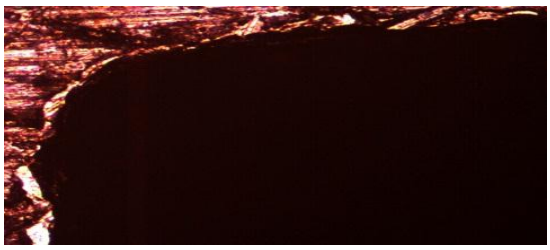

(c) Trial 9 (With magnetic strength, Gr powder, 6 g/L concentration, 2 A current, C18000 tool, 100 µs pulse-on duration)

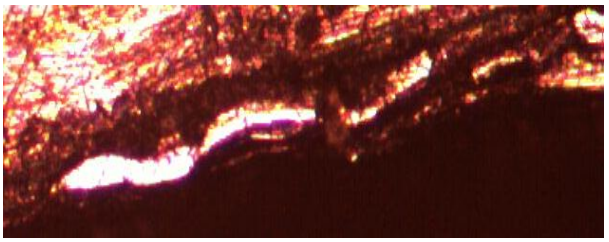

(d) Trial 10 (Without magnet, W powder, 2g/L concentration, 6 A current, C18000 tool, 100 µs pulse-on duration)

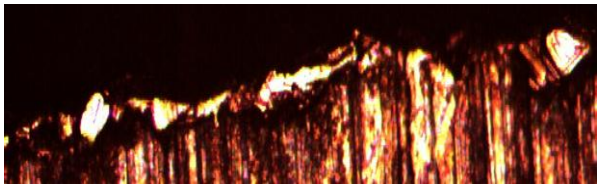

(e) Trial 11 (Without magnet, W powder, 4g/L concentration, 2 A current, Cu tool, 200 µs pulse-on duration)

(f) Trial 14 (Without magnet, Ti powder, 4 g/L concentration, 6 A current, Cu tool, 100 µs pulse-on duration)

(g) Trial 17 (Without magnet, Gr powder, 4 g/L concentration, 2 A current, C18000 tool, 50 µs pulse-on duration)

Figure 4.15: Trials with even profiles for H11 workpiece

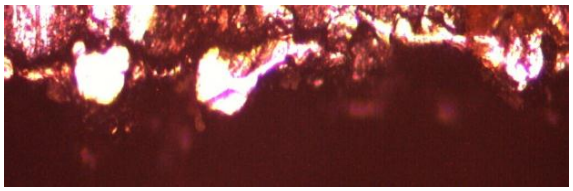

(a) Trial 3 (With magnetic strength 0.1 T, W powder, 2 g/L concentration, 2 A current, Cu tool, 50 µs pulse-on duration)

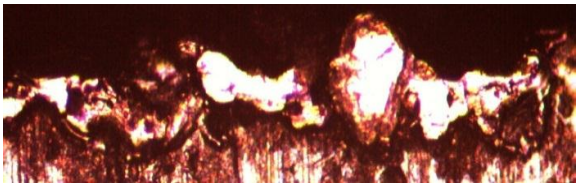

(b) Trial 7 (With magnetic strength 0.1 T, Gr powder, 2 g/L concentration, 4 A current, Cu tool, 200 µs pulse-on

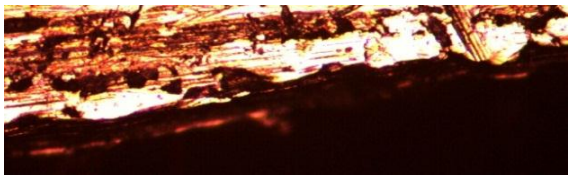

(c) Trial 8 (With magnetic strength 0.1 T, Gr powder, 4 g/L concentration, 6 A current, W tool, 50 µs pulse-on duration)

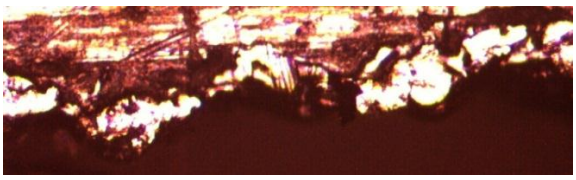

(d) Trial 13 (Without magnet, Ti powder, 2 g/L concentration, 4 A current, C18000 tool, 50 µs pulse-on duration)

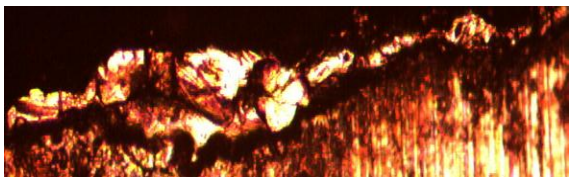

(e) Trial 15 (Without magnet, Ti powder, 6 g/L concentration, 2 A current, W tool, 50 µs pulse-on duration)

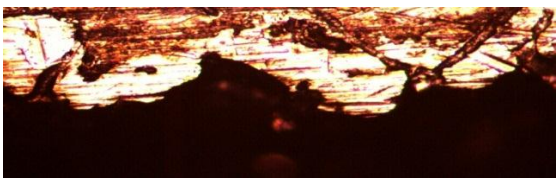

(f) Trial 16 (Without magnet, Gr powder, 2 g/L concentration, 6 A current, W tool, 200 µs pulse-on duration)

Figure 4.16: Trials with uneven profiles for H11 workpiece

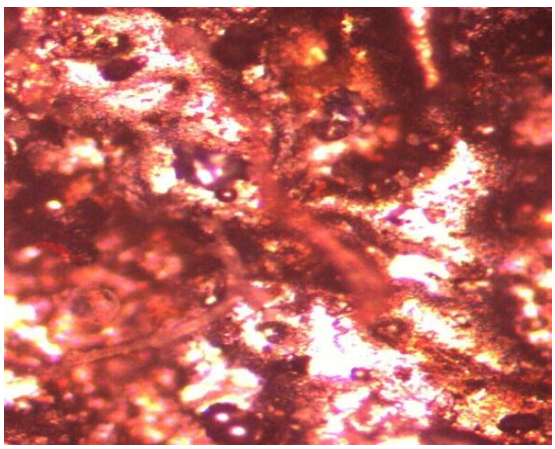

(a) Trial 4 (With magnetic strength 0.1 T, Ti powder, 2 g/L concentration, 2 A current, W tool, 100 µs pulse-on duration)

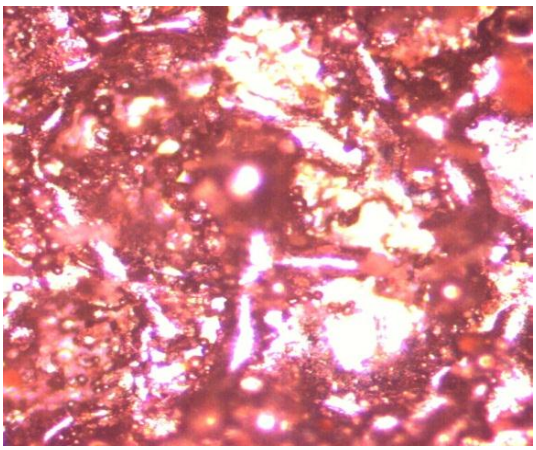

(b) Trial 6 (With magnetic strength 0.1 T, Ti powder, 6 g/L concentration, 6 A current, Cu tool, 50 µs pulse-on duration)

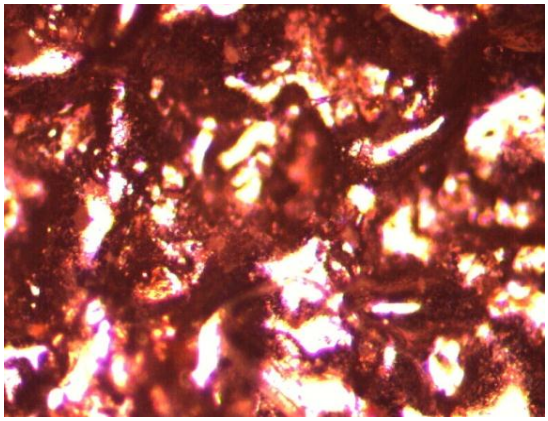

(c) Trial 12 (Without magnet, W powder, 6 g/L concentration, 4 A current, W tool, 50 µs pulse-on duration)

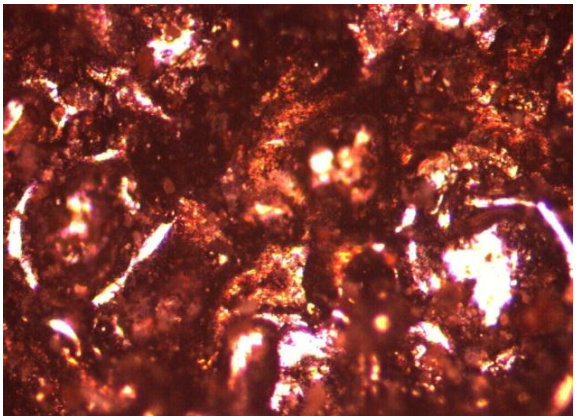

(d) Trial 15 (Without magnet, Ti powder, 6 g/L concentration, 2 A current, W tool, 200 µs pulse-on duration)

Figure 4.17: Profiles for cuts having fewer craters for H11 workpiece

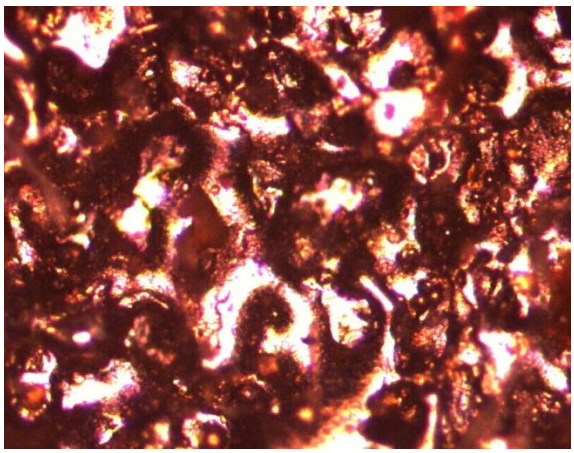

(a) Trial 1 (With magnetic strength 0.1 T, W powder, 2 g/L concentration, 2 A current, Cu tool, 50 µs pulse-on duration)

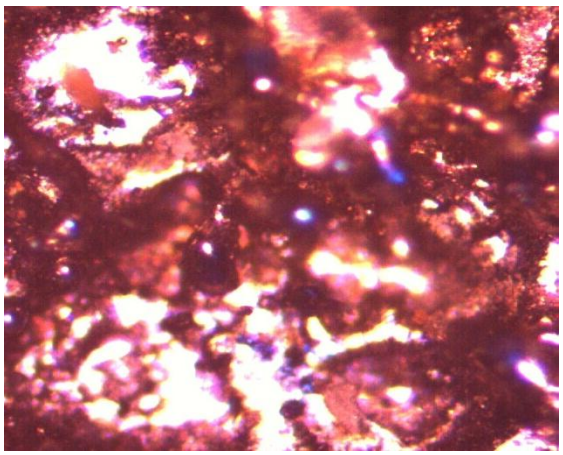

(b) Trial 3 (With magnetic strength 0.1 T, W powder, 6 g/L concentration, 6 A current, Cu tool, 50 µs pulse-on duration)

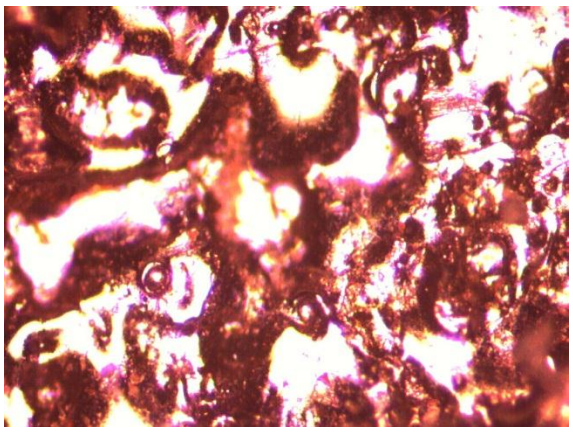

(c) Trial 8 (With magnetic strength 0.1 T, Cu powder, 4 g/L concentration, 6 A current, W tool, 50 µs pulse-on duration)

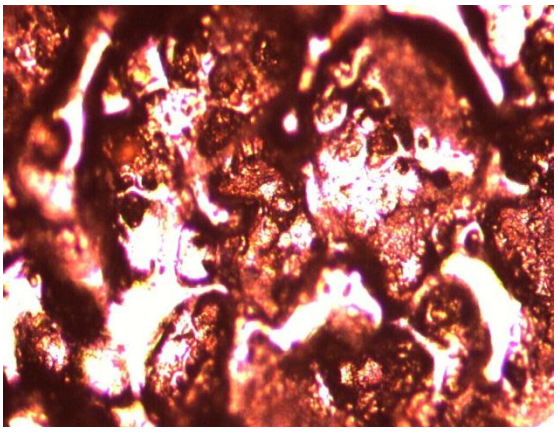

(d) Trial 16 (Without magnet, Cu powder, 2 g/L concentration, 6 A current, W tool, 200 µs pulse-on duration)

Figure 4.18: Profiles for cuts having large craters for H11 workpiece

4.6.2 Microstructure Analysis for H13 Workpiece

The photographic view for the boundaries of the cuts is shown in Fig. 4.13 and Fig 4.14. Fig. 4.13 shows the trials having even profiles and uneven profiles respectively. It has been found that in the case of H13 as the workpiece material trials conducted using copper as tool material irrespective of the current settings used form even profiles on boundaries and the trials using W and C18000 as tool material have formed uneven profiles. Fig. 4.15 and Fig. 4.16 show the microstructure for inner profiles of cuts. It shows that the trials conducted at low current settings or at less pulse-on duration show less area of craters formed this may be because less sparks have occurred compared to the trials conducted at high current settings or at pulse on duration of 200 µs. Also trials conducted using copper as the tool material irrespective of the current settings used also show large amount of craters formed this indicates that more number of sparks at high parameter settings resulting in more craters formed.

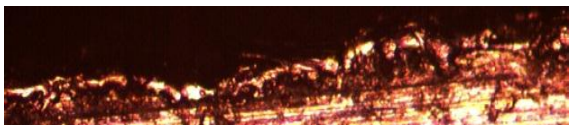

(a) Trial 11 (Without magnet, W powder, 4g/L concentration, 2 A current, Cu tool, 200 µs pulse-on duration)

(b) Trial 14 (Without magnet, Ti powder, 4 g/L concentration, 6 A current, Cu tool, 100 µs pulse-on duration)

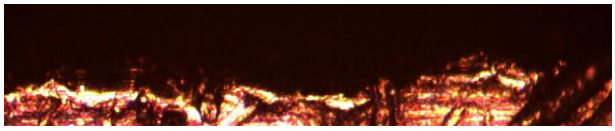

(c) Trial 18 (Without magnet, Gr powder, 6 g/L concentration, 4 A current, Cu tool, 100 µs pulse-on duration)

Figure 4.19: Trials with even profile for H13 workpiece

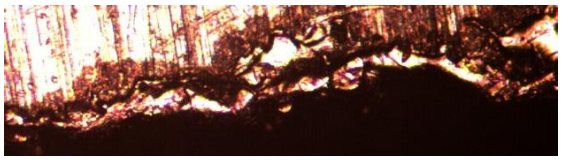

(a) Trial 5 (With magnetic strength 0.1 T, Ti powder, 4 g/L concentration, 4 A current, C18000 tool, 200 µs pulse-on duration)

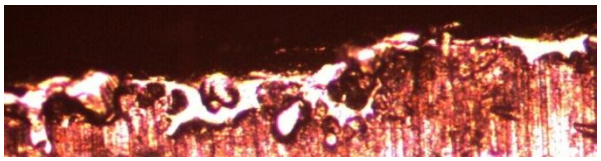

(b) Trial 10 (Without magnet, W powder, 2 g/L concentration, 6 A current, C18000 tool, 100 µs pulse-on duration)

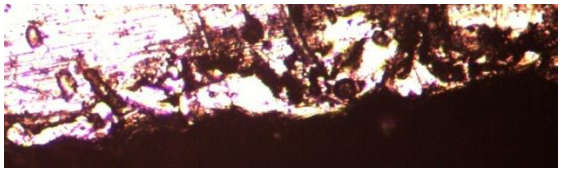

(c) Trial 13 (Without magnet, Ti powder, 2 g/L concentration, 4 A current, C18000 tool, 50 µs pulse-on duration)

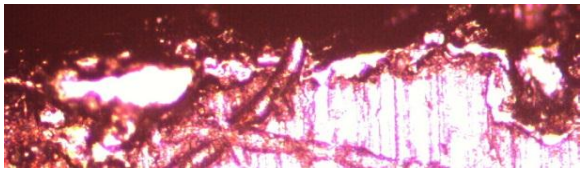

(d) Trial 16 (Without magnet, Gr powder, 2 g/L concentration, 6 A current, W tool, 200 µs pulse-on duration)

Figure 4.20: Trials with uneven profile for H13 workpiece

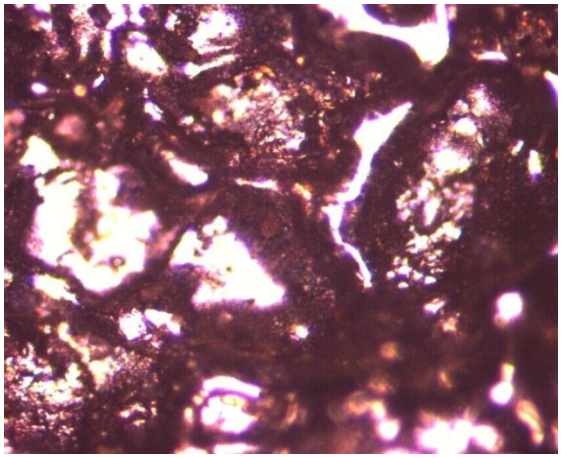

(a) Trial 5 (With magnetic strength 0.1 T, Ti powder, 4 g/L concentration, 4 A current, C18000 tool, 200 µs pulse-on duration)

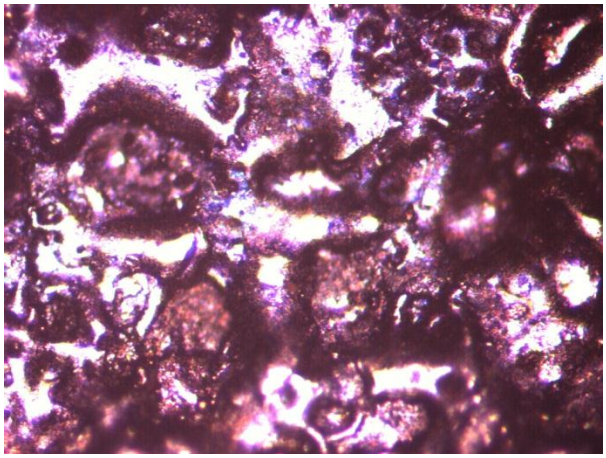

(b) Trial 6 (With magnetic strength 0.1 T, Ti powder, 6 g/L concentration, 6 A current, Cu tool, 50 µs pulse-on duration)

Figure 4.21: Profiles for cuts having fewer craters for H13 workpiece

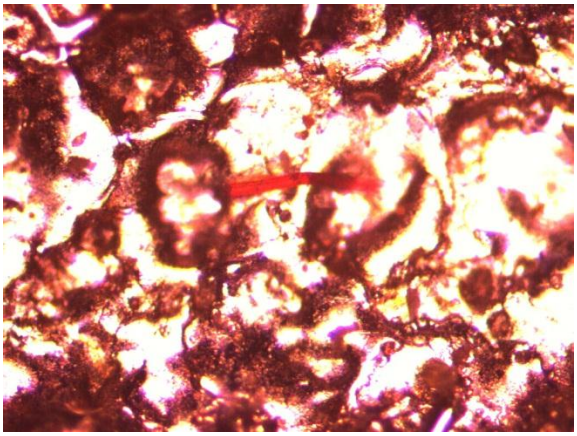

(a) Trial 11 (Without magnet, W powder, 4g/L concentration, 2 A current, Cu tool, 200 µs pulse-on duration)

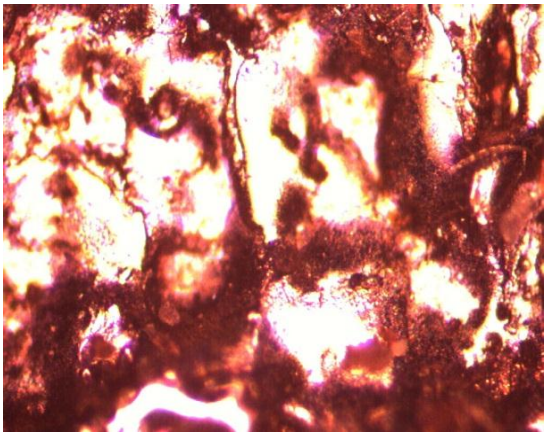

(b) Trial 16 (Without magnet, Gr powder, 2 g/L concentration, 6 A current, W tool, 200 µs pulse-on duration)

Figure 4.22: Profiles for cuts having larger craters for H13 workpiece

4.6.3 Microstructure Analysis for D3 Workpiece

The photographic view for the boundaries of the cuts is shown in Fig. 4.23 and Fig 4.24 shows the trials having even profiles and uneven profiles respectively. It has been found that in the case of D3 as the workpiece material trials conducted using copper as tool material irrespective of the current settings and pulse-on durations used form even profiles on boundaries and the trials using W and C18000 as well in some cases of copper as tool material at higher current settings have formed uneven profiles also trials conducted using copper as tool material with low current and high pulse-on settings also formed uneven profiles. Fig. 4.15 and Fig. 4.16 show the microstructure for inner profiles of cuts. Fig. 4.24 and Fig. 4.25 show the microstructure for inner profiles of cuts. It shows that the trials conducted at low current settings or at less pulse-on duration show less area of craters formed this may be because less sparks have occurred compared to the trials conducted at high current settings or at pulse on duration of 200 µs. Also trials conducted using copper as the tool material irrespective of the current settings used also show large amount of craters formed this indicates that more number of sparks at high parameter settings resulting in more craters formed.

(a) Trial 4 (With magnetic strength 0.1 T, Ti powder, 2 g/L concentration, 2 A current, W tool, 100 µs pulse-on duration)

(a) Trial 11 (Without magnet, W powder, 4g/L concentration, 2 A current, Cu tool, 200 µs pulse-on duration)

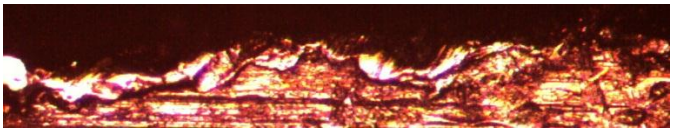

(c) Trial 12 (Without magnet, W powder, 6 g/L concentration, 4 A current, W tool, 50 µs pulse-on duration)

Figure 4.23: Trials with even profile for D3 workpiece

(a) Trial 6 (With magnetic strength 0.1 T, Ti powder, 6 g/L concentration, 6 A current, Cu tool, 50 µs pulse-on duration)

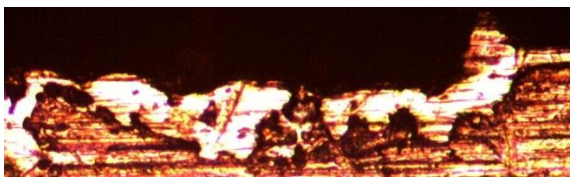

(b) Trial 10 (Without magnet, W powder, 2 g/L concentration, 6 A current, C18000 tool, 100 µs pulse-on duration)

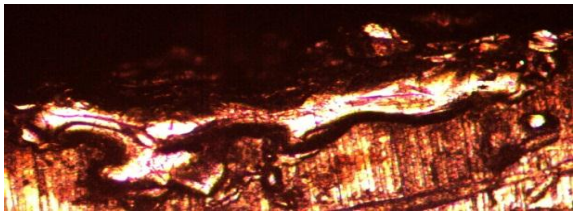

(b) Trial 14 (Without magnet, Ti powder, 4 g/L concentration, 6 A current, Cu tool, 100 µs pulse-on duration)

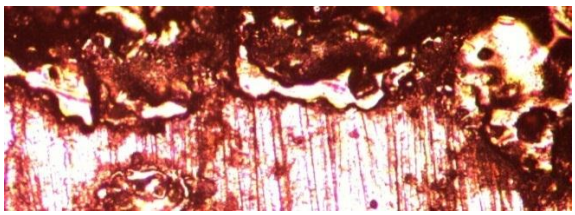

(d) Trial 15 (Without magnet, Ti powder, 6 g/L concentration, 2 A current, W tool, 200 µs pulse-on duration)

Figure 4.24: Trials with uneven profile for D3 workpiece

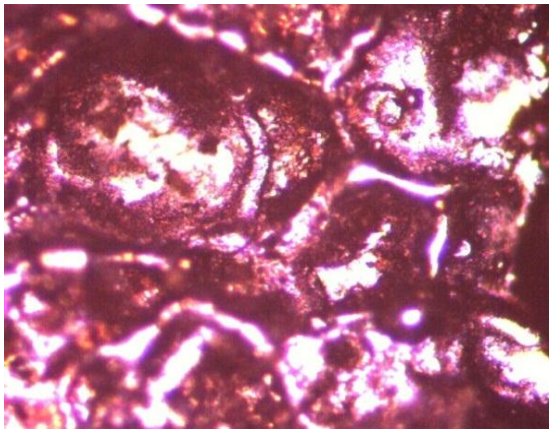

(a) Trial 1 (With magnetic strength 0.1 T, W powder, 2 g/L concentration, 2 A current, Cu tool, 50 µs pulse-on duration)

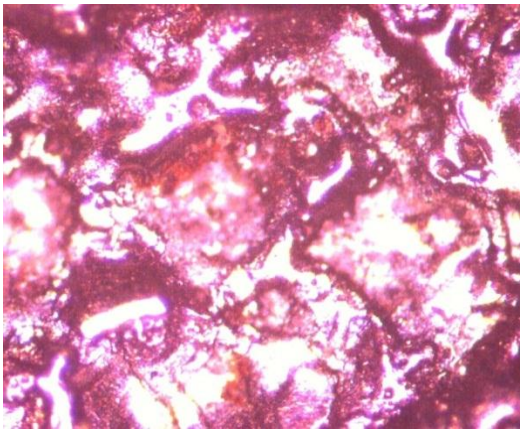

(a) Trial 4 (With magnetic strength 0.1 T, W powder, 4 g/L concentration, 4 A current, W tool, 100 µs pulse-on duration)

Figure 4.25: Profiles for cuts having fewer craters for D3 workpiece

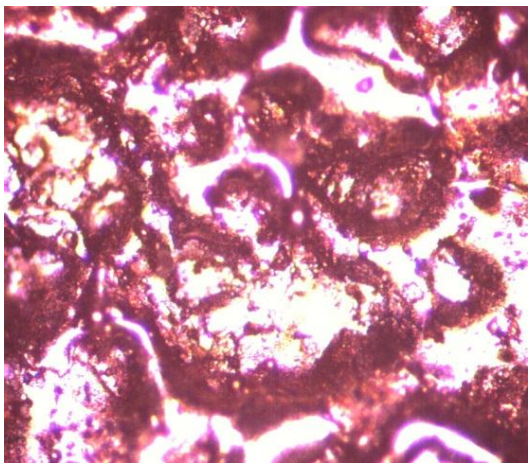

(a) Trial 5 (With magnetic strength 0.1 T, Ti powder, 4 g/L concentration, 4 A current, C18000 tool, 200 µs pulse-on duration)

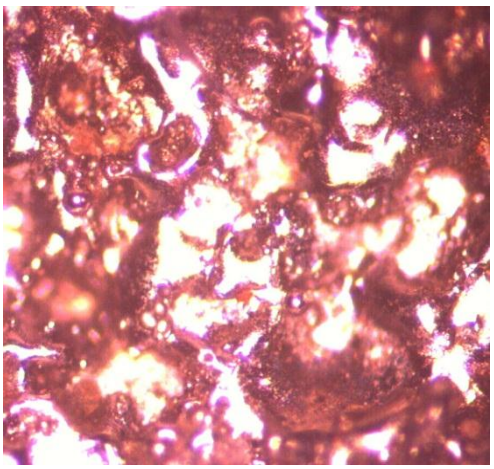

(b) Trial 10 (Without magnet, W powder, 2 g/L concentration, 6 A current, C18000 tool, 100 µs pulse-on duration)

Figure 4.26: Profiles for cuts having large craters for D3 workpiece

CHAPTER 5

Conclusion and Scope for Future Work

5.1 Conclusion

This experimental investigation was mainly aimed at comparing the tool wear behavior of the three tool material copper, C18000 and tungsten with and without using the external magnetic field. Different process parameters like current, pulse-on time, powder suspended in dielectric (tungsten, titanium and graphite) was varied at three levels with and without using magnetic field. Different output parameters measured are MRR, TWR, geometrical tool wear characteristics (corner wear, side wear), overcut. Some significant conclusions drawn on the basis of analysis of results.

For MRR achieved following conclusions have been observed

- Tool material is found to be the most significant factor in case of all the response variables measured with copper giving the highest MRR.
- Besides tool material current is found to be the significant factor in affecting MRR for H11 and D3 workpiece materials, type of powder suspended in dielectric is found to affect the MRR for H13 and D3 workpiece materials..
- AISI H13 workpiece material is found to have maximum MRR.
- Graphite powder has reported better MRR compared to the two other powders used.
- Trials conducted in the presence of external magnetic field have reported to show better MRR.
- Maximum MRR is achieved at the powder concentration of 2g/L as on increasing the concentration beyond this level rather than sparking arcing was observed.

  For TWR following conclusions have been drawn
- Tool material is found to be the most significant factor in case of all the response variables measured with copper giving highest TWR followed by C18000 alloy and tungsten.
- Maximum corner wear is reported in tool material C18000 alloy while maximum side wear is shown in tungsten tool.
- Including the tool material factor TWR is affected by pulse-on duration for H11 and D3 workpiece, by magnetic strength for H13 workpiece.

- Machining of D3 workpiece has shown minimum TWR.
- Trials conducted in the presence of external magnetic field have reported to show less TWR.

  Other conclusions drawn are as follows
- Overcut is found to decrease with increase in pulse-on duration, presence of magnetic strength is also found to decrease the overcut.
- Maximum depth of cuts is achieved using copper as a tool material and using 4 A of current setting.

5.2 Scope for Future Work

The future work can be carried out in the following areas

- Other than the one used other workpiece and tool materials can be explored for slot cutting.
- The length of cut and machining time can be increased and the difference in the MRR and TWR can be analyzed.
- Other conductive powders like copper and of other grit size besides the one used can also be explored.
- Magnets of higher strength and different shapes can also be explored.

References

Aas, K.L. (2004) Performance of two graphite electrode qualities in EDM of seal slots in a jet engine turbine vane. *Journals of Materials Processing Technology,* 149: 152-156.

Batish, A.; Bhattacharya, A. (2012) Mechanism of Material Deposition from Powder, Electrode and Dielectric for Surface Modification of H11 and H13 die steels in EDM Process. *Material Science Forum,* 701: 61-75.

Bhattacharya, A.; Batish, A. (2012) Surface Modification of Carbon High Chromium, EN31 and Hot Die Steel using Powder Mixed EDM Process. *Material Science Forum,* 701: 43-59.

Bhattacharya, A.; Batish, A.; Singh, G. (2011) Optimization of Powder Mixed Electric discharge Machining using Dummy treated Experimental Design with Analytic Hierarchy process. *Proceedings of Institution of Mechanical Engineers, Part B: Journal of Engineering Manufacture,* 226: 103–116.

Bhattacharya, A.; Batish, A. (2011) Optimal Parameter Settings for Rough and Finish machining of die steels in powder- mixed EDM. *International Journal of Advanced Manufacturing Technology,* 61(5-8): 537 – 548.

Bhattacharya, A.; Batish, A.; Bhatt G. (2014) Material transfer mechanism during magnetic field–assisted electric discharge machining of AISI D2, D3 and H13 die steel *Proceedings of Institution of Mechanical Engineers, Part B: Journal of Engineering Manufacture,* doi: 10.1177/09544054 14522797.

Bhatt, G. (2013) Experimental Investigation of magnetic field assisted electric discharge machining process, M.Tech Thesis, Thapar University, Patiala.

Chen, SL.; Yan, BH.; Huang, FY. (1999) Influence of kerosene and distilled water as dielectrics on the dielectric discharge machining characteristics of Ti-6Al-4V. *Journal of Materials Processing Technology*, 87:107-111.

Chow, H.M.; Yan, B.; Huang, F.; Hung, J. (2000) Study of added powder in kerosene for the micro-slit machining of titanium alloy using electro-discharge machining. *Journal of Materials Processing Technology,* 101:95–103.

Cogun, C.; Akaslan, S. (2002) The effect of machining parameters on tool electrode wear and machining performance in electric discharge machining. *KSME International Journal,* 16(1): 46-59.

Erden, S.; Bilgin. (1980) Role of impurities in electric discharge machining. in*: Proceedings of 21st International Machine Tool Design and Research Conference,* Macmillan, London, pp. 345–350.

Furutani, K.; Saneto, A.; Takezawa, H.; Mohri N. (2001) Miyake H., Accretion of titanium carbide by electrical discharge machining with powder suspended in working fluid. *International Journal of Precision Engineering,* 25: 138–144.

Ghoreishi, M.; Atkinson, J. (2002) A comparative experimental study of machining characteristics in vibratory, rotary and vibro-rotary electro-discharge machining. *Journal of Materials Processing Technology,* 120: 374-384.

Ghosh A.; Mallik A.K. (2005) Manufacturing Science. Affiliated east-west press private limited. New Delhi.

Govindan, P.; Gupta, A.; Joshi, S.S.; Malshe, A; Rajurkar, K.P. (2013) Single-spark analysis of removal phenomenon in magnetic field assisted dry EDM, *Journal of Materials Processing Technology,* 213: 1048–1058.

He, H.; Cheng, B.J.; Sheng L.Z.; Feng, G.Y. (2009) Electrode Wear Prediction in Milling Electrical Discharge Machining Based on Radial Basis Function Neural Network. *Journal Shanghai Jiaotong University (Sci),* 14: 736-741.

Heinz, K.; Kapoor, S.G.; Devor, R.E.; and Surla V. (2011) An Investigation of Magnetic-Field-Assisted Material Removal in Micro-EDM for Nonmagnetic Materials. *Journal of Manufacturing Science and Engineering,* doi: 10.1115/1.4003488.

Jilani, ST.; Pandey, PC. (1984) *Experimental investigation into the performance of water as dielectric in EDM. International Journal of Machine Tool Design and Research,* 24(1): 31-43

Kansal H.K.; Singh S.; Kumar P. (2007) Technology and Research Developments in Powder mixed electric discharge machining (PMEDM). *Journal of Materials Processing Technology,* 184: 32–41.

Klocke, F.; Schwade, K.A., Veselovac, D. (2013) Analysis of material removal rate and electrode wear in sinking EDM roughing strategies using different graphite grades. *The Seventh Conference on Electro Physical and Chemical Machining (ISEM),* 163-167.

Kobayashi, K.; Magara, T.; Ozaki, Y.; Yatomi T. (1992) The present and future developments of electrical discharge machining, in: *Proceedings of 2nd International Conference on Die and Mould Technology, Singapore,* pp. 35–47.

Koeing, W.; Weill, R.; Wertheim, R.; Jutzler WI. (1977) The flow fields in the working gap with electro-discharge machining. *Annals of CIRP – Manufacturing Technology*, 25(1): 71-76.

Koing, W.; Jorres, L. (1987) Aqueous solutions of organic compounds as dielectrics for EDM sinking. *Annals of CIRP- Manufacturing Technology*, 36(1): 105-109.

Koshy, P.; Tovey, J. (2011). Performance of electrical discharge textured cutting tools. *Annals of CIRP – Manufacturing Technology*, 60: 153-156.

Kung, K.; Horng, J.; Chiang, K. (2009) Material removal rate and electrode wear ratio study on the powder mixed machining of cobalt-bonded tungsten carbide. *International Journal of Advanced Manufacturing Technology*, 40: 95-104 .

Kung, K.Y.; Horng, J T.; Chiang, K.T. (2009) Material removal rate and electrode wear ratio study on the powder mixed electrical discharge machining of cobalt-bonded tungsten carbide. *International Journal of Advanced Manufacturing Technology*, 40: 95-104.

Kunieda, M.; Kobayashi, T. (2004) Clarifying mechanism of determining tool electrode wear ratio in EDM using spectroscopic measurement of vapor density. *Journal of Materials Processing Technology*, 149: 284- 288.

Kunieda, M.; Yanatori, K. (1997) Study on debris movement in EDM gap. *Interational Journal of Electrical Power and Energy Systems*, 2: 43–49.

Lee, SH.; Li, XP. (2001) Study of the effect of machining parameters on the machining characteristics in electrical discharge machining of tungsten carbide. *Journal of Materials Processing Technology*, 115: 344-358.

Li, Y.; Zhang, J.; Yu, C.; Zhang, Y. (2007) Analysis of the wear characteristics of an EDM electrode made by selective laser sintering. *Journals of Materials Processing Technology*, 138: 475-478.

Lin, Y.C.; Chen, Y.F.; Wang, D.A.; and Lee, H.S. (2009) Optimization of machining parameters in magnetic force assisted EDM based on Taguchi method. *Journals of Materials Processing Technology*, 209: 3374–3383.

Lonardo, PM.; Bruzzone, A.A. (1999) Effect of flushing and electrode material on die sinking EDM. *Annals of CIRP – Manufacturing Technology*, 48(1): 123-126.

Luis, C.J.; Puertas, I.; Villa, G. (2005) Material removal rate and electrode wear study on the EDM of silicon carbide. *Journals of Materials Processing Technology*, 164-165: 889-896.

Maradia, U.; Boccardo, M.; Stirnimann J.; Beltrami I.; Kuster F.; Wegner K. (2012) Die sinking EDM in meso-micro machining. *5th CIRP Conference on High Performance Cutting. Procedia Cirp1*, pp.166-177.

Marafona, J. (2007) Black layer characterization and electrode wear ratio in electrical discharge machining (EDM). *Journals of Materials Processing Technology*, 184: 27-31.

Marafona, J.; Wykes, C. (2000) A new method of optimizing material rate using EDM with copper-tugsten electrodes. *International Journal of Machine Tools and Manufacture,* 40(2): 153-164.

Masuzawa, T.; Heuvelman, C.J. (1983) A self flushing method with spark erosion machining. *Annals of CIRP – Manufacturing Technology*, 32(1): 109-111.

Mohri, N.; Suzuki, M.; Furuya, M.; Satio, N. (1995) Electrode wear process in electrical discharge machining. *Annals of CIRP – Manufacturing Technology*, 44(1): 165-168.

Ozgedik, A.; Cogun, C. (2006) An experimental investigation of tool wear in EDM. *International Journal of Advanced Manufacturing Technology*, 27: 488-500.

Pellicer, N.; Ciurana, J.; Delgado, J. (2011) Tool electrode geometry and process parameters influence on different feature geometry and surface quality in electrical discharge machining of AISI H13 steel. *Journal of intelligent manufacturing*, 22(4): 575-584.

Pham, D.T.; Ivanov, A.; Bigot, S.; Popov K., Dimov S. (2007) An investigation of tube and rod electrode wear in micro EDM drilling. *International Journal of Advanced Manufacturing Technology*, 33: 103-109.

Samuel, MP.; Phillip, P.K. (1997) Power metallurgy tool electrodes for electric discharge machining. *International Journal of Machine Tools and Manufacture*, 37(11): 1625-1633.

Sato, T.; Imai, Y.; Goto, A.; Magara, T. (2000) A new grooving method based on steady wear model in EDM. *International Journal of Electrical Machining*, 5: 41-49

Simao, J. (2003) Work piece surface modification using electrical discharge machining. *International Journal of Machine Tools and Manufacture*, 43: 121–128.

Sohani, M.S.; Gaitonde, V.N.; Siddeswarappa, B.; Deshpande, A.S. (2009) Investigations into the effect of tool shapes with size factor consideration in sink electrical discharge machining (EDM) process. *International Journal of Advanced Manufacturing Technology*, 45: 1131-1145.

Teimouri, R.; Baseri, H. (2012b) Study of tool wear and overcut in EDM process with rotary tool and magnetic field. *Advances in Tribology, Volume 2012, Article ID 895918, 8 pages*, doi: 10.1155/2012/895918.

Tzeng, Y.H.; Chen, F. (2003) A simple approach for robust design of high-speed electrical-discharge machining technology. *International Journal of Advanced Manufacturing Technology*, 43: 217–227.

Uno, Y.; A, Okada. (1997) Surface generation mechanism in electrical discharge machining with silicon powder mixed fluid. *International Journal of Electrical Machining*, 2: 13–18.

Wong, Y.S.; Lim, L.C.; Lee, L.C. (1995). Effect of flushing on electro-discharge machined surfaces. *Journal of Materials Processing Technology*, 48: 299–305.

Yan, BH.; Wang, C.C. (1999) The machining characteristics of Al2O3/6061 Al composite using rotary electro-discharge machining with a tube electrode. *Journal of Material Processing Technology,* 95: 107-111.

Yan, M.T.; Huang, K.Y.; Lo, C.Y. (2009) A study on electrode wear sensing and compensation in Micro-EDM using machine vision system. *International Journal of Advanced Manufacturing Technology,* 42: 1065-1073.

Yoshida, M.; Kunieda, M.; Taniguchi, N. (1997) Electrical discharge machining in gas. *Annals of CIRP – Manufacturing Technology*, 46(1): 143-146.

Yu, Z.Y.; Masuzawa, T.; Fujino, M. (1998a) 3D micro-EDM the simple shape electrode. *International Journal of Electrical Machining,* 3: 7-12.

Zarepour, H.; Tehrani, A.F.; Karimi, D.; Amini, S. (2007) Statistical analysis on electrode wear in EDM of tool steel DIN 1.2714 used in forging dies. *Journals of Materials Processing Technology,* 187-188: 711-714.

Zha, J.; Li, Y.; Zhang, J.; Yu, C.; Zhang, Y. (2003) Analysis of the wear characteristics of an EDM electrode made by selective laser sintering. *Journals of Materials Processing Technology*, 138: 475-478.

Zhao, W.S.; Meng, Q.G.; Wang, Z.L. (2002) The application of research on powder mixed EDM in rough machining. *Journal of Material Processing Technology*, 129: 30–33.

WEB REFERNCES

http://nptel.iitm.ac.in/courses/Webcoursecontents/IIT%20Kharagpur/Manuf%20Proc%20II/pdf/LM-39.pdf

http://www.iste.co.uk/data/doc_ayupatunrlmy.pdf